139

VERIFICATION OF THE FSU/FPL LIGHTNING MODEL AND ANALYSIS OF THE METEOROLOGICAL CONDITIONS LEADING TO THE HIGHEST FREQUENCY OF LIGHTNING DURING THE 2012 CONVECTIVE SEASON

Michelle Wilson[1] and J.E. Estupiñán[2,*]

[1] Division of Meteorology and Physical Oceanography, Rosenstiel School of Marine and Atmospheric Science, University of Miami

[2]*Miami Weather Forecast Office, National Weather Service, NOAA, Miami, FL*

ABSTRACT

The results presented in this study will allow forecasters in the NWS Miami Weather Forecast Office, in a more quantitative basis, to increase their knowledge on the atmospheric conditions suitable for active lightning days and provide a better understanding of the performance of the Florida State University/Florida Power and Light Corporation (FSU/FPL) model in predicting lightning. The FSU/FPL model produces statistically-derived forecast spatial fields of categorical lightning occurrence at various times throughout the day using meteorological parameters as input. This presentation will outline how the lightning forecasts for the 2012 convective season (1 June-30 September) were analyzed in two ways: 1) comparing the forecast lightning from the FSU/FPL SREF model to the observed lightning from the National Lightning Detection Network in South Florida; and 2) analyzing the weather conditions that caused the highest frequency of lightning.

The FSU/FPL model predicted 53% of all the lightning in the highest probability range for 15Z, 67% of all the lightning for 18Z, and 57% of all the lightning for 21Z in the highest probability range indicating that the model was able to predict the general area where lightning was observed for the 2012 convective season. Large fluctuations in 500 mb temperature can explain one of the important physical processes related to lightning activity over South Florida. Decreases in 500 mb temperatures were generally correlated with an increase in lightning activity. However, a decrease in 500 mb temperature did not result in an increase in lightning activity if sufficient moisture was not available, if cloud cover inhibited surface heating, or if the surface wind speeds were too strong to allow for intensification of sea breeze fronts. Diagnosing the 500 mb temperatures alone was not sufficient to explain why lightning occurred on certain days but not others, as there are many atmospheric variables to consider. The combination of low 500 mb temperatures with a moist airmass at the leading edge of a Saharan air mass led to increases in lightning activity in South Florida. In addition to these results, images of detailed weather patterns intended to help the NWS Miami forecasters identify the days with the greatest potential of active lightning are presented.

*_Corresponding author address:_ Jeral Estupiñán, Miami Weather Forecast Office, National Weather Service, 11691 SW 17th Street, Miami, FL 33165; e-mail: jeral.estupinan@noaa.gov

1. INTRODUCTION

The National Severe Storms Laboratory states that 62 people die and 300 are injured from being struck by lightning on average in the United States every year. There were 74 recorded deaths in the state of Florida alone from 1998 to 2008 ("Lightning Deaths 1998-2008"). In 2012, the National Weather Service reported 5 deaths that occurred due to lightning in Florida, two of them in South Florida ("Lightning Safety").

This project is a collaborative effort between the Rosenstiel School of Marine and Atmospheric Science at the University of Miami, the National Weather Service (NWS) Miami Weather Forecast Office and the Meteorological Development Laboratory, both a part of the National Oceanic and Atmospheric Administration (NOAA). The project aims to look at an existing statistical model for predicting lightning and to verify the guidance using lightning observations for the 2012 convective season over land in South Florida. Along with the verification of the guidance, a meteorological analysis of the atmospheric conditions for days with high number of strikes will be performed as well as analyzing the conditions for days with low lightning activity over land and adjacent coastal waters.

The model that is to be used to verify is the Short Range Ensemble Forecast (SREF). Phil Shafer produced the existing lightning guidance as his Ph.D. dissertation at the Florida State University for Florida Power and Light (FP&L). The project focused on the regions in Miami-Dade and Broward Counties to which FP&L provides services. The model was created to predict where dangerous lightning could occur from noon to midnight that could lead to power outages in the region (Shafer 2004).

The biggest producer of lighting during the convective season in South Florida is the sea breeze front (Wexler 1946; Simpson 1994; Shafer 2004). The shape of Florida in the south is very narrow allowing the region to experience sea breezes from both coasts: the west and the east. Another important feature of South Florida is that the majority of the center is made up of wetlands, the Everglades. This area can develop its own circulation that can interact and converge with the sea breeze front. The metropolitan areas of South Florida lie close to the coast. This location creates favorable conditions for lightning when the sea breeze comes from the east and converges with the Everglades' circulation. The direction and speed of the low level winds also play a major role in how strong and how far inland the sea breeze will propagate. A strong east wind will create a weak sea breeze front that will affect the west coast of South Florida, whereas a light east wind will be favorable for a strong sea breeze front located on or near the east coast affecting the metropolitan areas (Lopez and Holle 1987; Arritt 1993; Lericos et al. 2002; Shafer 2004). Other factors that create convection and lightning in South Florida are outflow boundaries from already existing storms, synoptic disturbances and lake breezes (Shafer 2004).

The lightning guidance was created during the convective seasons from 1989 to 2004 (Shafer 2004). The atmospheric variables important for sea breeze formation were considered in the generation of the lightning guidance: wind, stability and moisture. These parameters were extracted from the 12Z radiosonde soundings from West Palm Beach and Miami, Florida. Days affected by synoptic disturbances and tropical cyclones were removed from the data set whereas atmospheric variables important to the formation of lake breezes and outflow boundaries were not considered (Shafer 2004). The end result was a statistical model produced and evaluated for the years 1989-2004 to predict where at least one lightning strike could occur during the convective season in Miami Dade and Broward Counties.

This project will verify the accuracy of the statistical model in predicting lightning strikes for the 2012 convective season over the land in South Florida. The observed lightning for the time period is obtained from the National Lightning Detection Network (NLDN) of Vaisala Inc., and compared with the guidance for verification ("National Lightning Detection Network"). The purpose of this study is to give forecasters at the Miami National Weather Service Office detailed information about the accuracy of the lightning model to increase the situational awareness of the

conditions favorable for active lightning in the region. This will help improve the convective forecasts. The forecasters will be presented with the meteorological analysis of the 2012 convective season describing the atmospheric conditions that were present for high number of lightning strike days and for days with few strikes.

2. METHODS

This section explains how the observed and forecast lightning information was collected and compared to each other as well as which data was used. Cloud to ground lightning observations are obtained from the NLDN run by Vaisala Inc., which contains a little over a hundred sensors across the United States. This network detects the cloud to ground lightning with the IMProved Accuracy from Combined Technology (IMPACT) method (Cummins et al. 1998; Shafer 2004). The observations are collected just for the South Florida region and adjacent waters, for the whole day from 00Z to 00Z from June 1st through September 30th, 2012. The total number of lightning strikes for the day was recorded.

2.1 Lightning Observations Maps

This section explains the reasoning for creating lightning maps. The KML file that contains detailed information about the lightning (the time of each strike, the multiplicity and if the strike is positive or negative) is utilized in the analysis. It needs to be noted that for June and July there was some missing data due to an issue in archiving the observations. June had five missing days of lightning data (June 1-5) and July had sixteen missing days of lightning data (July 1-16). The lightning maps were created to visually understand the accuracy of the model compared with the actual lightning that occurred for each active day in the convective season. The model data exists only for the land areas, therefore lightning observations over the ocean were removed when comparing lightning observations to the model lightning forecast. Lightning observation maps were created first to visually see where lightning occurred in comparison to the probabilities created by the model. The second maps were built from the first lightning observation maps, except instead of the observed lightning, the number of lightning strikes that occurred in each probability created by the model were displayed. This is to put a number on the visual observation map. Percentages were calculated to assess the accuracy of the model to the lightning that occurred. Lastly, lightning densities were calculated to account for the different areas of the probability ranges, which produce a more accurate verification of the model.

The KML file is converted into a layer in the ArcGIS 10 program. This allows for manipulation of a large data set into an organized image representing the lightning for each day. The symbology is changed to display the location of positive lightning strikes and negative lightning strikes in the South Florida region. The South Florida Forecast Zones shapefile is added to the data frame for spatial reference. The attribute tables of each KML files representing different days in the summer of 2012 is edited to maximize the information that can be displayed in the map.

The lightning guidance data comes from the Short Range Ensemble Forecast (SREF) model and for this project will only look at the probability of 1 or more cloud to ground lightning strikes in a three-hour period. The SREF was chosen to be verified due to a previous analysis comparing the accuracy of the different lightning models by the National Weather Service of Miami. That project assessed the accuracy of six different models by how well each of them predicted lightning from the 18 to 21Z time period during the 2012 convective season. The SREF performed the best over the other models. Therefore we chose the SREF for this study. The SREF guidance data is provided in a form compatible with ArcGIS 10. This project is to verify the day 1 forecast from the 15Z model run valid for the 15-18Z, 18-21Z, and 21-00 periods. For example, the 18Z model run includes the model valid time from 18-21Z. Each forecast time is valid for three hours prior to the forecast hour. The file is placed into ArcMap and the symbology is changed to display the probability of one or more strikes. The data is interpolated by an inverse distance weighted (IDW) interpolation to display the probabilities as a surface rather than gridded points. With both the observed lightning data and the guidance data in ArcMap, the process of verifying the guidance can

begin. The observed lightning layer is plotted to just include the forecast times in the guidance data. The observed lightning data layer for the correct times is placed over the interpolated guidance layer. From this, it is seen where the guidance lines up most with the observed lightning. Maps are made for each forecast time.

2.2 Total Number of Observed Lightning for each SREF Probability Maps

From the set up produced by creating the lightning observations map, a map for each forecast time is produced showing the number of lightning strikes that falls in each forecast probability range. The probabilities produced by the SREF model are arranged into the following ranges: 0-10%, 10-20%, 20-40%, 40-60%, and 60-80%. The data is joined with the observed lightning data to be able to quantitatively show how many strikes occurred in each probability range. This map is created for each forecast time for each day and displays a number in each probability range representing the lightning strike total for each range.

2.3 Percentages and Lightning Densities of Observed Lightning in Top Two Probability Ranges

The percentages that were created give a quantitative picture of how well the model did at predicting the observed lightning. The two probability ranges that are evaluated are only the top two for each time period, 15, 18 and 21Z. These percentages are calculated in ArcGIS by using the previously created map with the total number of lightning strikes per probability range. Starting with the 15Z period, the top probability range's total lightning is divided by the total number of lightning strikes for the whole time period. The second highest probability range's total lightning is divided by the total number of lightning strikes for the whole time period. This process is repeated for the other two time periods, 18 and 21Z.

The probabilities produced by the model make up different areas. For this reason the data was normalized to account for these different areas. Lightning densities were calculated for each time period and the top two probability ranges. The densities were created by taking the number of lightning strikes in the highest probability range and dividing it by the area, in square kilometers, of the highest probability range. The same was done for the second highest probability range.

2.4 Atmospheric Conditions Analysis

Along with verifying the guidance for the probability of lightning in the convective season of 2012 in South Florida, a meteorological analysis is also conducted. The analysis provides insight to the meteorological conditions present that favor the most active lightning days, compared with days with very little lightning activity. This includes observing the surface analysis plots from NOAA's Hydrometeorological Predication Center (HPC) for 21Z for each day, and the 500 mb mean temperature and geopotential heights for the day from NOAA's Earth System Research Laboratory (ESRL) daily mean composites, moisture and stability. The 00Z atmospheric sounding for each of the days is also analyzed. It should be noted that active days contain more moisture and instability. However, atmospheric conditions change frequently throughout the day. The convection towards the end of the convective season is less affected by other dynamics unlike in June. Select soundings for active and non-active days are displayed in Appendix J and K.

For each day in the summer of 2012 the 500 mb temperatures, interpolated freezing level and precipitable water are obtained from both the 12Z and 00Z atmospheric sounding. With this data each variable is averaged for the active days and for the non-active days and placed in table 4. The days in the summer with lightning data are plotted together in a bar graph as seen in figure 1. This graph shows each day and the number of lightning strikes that occurred during the day over land and adjacent waters. From this figure the active days are arbitrarily defined as days with greater than 2,000 strikes and the non-active days are defined as days with less than 2,000 strikes.

The Miami National Weather Service area forecast discussions (AFDs) are reviewed for each of the active days to rule out any days where lightning was produced by synoptic forcing. The only days to be considered are ones where the sea breeze is the main forcing mechanism behind the

lightning generation. Certain patterns are expected to come out of these area forecast discussions that will help narrow down certain weather patterns that lead to the most lightning or least lightning activity.

3. RESULTS AND DISCUSSION

There were 97 days in the convective season of 2012 with usable lightning data for this project. Of the 97 days with data, 31 of those days had greater than 2,000 strikes and were considered active days. There were seven active days in June, six days in July, thirteen in August and five in September. June had five missing days of lightning data (June 1-5) and three days, June 18, 19 and 26, with a record of zero strikes for the day. July had sixteen missing days of lightning data (July 1-16) and one day, July 25, with zero strikes. The day with the greatest number of lightning strikes for the 24-hour period was on June 15th with 8,972 strikes (Figure 1).

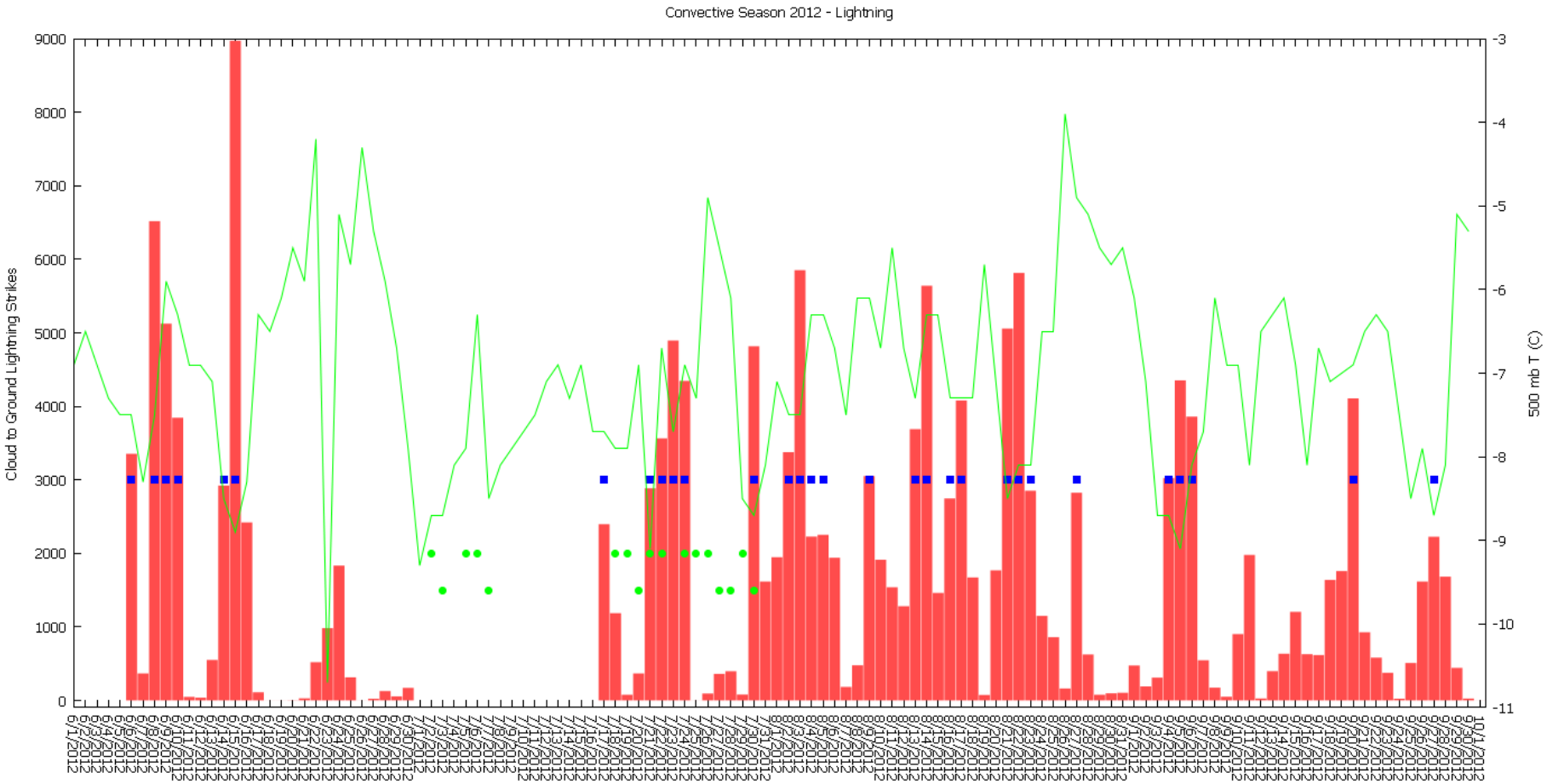

Figure 1. Plot of observed lightning over land and adjacent waters of South Florida for the whole convective season indicated by the orange bar graph with the green line depicting the 00Z 500 mb temperatures. The blue squares over the lightning represent the days with lightning strikes greater than 2,000 strikes. The green circles at the 2,000 level indicate a very high Saharan dust event and the green circles at 1,500 indicate a moderate Saharan Dust event. Note the Saharan dust data is only available for July

To assess the accuracy of the model, two maps were created: one showing the interpolated probabilities that at least one strike or more will occur within a 10-km radius of a point during a three hour period and the location of the observed lightning for the day, and another map showing the same interpolated probabilities with the number of lightning strikes that occurred within those interpolated probabilities. The maps for each active day in June, July, August and September can be found in Appendices A, B, C and D. Figure 2 is of June 15th, the most active day of the convective season. Figure 2a shows a map with all three time periods, 15Z, 18Z, and 21Z. This indicates that there was lightning activity present in all three time periods. This is not always the case for every active day as can be seen in the Appendix. The map on the left in Figure 2 visually represents where the observed lightning occurred during each time period depicted by blue minus signs for negatively charged lightning strikes and gray positive signs for positively charged lightning strikes. The colors represent the probabilities that were created by the SREF model to predict where lightning can occur. This map visually lets the viewer see if the observed lightning fell into the probability range that was highest indicating where lightning activity should occur. The map on the right in figure 2 has the same information present keeping the probabilities interpolated by the model, but removing the lightning positions and adding numbers in each colored polygon. The numbers represent the number of observed lightning strikes that occurred in each probability range (colored polygon). From this information, statistics of how well the model did at predicting the lightning activity are calculated
.

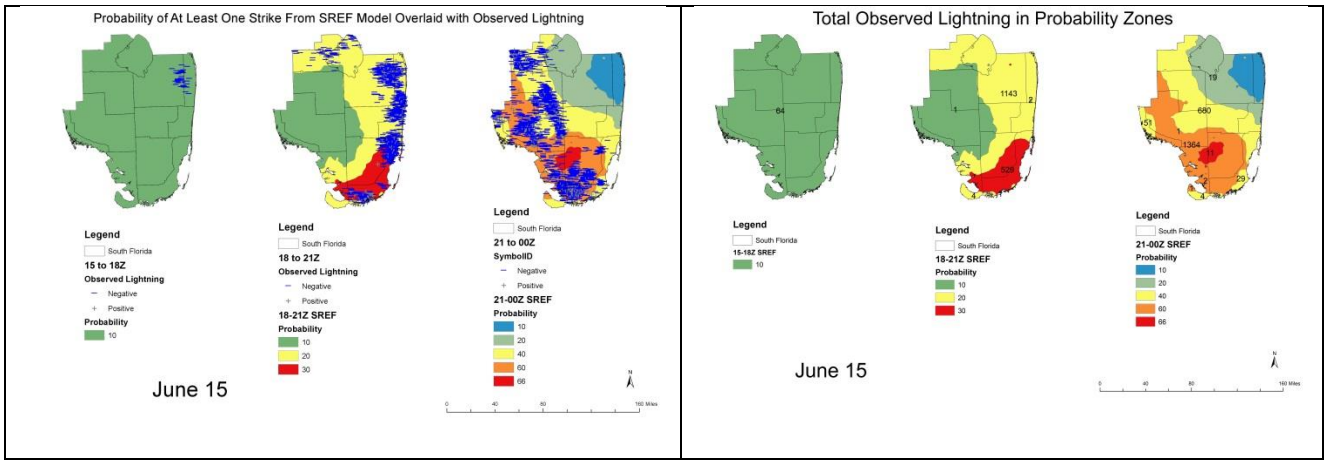

Figure 2. ArcGIS maps produced from analyzing the SREF model depicting on the left where the observed lightning occurred in respect to the model's predictions for each time period, 15Z, 18Z and 21Z and on the right how many lightning strikes occurred in each probability range for each time period, 15Z, 18Z and 21Z. In figure a) the observed lightning is represented by blue minus signs for negatively charged and gray positive signs for positively charged lightning and the probabilities are represented by colored polygons. In figure b) the probabilities remain the same represented as colored polygons and the numbers represent the number of observed lightning strikes that occurred for each probability zones

Quantitative results derived from the verification maps are shown in tables 1-3. Table 1 represents all data from the 15Z time period (15Z-18Z). The days that had lightning strikes during this time period are listed and each is given a percentage based on how many lightning strikes out of the total for the time period occurred in the highest probability range and the second highest probability range as well as the lightning densities for the two probability ranges. These probability ranges can be explained using figure 2. It should be noted that both maps have the same probabilities for the day, as there were no changes made to the model. As stated in the methods, the probabilities are arranged into the following ranges for every single active day: 0-10%, 10-20%, 20-40%, 40-60% and 60-80%. In figure 2 for 15Z, there is only one probability, 10. This 10 indicates the probability range from 0-10%. During the 18Z time period for June 15th (figure 2) the model produced probabilities 10, 20 and 30. This corresponds to the probability ranges of 0-10%, 10-20% and 20-30%. The reason 30% is not 40 as indicated in our arrangement of the ranges is because the probabilities produced by the model for that time period did not exceed 30%. For the 18Z time period the top probability range is 20-30% and the second highest probability range is 10-20%. It should be noted the different areas of each probability range. The top probability range has a smaller area than that of the second highest probability range. The 21Z time period for June 15th (figure 2) had model probabilities of 10, 20, 40, 60, and 66. This corresponds to the probability ranges of 0-10%, 10-20%, 20-40%, 40-60% and 60-66%. The highest probability range for this time period would be 60-66% and the second highest probability range would be 40-60%. Analyzing the probability ranges again, it is evident that the highest probability range's area is quite small compared to the second highest probability range. This occurs for almost every active day shown in appendices A-D.

.

The lightning densities were created to account for the differences in the areas of the top two probability ranges. The values are found in the same table (table 2). By doing the lightning densities, 10 out of the 19 days (53%), had the highest probability range predict the greatest number of lightning strikes. The second highest probability range only predicted 47% of all the lightning in the 15Z time period for all 19 days. To continue to analyze June 15th, the percentages for 15Z were not included in table 1 because there was only one probability range and the model predicted this probability for all of South Florida. Therefore there would be no comparison of the highest and second highest probability ranges as there was only one range

Date	Highest Probability Range (%)	Lightning Density for Highest Range (strikes/km^2)	Second Highest Probability Range (%)	Lightning Density for Second Highest Range (strikes/km^2)
June 8	21.40	0.158	78.20	0.115
July 17	28.51	0.072	63.21	0.012
July 22	49.50	0.031	49.40	0.038
July 23	0.00	0.00	14.20	0.006
July 24	0.00	0.00	100.0	0.001
July 30	28.30	0.011	71.70	0.004
August 3	35.40	0.483	43.60	0.223
August 5	9.62	0.003	90.40	0.004
August 9	0.00	0.00	100.00	0.00004
August 13	88.00	0.002	12.00	0.0001
August 14	29.50	0.016	70.20	0.014
August 16	50.30	0.067	46.30	0.027
August 17	16.10	0.004	83.90	0.001
August 22	0.00	0.00	100.00	0.002
August 27	70.00	0.057	30.00	0.007
September 4	0.00	0.00	75.00	0.003
September 6	27.20	0.032	39.00	0.012
September 20	0.00	0.00	25.30	0.002
September 27	1.18	0.014	74.00	0.015
Total	21.10	53%	78.95	47 %

Table 1. Lightning densities calculated for the highest and second highest probability ranges to account for the different areas of each probability range during the 15Z time period. Percentages were also calculated of the lightning falling in the highest probability range or the second highest probability range interpolated from the SREF statistical model

Time Period	Number of Days (out of 31)
15Z	19
18Z	30
21Z	28

Table 2. Table of the number of active days per time period

Table 3 refers to the active days with lightning that occurred during the 18Z time period (18Z-21Z). There are 30 out of the 31 active days that had lightning occur in the 18Z time period (table 2). Accounting for the differences in areas by calculating the lightning densities (table 3), the highest probability range predicted the greatest number of lightning strikes at 67% for the 30 days with lightning during the 18Z time period, whereas the second highest probability range only predicted 33%. Now analyzing the lightning densities for June 15th, the lightning density for the highest probability range was 0.173 strikes/km^2 whereas the lightning density for the second highest probability range was 0.082 strikes/km^2

.

Date	Highest Probability Range (%)	Lightning Density for Highest Range (strikes/km^2)	Second Highest Probability Range (%)	Lightning Density for Second Highest Range (strikes/km^2)
June 6	92.30	0.022	7.69	0.0002
June 8	34.90	0.103	60.50	0.035
June 9	19.20	0.025	80.60	0.096
June 10	97.60	0.129	2.40	0.001
June 14	0.00	0.00	15.00	0.0002
June 15	31.30	0.173	68.00	0.082
June 16	72.60	0.008	22.60	0.004
July 17	12.20	0.0111	43.68	0.0114
July 21	0.00	0.00	97.20	0.057
July 22	39.10	0.011	35.10	0.007
July 23	2.80	0.047	88.80	0.073
July 24	3.60	0.033	76.80	0.084
July 30	22.50	0.036	45.20	0.035
August 2	11.10	0.019	88.70	0.066
August 3	40.20	0.130	42.60	0.047
August 4	69.30	0.025	30.50	0.015
August 5	44.50	0.063	52.00	0.021
August 9	4.40	0.023	87.80	0.005
August 13	21.70	0.089	73.70	0.042
August 14	64.40	0.063	35.50	0.037
August 16	34.00	0.051	57.40	0.029
August 17	25.20	0.082	61.00	0.030
August 21	0.11	0.064	61.10	0.084
August 22	0.00	0.102	51.10	0.040
August 23	16.20	0.056	83.80	0.034
September 4	0.00	0.00	0.81	0.001
September 5	0.00	0.00	64.10	0.089
September 6	16.00	0.166	69.00	0.102
September 20	16.90	0.216	76.40	0.084
September 27	1.14	0.065	17.00	0.052
Total	80.00	67%	20.00	33%

Table 3. Lightning densities calculated for the highest and second highest probability ranges to account for the different areas of each probability range during the 18Z time period. Percentages were also calculated of the lightning falling in the highest probability range or the second highest probability range interpolated from the SREF statistical model

Table 4 represents the active days that had lightning strikes during the 21Z time period (21Z-00Z). There are 28 of the 31 active days with lightning activity during the 21Z time period (table 2). The lightning densities for the 21Z time period are also presented in table 4 to account for the differences in area. There were 16 out of the 28 days (57%) that had the lightning density of the highest probability range predict the greatest number of lightning strikes. The lightning densities for the second highest probability range only predicted 43% of the lightning strikes for the 28 days that had lightning during the 21Z time period. The lightning density for the highest probability range on June 15th was 0.017 strikes/km^2 whereas the lightning density for the second highest probability range was 0.157 strikes/km^2. In this case, June 15th at 21Z was one of the 12 days where the lightning density for the second highest probability range was greater than that of the highest probability range

.

Date	Highest Probability Range (%)	Lightning Density for Highest Range (strikes/km^2)	Second Highest Probability Range (%)	Lightning Density for Second Highest Range (strikes/km^2)
June 8	14.80	0.032	65.80	0.049
June 9	14.40	0.152	69.80	0.063
June 10	68.90	0.062	30.20	0.010
June 14	7.21	0.093	91.70	0.079
June 15	0.59	0.017	63.10	0.157
June 16	51.70	0.010	48.30	0.003
July 17	59.20	0.035	40.85	0.004
July 21	0.30	0.00	68.20	0.053
July 23	88.30	0.091	11.70	0.019
July 24	88.50	0.096	11.50	0.029
July 30	5.80	0.078	54.10	0.127
August 2	21.30	0.066	33.90	0.057
August 3	98.00	0.009	1.96	0.0001
August 4	52.40	0.121	43.30	0.085
August 5	19.30	0.005	9.20	0.002
August 9	2.01	0.116	89.70	0.197
August 13	55.80	0.163	43.30	0.064
August 14	54.70	0.045	44.80	0.023
August 16	18.40	0.003	81.60	0.004
August 17	58.30	0.222	41.30	0.063
August 21	0.00	0.00	25.90	0.104
August 22	70.70	0.429	29.30	0.040
August 23	0.19	0.010	12.40	0.062
September 4	2.40	0.021	20.60	0.044
September 5	0.00	0.00	8.04	0.021
September 6	39.30	0.022	53.40	0.009
September 20	39.80	0.028	46.90	0.018
September 27	37.10	0.021	61.10	0.011
Total	42.86	57 %	57.14	43 %

Table 4. Lightning densities calculated for the highest and second highest probability ranges to account for the different areas of each probability range during the 21Z time period. Percentages were also calculated of the lightning falling in the highest probability range or the second highest probability range interpolated from the SREF statistical model

From this analysis of the statistical model, for the 2012 convective season, the highest probability range predicted the majority of the lightning that was observed over the second highest probability range. Interpreting the maps that were created (Appendices A-D) the highest probability ranges seemed to be small specific areas. By normalizing the data into lightning densities, the highest probability range predicted the greatest number of lightning strikes by accounting for the differences in the areas. To conclude, the model predicted 53% of all the lightning in the highest probability range for 15Z, 67% of all the lightning for 18Z, and 57% of all the lightning for 21Z in the highest probability range indicating that the model was able to predict the general area where lightning was observed for the 2012 convective season.

To assess the atmospheric conditions that were present during the active days and the 12Z and 00Z 500mb temperature, freezing level and precipitable water were analyzed. Table 5 includes 500 mb temperatures, freezing levels and precipitable water for both the active and the non-active days at 00 and 12Z. The variables freezing level and precipitable water have very little variability from active to non-active days. Even though there is some correlation (R^2 = 0.2) between the freezing level and 500 mb temperatures, the colder the 500 mb temperatures the more unstable the atmosphere will be, which will allow for clouds to grow vertically above the freezing level. For example, in South Florida, the average freezing level height is 4,439 m and the average 500 mb temperatures height is 5,500 m. When the freezing level is colder the cloud has the opportunity to grow more effectively. In this case this corresponds to 1,000 m of the cloud located in the mixed phase which is known to enhance lightning.

Month	12Z 500mb Temperature (C)	00Z 500mb Temperature (C)	12Z Freezing Level (ft)	00Z Freezing Level (ft)	12Z Precipitable Water (in)	00Z Precipitable Water (in)
JUNE						
Active (7)	-8.2	-7.6	14743.4	14648.5	1.77	1.82
Non-Active (15)	-6.7	-6.6	15343.0	15491.8	1.87	1.88
JULY						
Active (6)	-7.9	-7.8	14803.4	14808.4	1.94	1.98
Non-Active (8)	-7.1	-7.0	15433.3	15427.1	1.54	1.65
AUGUST						
Active (13)	-6.9	-7.0	14738.0	15388.1	1.96	2.03
Non-Active (18)	-6.5	-6.2	15587.0	15538.4	1.92	2.02
SEPTEMBER						
Active (5)	-9.2	-8.3	14476.7	14179.1	1.90	2.07
Non-Active (25)	-6.7	-6.7	14663.4	14801.7	1.84	2.00

Table 5. A table of 12 and 00Z 500 mb temperatures, freezing level, and precipitable water from atmospheric soundings for the active days and non-active days. The number of active and non-active days is noted for each month in parenthesizes

Figure 1 includes the 500 mb temperatures for 00Z represented by the green line. The 12Z 500 mb temperatures were compared to 00Z and found to have the same trends with minor differences; therefore, only the 00Z 500 mb temperatures are displayed in figure 1. From visual analysis of figure 1 there are highs and lows in the lightning activity grouped together and for most of the days the dips/highs in the 500 mb temperatures correlate to increased/decreased lightning activity. It should be noted from figure 1 that when the 500 mb temperatures reach -6 degrees C lightning is actually suppressed. The days for which this was an exception are explained later on. From this figure, days with greater than 2,000 strikes were considered to be active. To better understand the active days and what atmospheric set up allowed for the high activity the average 500 mb temperature for each day were produced from NOAA's Earth System Research Laboratory (ESRL) reanalysis. Lightning is enhanced when the mid-levels cool, bringing in instability that allows for convective initiation and stronger updrafts. Another variable that is important and needs to be present when the mid-levels cool is sufficient moisture. Analysis of the 500 mb temperature maps shows trends in the geographic distribution of the mid-levels. The cooler mid-levels are found to increase lightning activity on days conducive for sea breeze formation. The mechanism by which this occurs is that when the mid-levels are cooler and there is low level convergence due to the sea breeze, the difference in temperature between the surface and mid-levels increase instability allowing for an active lightning day. Along with these maps a corresponding 21Z surface map was included. After pointing out specific features the AFD for the day was analyzed to add and verify the features. The analysis of the active days for the whole convective season is presented in Appendices F, G, H and I

.

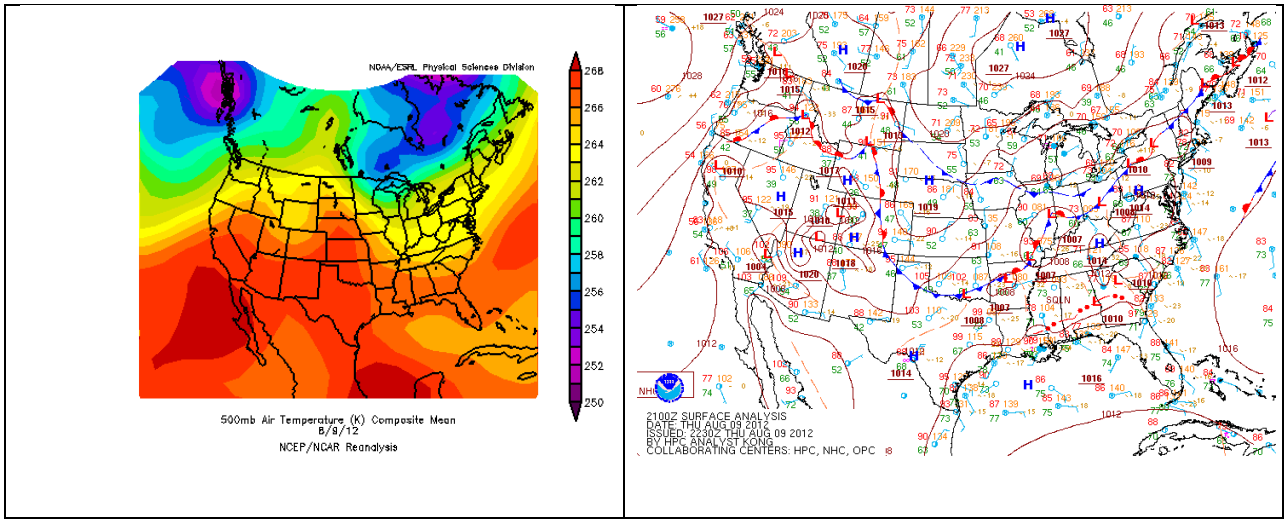

Figure 3. The two figures are of the synoptic set-up for August 9 with the image on the left being a reanalysis map from NOAA's Earth System Research Laboratory (ESRL) daily mean composites of the 500 mb temperatures and the image on the right being a surface analysis map for 21Z from NOAA's Hydrometeorological Predication Center (HPC)

An analysis of August 9th is presented in figure 3 with the mean 500 mb temperatures in figure 3a and the 21Z surface analysis in figure 3b. August 9th had 3050 lightning strikes for the day and is considered an active day. The mean 500 mb temperatures indicate an area of higher temperatures across the central United States with a trough of lower temperatures in the Northeast. A day in June with this same general synoptic pattern is June 8th. For July, the 23rd mean 500 mb temperatures indicate lower temperatures in the Northeast and warmer temperatures across the central United States. In September the pattern is a bit more northward but follows the same general synoptic set-up. September 5th has lower temperatures across the northern portion of the country and warmer temperatures across the southern portion of the country. This set-up can be found in all of the active days in Appendices F-I. Another feature that is found in some active days is a cold pool just south of South Florida. This feature is present in figure 3a but not as strong as other days. This cold pool tends to be present in most of the active days in September. For August 9th the AFD states that dry air was located over the Bahamas and expected to be travelling towards the forecast area due to deep ridging over central Florida. The storm activity was expected to occur by diurnal heating and collision of sea breeze fronts.

Investigating the highs and lows in the 500 mb temperatures in figure 1 and figure 4 is important to understand why lightning occurred and why it did not. Generally speaking, over the month of June there is strong variability in the 500 mb temperatures with lightning dependent on the 500 mb temperature, but as the season progresses, the variability becomes small and less dependent on the 500 mb temperature according to figure 1. From NOAA's Earth System Research Laboratory (ESRL) reanalysis of the 500 mb temperature monthly mean from 1981 to 2010 was created as a reference to use in investigating figure 1. These climatologies can be found in Appendix E. The June 500mb temperature climatology indicates a 500 mb temperature of about -7 to -8 degrees C. The July 500 mb temperature climatology from the reanalysis shows a temperature of about -7 to -8 degrees C. The August 500 mb temperature climatology indicates a temperature of about -6 to -7 degrees C. The September 500 mb temperature climatology indicates a temperature of about -6 to -7 degrees C. The climatology of 500 mb temperatures shows that temperatures increase as the summer progresses

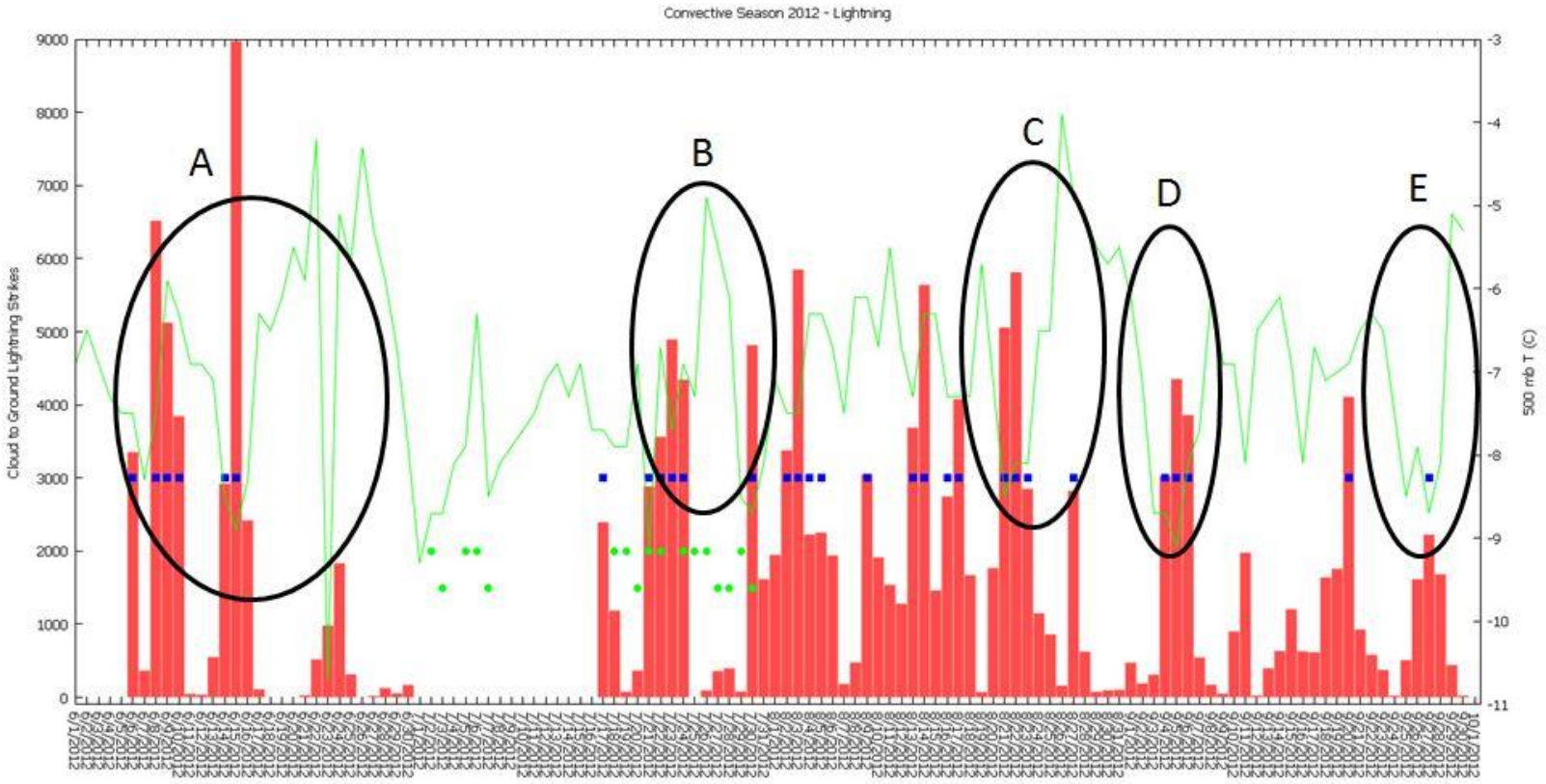

Figure 4. Plot of observed lightning over land and adjacent waters of South Florida for the whole convective season indicated by the orange bar graph with the green line depicting the 00Z 500 mb temperatures. The blue squares over the lightning represent the days with lightning strikes greater than 2,000 strikes. The green circles at the 2,000 level indicate a very high Saharan Dust event and the green circles at 1,500 indicate a moderate Saharan dust event. Note the Saharan dust data is only available for July. The circles A, B, C, D, and E indicate areas to be analyzed

Beginning with the month of June, analyzing figure 4, oval A, there is a dip in 500 mb temperatures at June 7th with only 365 strikes. It is indicated in the AFD that mostly cloudy skies were expected due to a frontal boundary to the north of the forecast area which would keep activity, especially from diurnal heating, at a minimum. The mostly cloudy skies allow for an increase in stability in the lower levels inhibiting convective initiation. The next area of concern in oval A in figure 4 for the active days is June 9th and 10th where 500 mb temperatures were relatively warm. Both days had abundant moisture and ability for the sea breezes to initiate convection but the wind speed on June 10th found on the 21Z surface analysis plot in Appendix F is about 15 knots. Strong wind speeds will inhibit the sea breezes from becoming well developed to initiate convection. The next dip in the 500 mb temperatures in figure 4, oval A corresponds to the most active day in the season June 15th and then an increase in temperature with a decrease in activity until a major drop in the 500 mb temperatures on June 23rd. June 23rd recorded 980 lightning strikes. The AFD states there is abundant moisture from the southerly flow but mentions mostly cloudy skies over the forecast area for the afternoon. The beginnings of tropical storm Debby were located in the eastern Gulf of Mexico and from satellite analysis indicated that the location of tropical storm Debbie kept the forecast area under cloudy skies during the day of June 23rd. Typically tropical cyclones warm the mid-levels due to their warm core characteristics. The decrease in 500 mb temperatures associated with this day was just a small pocket of cold air associated with the tropical storm to enhance lightning activity. Even though the 500 mb temperatures were low and near that of the most active day, June 15th, the conditions did not allow for any significant activity to occur. The rest of the month saw an increase in 500 mb temperatures and decrease in lightning activity after tropical storm Debby moved through bringing dry air into the forecast area.

The month of July is interesting because the National Weather Service of Miami analyzed the Saharan dust events that affected the forecast area in the month of July 2012. Analyzing figure 4 oval B, warmer temperatures correspond to a decrease in lightning activity and cooler temperatures correspond to an increase in lightning activity. July 29th was a day depicting a dip in the 500 mb temperatures. This day produced only 78 lightning strikes. From analysis of the 850-500 mb relative humidity (RH) map at 12 and 00Z for this day there is significant dry air present (Appendix L). This knowledge can be related to the dust events that occurred and were recorded for the month of July (figure 5) as July 29th was a day during a dust event. Table 6 relates these dust events to the amount of lightning that occurred the day before the event, the days during the event and the day after the event. Dust could affect the number and updraft strength in thunderstorms, possibly causing more updrafts during a dust event (Susan et al. 2009; Estupiñán et al 2012). At the leading edge of the dust airmass, an existing airmass with ample moisture is still present over the area. The combination of this existing moisture with the possibility of increased updrafts, as found by Susan et al. 2009, could be a possible explanation for the increased lightning activity at the interface of the two airmasses. From the results in table 5, lightning activity is increased the day before an event and the day after. It should be noted that dust was found in small amounts on the 27th and 28th which could be why the lightning activity was not as intense as other days before or after the event.

The month of August has very little variability in the change of 500 mb temperatures as indicated in figures 1 and 4. This month was the most active with 13 out of the 31 days being considered active, and only 9 days with lightning less than 1,000 strikes. August 20th was a non-active day with one of the only notable dips in the 500 mb temperatures for August found in figure 4, oval C. The moisture content was analyzed by the 850-500 mb relative humidity map and the 850 mb wind map found in Appendix L. The AFD stated a subtropical ridge was over the forecast area with a frontal boundary to the north and any activity would be diurnal, forced by sea breezes. The 850-500 mb moisture map indicated a dry patch of air

to the east of South Florida at 12Z with some moisture but nothing ideal for convective initiation .

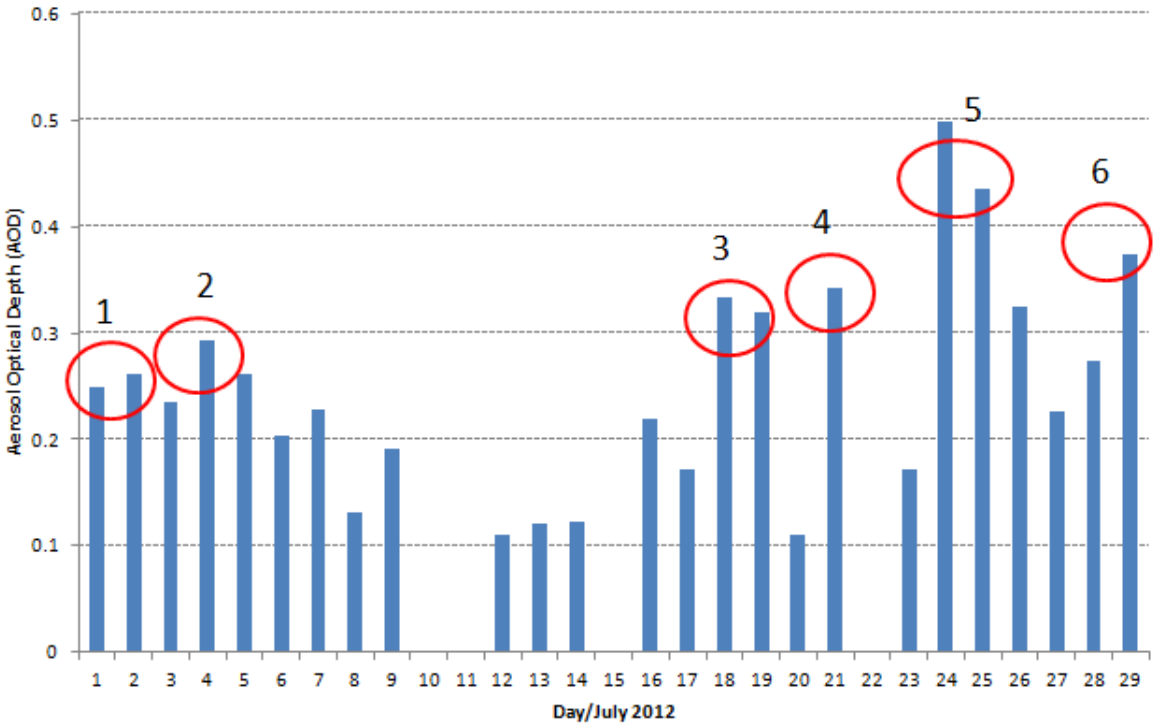

Figure 5. The plot is of July 2012 plotted with aerosol optical depth to indicate when the Saharan Dust events occurred. Red circles and corresponding numbers above indicate a Saharan dust event (Estupiñán et al 2012)

Event Number	Time Frame of Dust Event	Number of Strikes-Day Before	Number of Strikes-Days During	Number of Strikes-Day After
3	18^{th}- 20^{th}	17^{th}- 2396	18^{th}-1185 19^{th}-75 20^{th}- 364	21^{st}- 2884
4	21^{st}- morning of 22^{nd}	20^{th}- 364	21^{st}-2884 22^{nd}- 3563	23^{rd}- 4894
5	24^{th}- 26^{th}	23^{rd}- 4894	24^{th}-4345 25^{th}-0 26^{th}- 93	27^{th}- 359
6	29^{th}- 30^{th}	28^{th}- 395	29^{th}-78 30^{th}- 4817	31^{st}- 1615

Table 6. Days in July affected by the Saharan dust events and the associated number of lightning strikes for each day before, during and after

The winds from the 850 wind map indicate that it would advect high moisture into the area by August 21st at 00Z and push out that dry patch. To conclude on the lack of activity the ideal moisture was not able to make it into the air until early evening. The one notable active day with increased lightning but very warm 500 mb temperatures was August 27th (figure 4, oval C). Tropical Storm Isaac was located in the eastern Gulf of Mexico during this day and was, according to the AFD, continuing to bring outer rain bands to the forecast area. With widespread clouds it can decrease significantly the convection initialization over the local area and reduce lightning activity by keeping the land from heating up during the day. This does not allow for a sufficient temperature gradient between the ocean temperature and the land temperature producing a weak to non-existent sea breeze front.

September had more variation in changes in the 500 mb temperatures than August but corresponded to the same pattern seen for the other months (figures 1, 4). The pattern is when the temperatures increase there is a lack or decrease in lightning activity and when the 500 mb temperatures decrease there is an increase in activity. The biggest increase in temperatures is at the beginning of the month with little activity. Shortly after the increase in temperatures, the 500 mb temperatures decrease and activity sharply increases (figure 4, oval D). The end of the month has a sharp decrease in 500 mb temperatures in oval E where investigation of the moisture content in Appendix L indicates significant levels of moisture to aid in convective initiation. The AFD stated for the 27th (an active day) that a mid to upper level shortwave in the area would help to enhance convection created by the sea breeze with a mid to upper level low located over the eastern Gulf of Mexico on the 28th that was expected to either enhance or bring subsidence into the forecast area. After this dip in temperatures, it rises again at the end of the month with very little activity.

4. CONCLUSIONS

The convective season of 2012 and associated observed lightning was used to verify the statistical model created by Philip Shafer used to predict where lightning can occur. The 15Z model cycle was used for the verification. The valid times verified were the 15, 18 and 21Z for day one. Two different lightning maps were created to visually show how well the observed lightning matched up with the probability of lightning that can occur from the model. Percentages and lightning densities were produced to analyze the accuracy of the model to the observed lightning in the top two probability ranges. Certain atmospheric conditions, 500 mb temperatures, stability, moisture, and synoptic features, were analyzed to determine what conditions lead to an enhancement or decrease in lightning activity.

The following are the main conclusions:

(1) The forecast lightning is verified with the Vaisala lightning data over the land only. By analyzing the model by lightning densities, it was found that the different areas of the probability ranges did matter in verifying the models' accuracy. The model predicted 53% of all the lightning in the highest probability range for 15Z, 67% of all the lightning for 18Z, and 57% of all the lightning for 21Z in the highest probability range indicating that the model was able to predict the general area where lightning was observed for the 2012 convective season.

(2) The changes in the 500 mb temperatures were examined in figures 1and 4 as it correlated with a relative increase or decrease in the lightning activity over South Florida and adjacent waters. Diagnosing the 500 mb temperatures alone is not enough to explain why lightning occurred on certain days over days where little activity occurred, as there are many variables to consider. The 500 mb temperature

conveys the overall trend well but it does not explain the entire physical process. A decrease in 500 mb temperatures does not necessarily correlate to an increase in lightning activity if there is not sufficient moisture available or the surface wind speeds are too strong to allow for intensification of sea breeze fronts. Another inhibiting factor would be significant cloud cover decreasing the amount of lightning developed over land during the day.

(3) It was found that lower pressure across the northeastern United States and higher pressure in the central United States at the mid-levels helps to funnel in colder air into South Florida to bring instability in the middle atmosphere to help initiate thunderstorm activity. Increases in lightning activity were also noted with mid-level cutoff lows around the Florida peninsula.

(4) From the small amount of Saharan dust data in July, a conclusion was made based on the amount of lightning that occurred during the dust events. Lightning activity tends to increase before the dust arrives and right after the dust event is over. It is possible that the combination of the dust and the dry air associated with it combined with the moisture still present along the leading edge of the dust could be enhancing the lightning activity.

(5) Tropical cyclones that brushed by South Florida in 2012, Debbie and Isaac, brought significant cloud cover over the area and brought in dry air behind each storm and limited activity. As stated prior, cloud cover diminishes vigorous daytime convection over the land therefore decreasing the overall lightning activity.

(6) It should be noted that this was a study of only one convective season that examined trends in 500 mb temperatures along with variables like moisture and stability that are of use to operational meteorology. Future work would include adding more convective years to the study, and investigating further the relationship between Saharan dust and lightning activity. The lightning data that was obtained was for a 24 hour period. Another question that could be investigated would be if the cooling of the mid-levels increases the number of hours lightning activity occurs in South Florida. A more detailed analysis of other variables possibly affecting lightning can be investigated in the future (e.g. upper level divergence, low level convergence, vorticity maxima, etc.).

The results will allow forecasters in the South Florida Forecast Office to increase their knowledge on the atmospheric conditions suitable for lightning and provide a better understanding of the model and how it performs in predicting lightning. Small changes in the 500 mb temperatures can have a significant effect in the overall lightning activity expected on a given day. The combination of cool 500 mb temperatures with a moist airmass at the leading edge of a Saharan air mass can lead to increases in lightning activity in South Florida. The images presented in the appendices of this paper will help the Miami forecasters identify the days with the greatest potential of active lightning.

Acknowledgements

I would like to first and foremost thank my advisor and mentor, Jeral Estupinan for all his guidance and support during this project. He has taken his time to aid me in analyzing my data, suggesting ways to improve the project, listening to my ideas, and trusting me to use GIS to present my findings.

Thank you to the Miami National Weather Service Office for allowing me to intern at your facility. I cannot thank the meteorologists enough for allowing me to ask questions and experience the everyday life of a weather forecaster as I have learned an abundance of information I would not have in a classroom.

I would like to thank my remaining committee members, David Nolan and Paquita Zuidema for their time, continued support, and expert advice.

I am grateful to Phil Shafer for allowing me to analyze and assess the model he created. Thank you for enabling me to utilize the observed lightning data and taking the time to help me to sort out the files so they were compatible with ArcGIS.

I want to express my gratitude to Maria Estenvez for her patience and time given to me to help me work through and figure out ways to make this project work using ArcGIS. I could not have finished this project without your expertise in GIS and your continued suggestions to improve my project.

5. *References Cited*

Arritt, R. W., 1993: Effects of the Large-Scale Flow on Characteristic Features of the Sea Breeze. *J. Appl. Meteor. Climatol.*, **32,** 116-125.

Cummins, K. L., M. J. Murphy, E. A. Bardo, W. L. Hiscox, R. B. Pyle, and A. E. Pifer, 1998: A Combined TOA/MDF Technology Upgrade of the U.S. National Lightning Detection Network. *J. Geophys. Res.*, **103,** 9035-9044.

Earth System Research Laboratory, cited 2013: Daily Mean Composites. [http://www.esrl.noaa.gov/psd/data/composites/day/.]

Estupiñán, J.E., Dan Gregoria, Roberto Arias, and K. Voss, 2012: Characteristics of the Saharan Dust Events of July 2012 at Miami Florida: Aerosol Physical Characteristics and Vertical Distribution - Presentation, 2012 SPoRT / NWS Partners Virtual Workshop.

Lericos, T. P., H. E. Fuelberg, A. I. Watson, and R. L. Holle, 2002: Warm Season Lightning Distributions over the Florida Peninsula as Related to Synoptic Patterns. *Wea. Forecasting*, **17**, 83-98.

Infoplease, cited 2013: Lightning Deaths 1998-2008. [http://www.infoplease.com/science/weather/lightning-deaths.html.]

National Weather Service, cited 2013: Lightning Safety. [http://www.lightningsafety.noaa.gov/fatalities.htm.]

López, R. E., and R. L. Holle, 1987: The Distribution of Summertime Lightning as a Function of Low-Level Wind Flow in Central Florida. NOAA Tech. Memo. ERL ESG-28, National Severe Storms Laboratory, Norman, OK, 43 pp.

Vaisala, cited 2013: National Lightning Detection Network. [http://www.vaisala.com/en/products/thunderstormandlightningdetectionsystems/Pages/NLDN.aspx.]

Vaisala, cited 2013: North American Lightning Detection Network. [http://www.vaisala.com/Vaisala%20Documents/Brochures%20and%20Datasheets/0537_2011%20WCO-WEN%20Lightning%20Map.pdf.]

Shafer, Phillip E., 2007: Developing Statistical Guidance for Forecasting the Amount of Warm Season Afternoon and Evening Lightning in South Florida. Dissertation, Florida State University, 87 pp.

Simpson, J. E., 1994: *Sea Breeze and Local Wind.* Cambridge University Press, 234 pp.

Susan C. van den Heever, Gustavo G. Carrio, William R. Cotton, Paul J. DeMott and Anthony J. Prenni, 2009: Saharan dust particles nucleate droplets in eastern Atlantic Cloud. *Geophys. Res. Lett.*, **36**, doi:10.1029/2008GL035846.

Unisys Weather, cited 2013: Image and Map Archive. [http://weather.unisys.com/archive/eta_init/.]

Weather Prediction Center, cited 2013: WPC's Surface Analysis Archive.

[http://www.hpc.ncep.noaa.gov/html/sfc_archive.shtml.]

Wexler, R., 1946: Theory and Observations of Land and Sea Breezes. *Bull. Amer. Meteor. Soc.*, **27,** 272-287.

]

Wyoming Weather Web, cited 2013: Atmospheric Soundings. [http://weather.uwyo.edu/upperair/sounding.html.

Appendix

Appendix A. June Lightning Maps

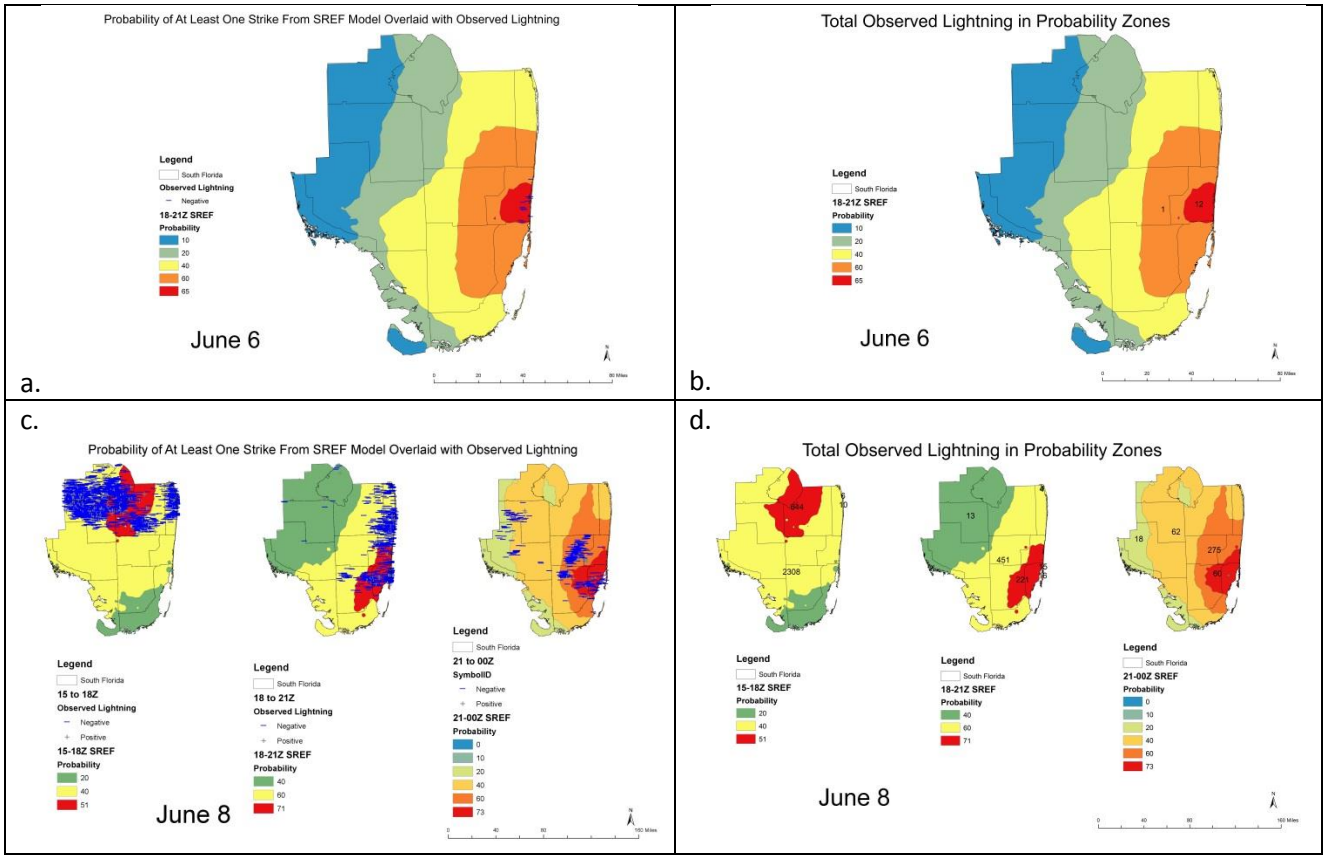

e.

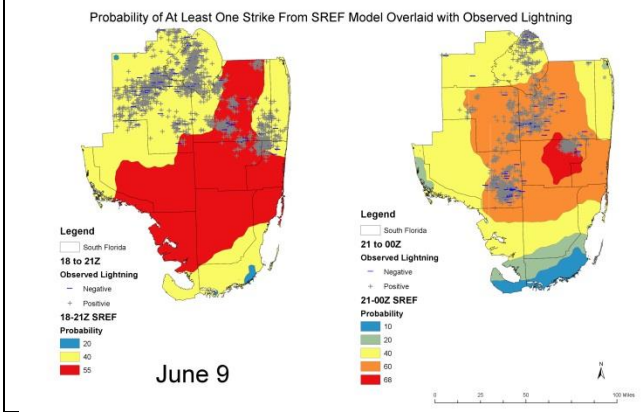
Probability of At Least One Strike From SREF Model Overlaid with Observed Lightning
Legend
South Florida
18 to 21Z
Observed Lightning
Negative
Positive
18-21Z SREF
Probability
20
40
55
Legend
South Florida
21 to 00Z
Observed Lightning
Negative
Positive
21-00Z SREF
Probability
10
20
40
60
68
June 9

f.

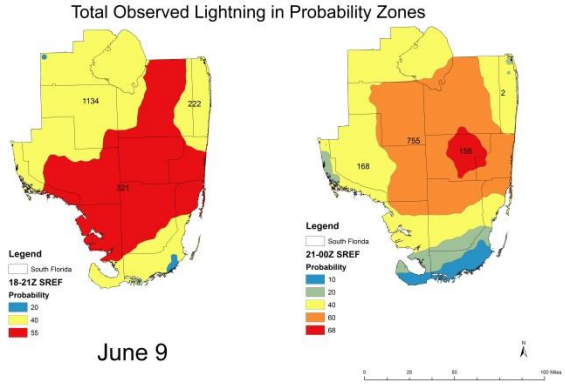
Total Observed Lightning in Probability Zones
1134
222
321
2
755
156
168
Legend
South Florida
18-21Z SREF
Probability
20
40
55
Legend
South Florida
21-00Z SREF
Probability
10
20
40
60
68
June 9

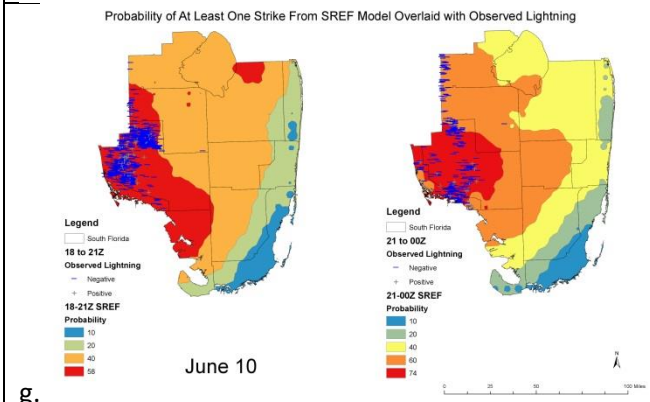
Probability of At Least One Strike From SREF Model Overlaid with Observed Lightning
Legend
South Florida
18 to 21Z
Observed Lightning
Negative
Positive
18-21Z SREF
Probability
10
20
40
58
Legend
South Florida
21 to 00Z
Observed Lightning
Negative
Positive
21-00Z SREF
Probability
10
20
40
60
74
June 10

g.

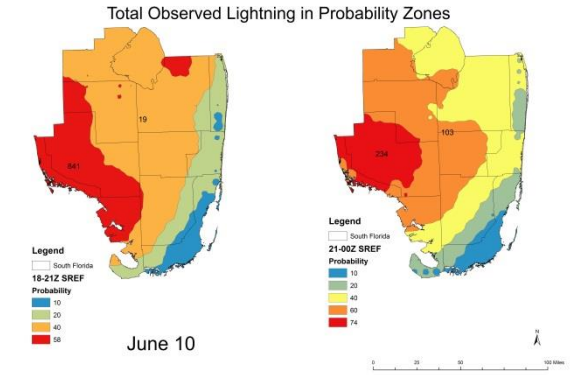
Total Observed Lightning in Probability Zones
19
841
103
234
Legend
South Florida
18-21Z SREF
Probability
10
20
40
58
Legend
South Florida
21-00Z SREF
Probability
10
20
40
60
74
June 10

h.

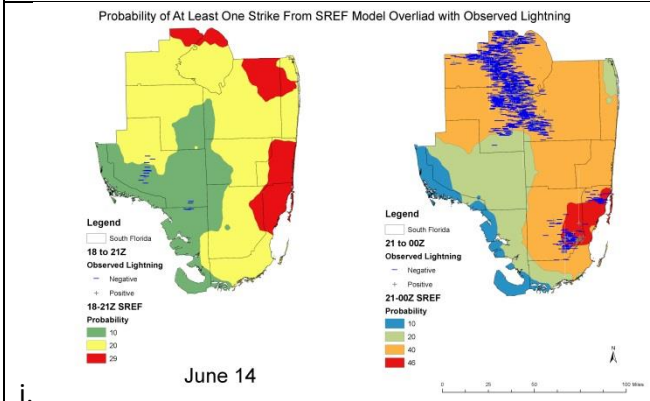
Probability of At Least One Strike From SREF Model Overliad with Observed Lightning
Legend
South Florida
18 to 21Z
Observed Lightning
Negative
Positive
18-21Z SREF
Probability
10
20
29
Legend
South Florida
21 to 00Z
Observed Lightning
Negative
Positive
21-00Z SREF
Probability
10
20
40
46
June 14

i.

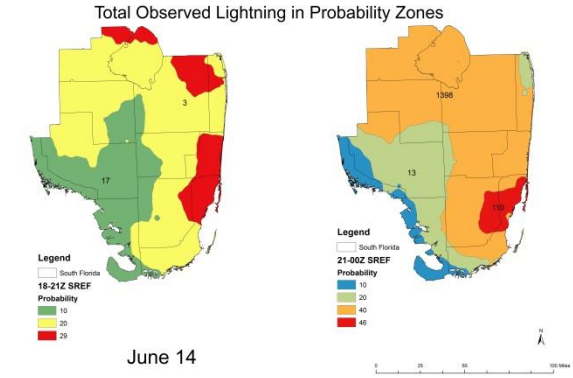
Total Observed Lightning in Probability Zones
3
17
1398
13
110
Legend
South Florida
18-21Z SREF
Probability
10
20
29
Legend
South Florida
21-00Z SREF
Probability
10
20
40
46
June 14

j.

k.

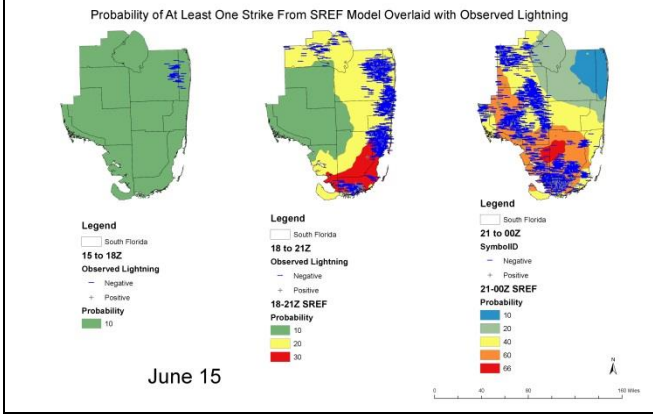
Probability of At Least One Strike From SREF Model Overlaid with Observed Lightning
Legend
South Florida
15 to 18Z
Observed Lightning
Negative
Positive
Probability
10
Legend
South Florida
18 to 21Z
Observed Lightning
Negative
Positive
18-21Z SREF
Probability
10
20
30
Legend
South Florida
21 to 00Z
SymbolID
Negative
Positive
21-00Z SREF
Probability
10
20
40
60
66
June 15

l.

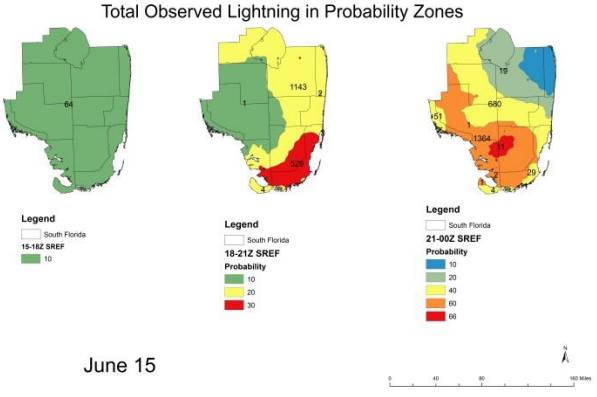
Total Observed Lightning in Probability Zones
64
1143
1
2
525
19
680
51
1364
11
29
Legend
South Florida
15-18Z SREF
10
Legend
South Florida
18-21Z SREF
Probability
10
20
30
Legend
South Florida
21-00Z SREF
Probability
10
20
40
60
66
June 15

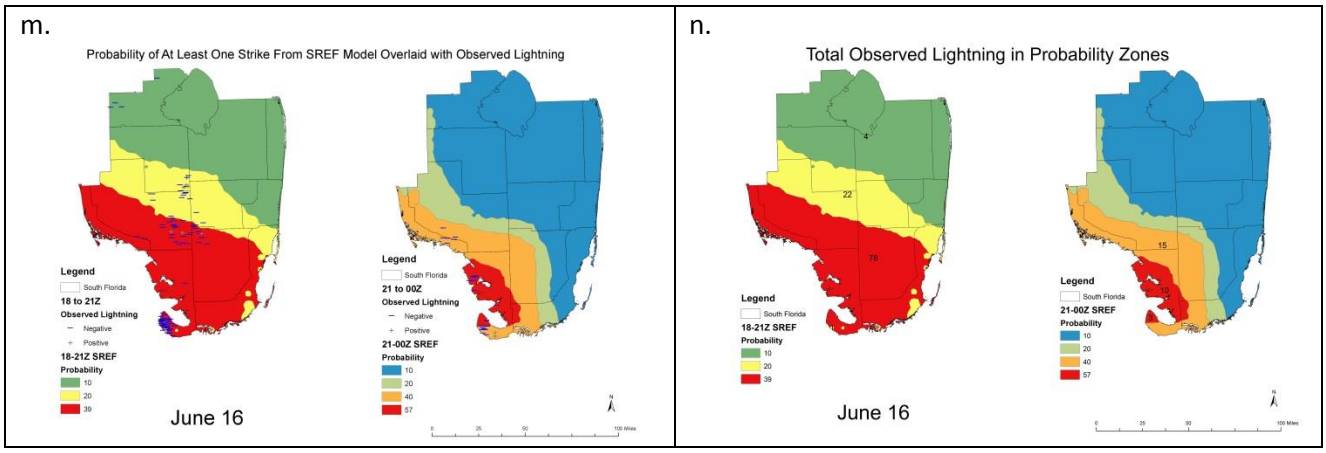

ArcGIS maps produced from analyzing the SREF model for active days in June depicting in a, c, e, g, i, k, m where the observed lightning occurred in respect to the model's predictions for each time period, 15Z, 18Z and 21Z and in b, d, f, h, j, l, n how many lightning strikes occurred in each probability range for each time period, 15Z, 18Z and 21Z. In figures a, c, e, g, i, k, m the observed lightning is represented by blue minus signs for negatively charged and gray positive signs for positively charged lightning and the probabilities are represented by colored polygons. In figures b, d, f, h, j, l, n the probabilities remain the same represented as colored polygons and the numbers represent the number of observed lightning strikes that occurred. Note that not all active days had lightning that occurred during all three time periods (15, 18 and 21Z). June 8th and 15th had all lightning activity during all three time periods. From the second map, figures b, d, f, h, j, l and n, the statistics were calculated to evaluate the accuracy of the SREF model.

Appendix B. July Lightning Maps

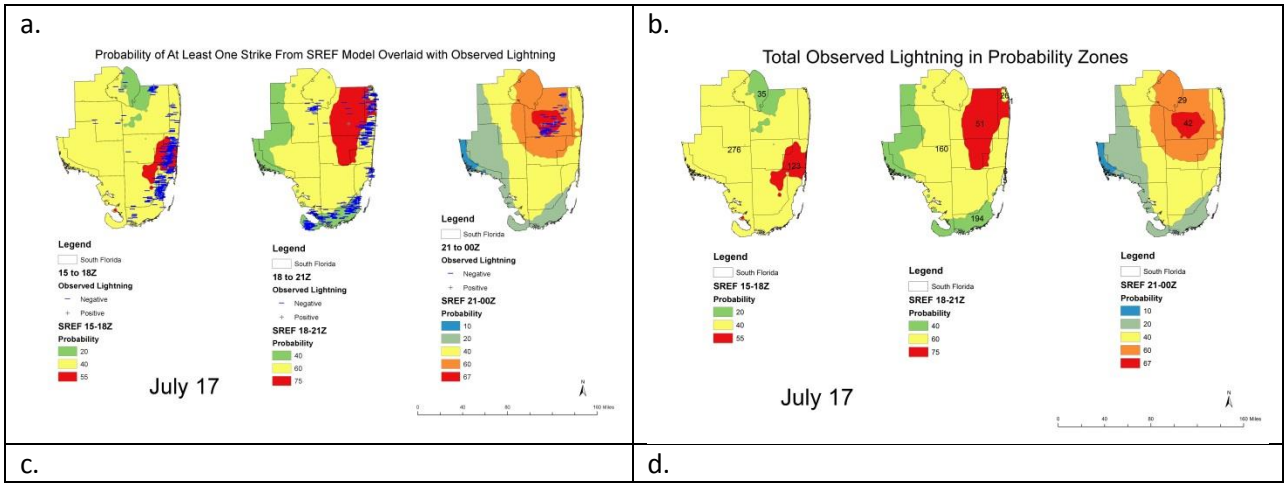

c.

d.

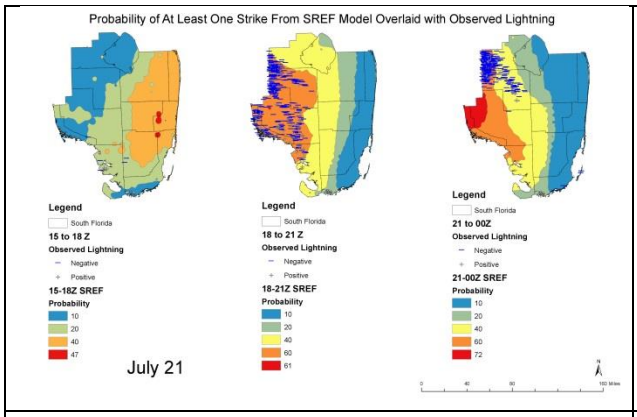
Probability of At Least One Strike From SREF Model Overlaid with Observed Lightning
Legend
South Florida
15 to 18 Z
Observed Lightning
Negative
Positive
15-18Z SREF
Probability
10
20
40
47
Legend
South Florida
18 to 21 Z
Observed Lightning
Negative
Positive
18-21Z SREF
Probability
10
20
40
60
61
Legend
South Florida
21 to 00Z
Observed Lightning
Negative
Positive
21-00Z SREF
Probability
10
20
40
60
72
July 21

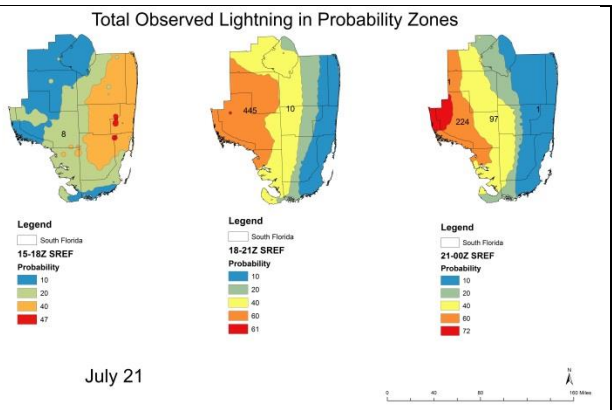
Total Observed Lightning in Probability Zones
8
445
10
224
97
1
3
Legend
South Florida
15-18Z SREF
Probability
10
20
40
47
Legend
South Florida
18-21Z SREF
Probability
10
20
40
60
61
Legend
South Florida
21-00Z SREF
Probability
10
20
40
60
72
July 21

e.

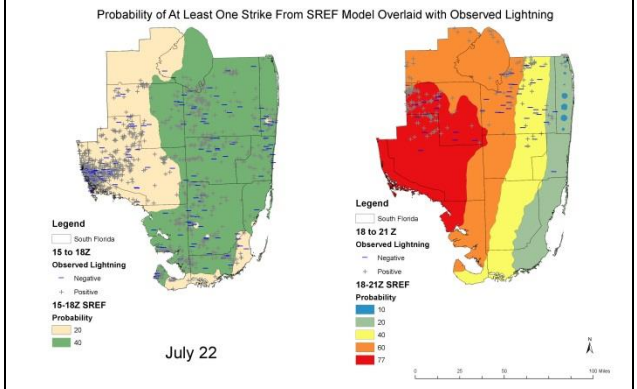
Probability of At Least One Strike From SREF Model Overlaid with Observed Lightning
Legend
South Florida
15 to 18Z
Observed Lightning
Negative
Positive
15-18Z SREF
Probability
20
40
Legend
South Florida
18 to 21 Z
Observed Lightning
Negative
Positive
18-21Z SREF
Probability
10
20
40
60
77
July 22

f.

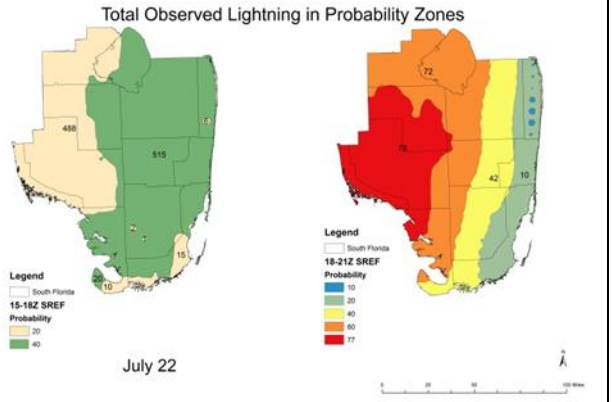
Total Observed Lightning in Probability Zones
458
515
15
10
72
78
42
10
Legend
South Florida
15-18Z SREF
Probability
20
40
Legend
South Florida
18-21Z SREF
Probability
10
20
40
60
77
July 22

g.

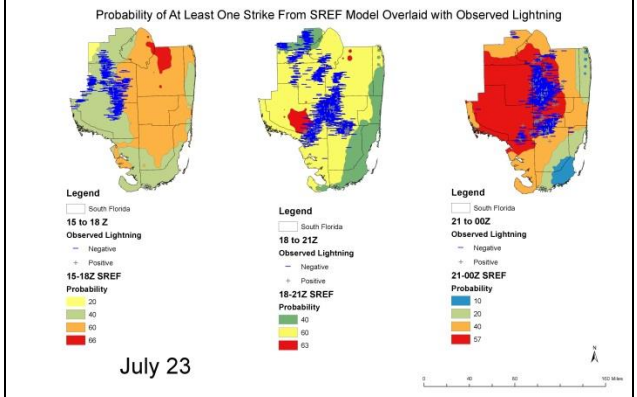
Probability of At Least One Strike From SREF Model Overlaid with Observed Lightning
Legend
South Florida
15 to 18 Z
Observed Lightning
Negative
Positive
15-18Z SREF
Probability
20
40
60
66
Legend
South Florida
18 to 21Z
Observed Lightning
Negative
Positive
18-21Z SREF
Probability
40
60
63
Legend
South Florida
21 to 00Z
Observed Lightning
Negative
Positive
21-00Z SREF
Probability
10
20
40
57
July 23

h.

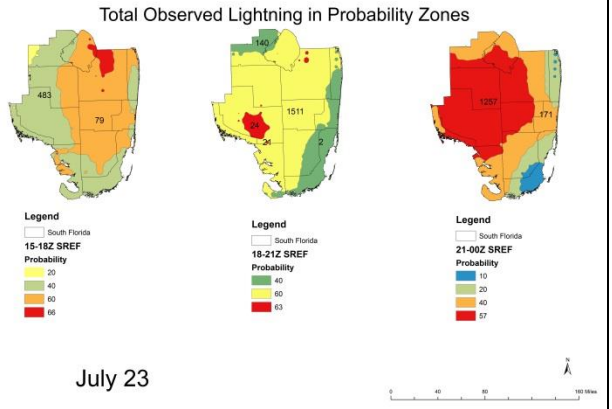
Total Observed Lightning in Probability Zones
483
79
140
1511
24
34
2
1257
171
Legend
South Florida
15-18Z SREF
Probability
20
40
60
66
Legend
South Florida
18-21Z SREF
Probability
40
60
63
Legend
South Florida
21-00Z SREF
Probability
10
20
40
57
July 23

i.

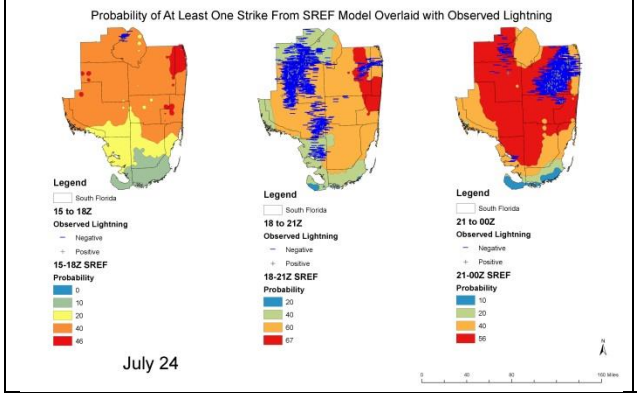
Probability of At Least One Strike From SREF Model Overlaid with Observed Lightning
Legend
South Florida
15 to 18Z
Observed Lightning
Negative
Positive
15-18Z SREF
Probability
0
10
20
40
46
Legend
South Florida
18 to 21Z
Observed Lightning
Negative
Positive
18-21Z SREF
Probability
20
40
60
67
Legend
South Florida
21 to 00Z
Observed Lightning
Negative
Positive
21-00Z SREF
Probability
10
20
40
55
July 24

j.

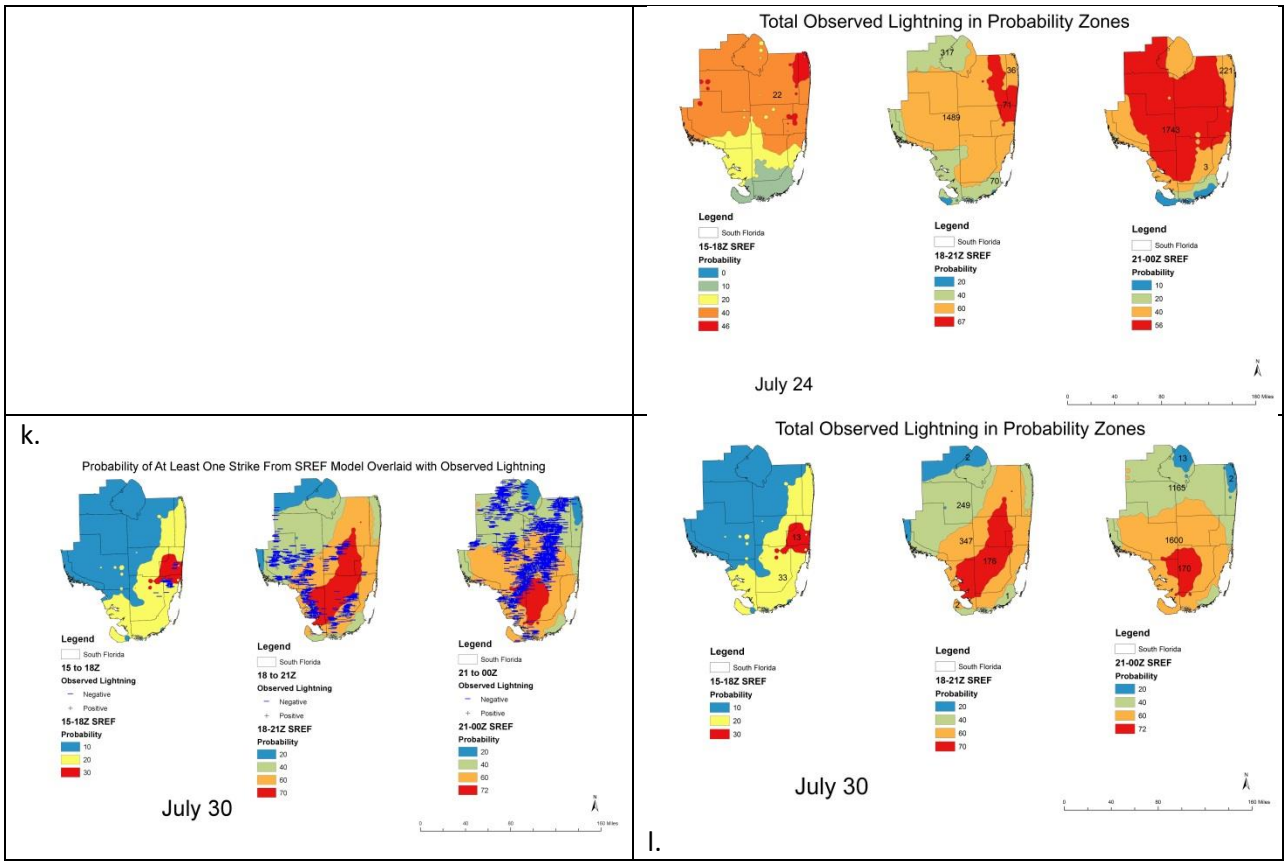

ArcGIS maps produced from analyzing the SREF model for active days in July depicting in a, c, e, g, i, k where the observed lightning occurred in respect to the model's predictions for each time period, 15Z, 18Z and 21Z and in b, d, f, h, j, l how many lightning strikes occurred in each probability range for each time period, 15Z, 18Z and 21Z. In figures a, c, e, g, i, k the observed lightning is represented by blue minus signs for negatively charged and gray positive signs for positively charged lightning and the probabilities are represented by colored polygons. In figures b, d, f, h, j, l the probabilities remain the same represented as colored polygons and the numbers represent the number of observed lightning strikes that occurred. Note that not all active days had lightning that occurred during all three time periods (15, 18 and 21Z). For July, the 22nd did not have lightning during all three time periods, only during the 18 and 21Z time periods. From the second map, figures b, d, f, h, j and l, the statistics were calculated to evaluate the accuracy of the SREF model.

Appendix C. August Lightning Maps

a.	b.

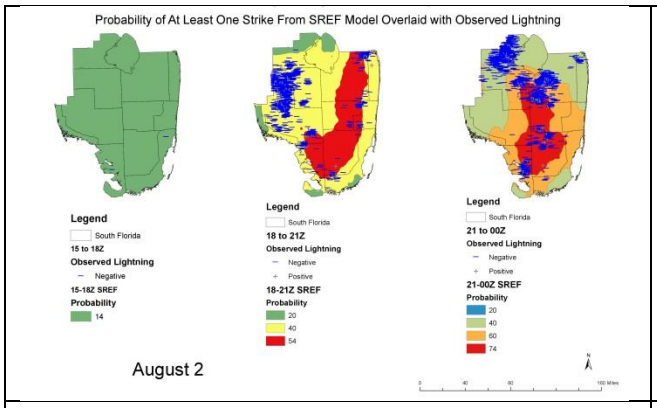
Probability of At Least One Strike From SREF Model Overlaid with Observed Lightning
Legend
South Florida
15 to 18Z
Observed Lightning
Negative
15-18Z SREF
Probability
14
Legend
South Florida
18 to 21Z
Observed Lightning
Negative
Positive
18-21Z SREF
Probability
20
40
54
Legend
South Florida
21 to 00Z
Observed Lightning
Negative
Positive
21-00Z SREF
Probability
20
40
60
74
August 2

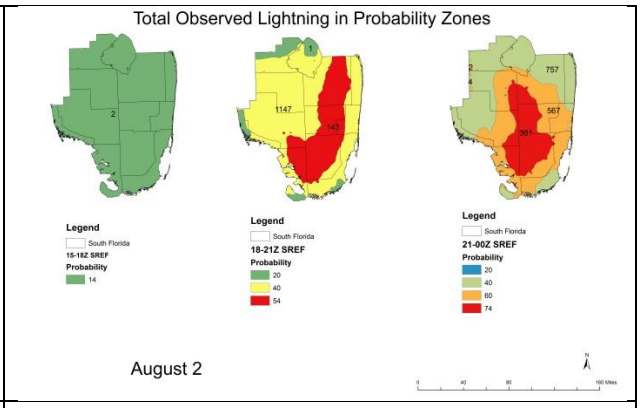
Total Observed Lightning in Probability Zones
2
1147
143
1
757
567
961
Legend
South Florida
15-18Z SREF
Probability
14
Legend
South Florida
18-21Z SREF
Probability
20
40
54
Legend
South Florida
21-00Z SREF
Probability
20
40
60
74
August 2

c.

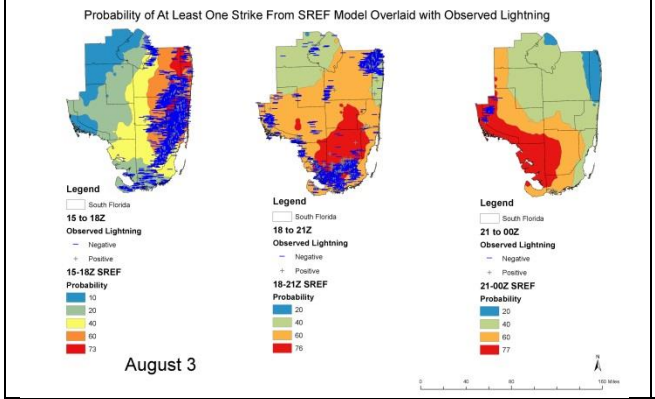
Probability of At Least One Strike From SREF Model Overlaid with Observed Lightning
Legend
South Florida
15 to 18Z
Observed Lightning
Negative
Positive
15-18Z SREF
Probability
10
20
40
60
73
Legend
South Florida
18 to 21Z
Observed Lightning
Negative
Positive
18-21Z SREF
Probability
20
40
60
76
Legend
South Florida
21 to 00Z
Observed Lightning
Negative
Positive
21-00Z SREF
Probability
20
40
60
77
August 3

d.

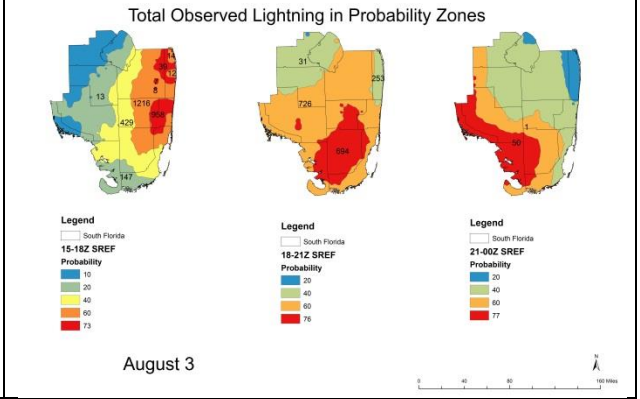
Total Observed Lightning in Probability Zones
13
1216
429
147
31
253
726
594
1
50
Legend
South Florida
15-18Z SREF
Probability
10
20
40
60
73
Legend
South Florida
18-21Z SREF
Probability
20
40
60
76
Legend
South Florida
21-00Z SREF
Probability
20
40
60
77
August 3

e.

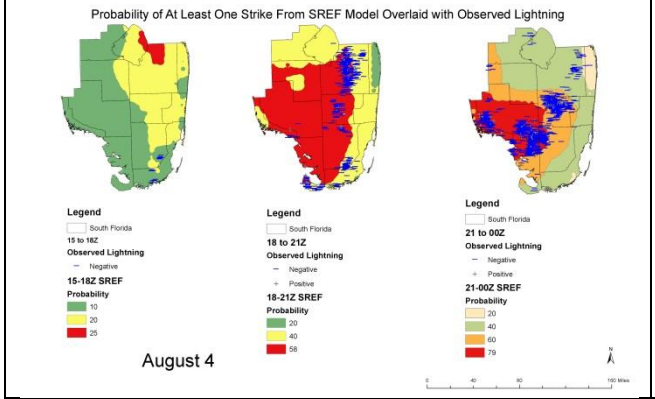
Probability of At Least One Strike From SREF Model Overlaid with Observed Lightning
Legend
South Florida
15 to 18Z
Observed Lightning
Negative
15-18Z SREF
Probability
10
20
25
Legend
South Florida
18 to 21Z
Observed Lightning
Negative
Positive
18-21Z SREF
Probability
20
40
58
Legend
South Florida
21 to 00Z
Observed Lightning
Negative
Positive
21-00Z SREF
Probability
20
40
60
79
August 4

f.

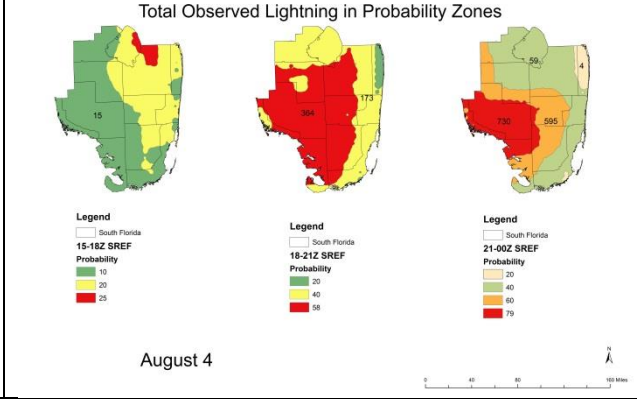
Total Observed Lightning in Probability Zones
15
364
173
59
4
730
595
Legend
South Florida
15-18Z SREF
Probability
10
20
25
Legend
South Florida
18-21Z SREF
Probability
20
40
58
Legend
South Florida
21-00Z SREF
Probability
20
40
60
79
August 4

g.

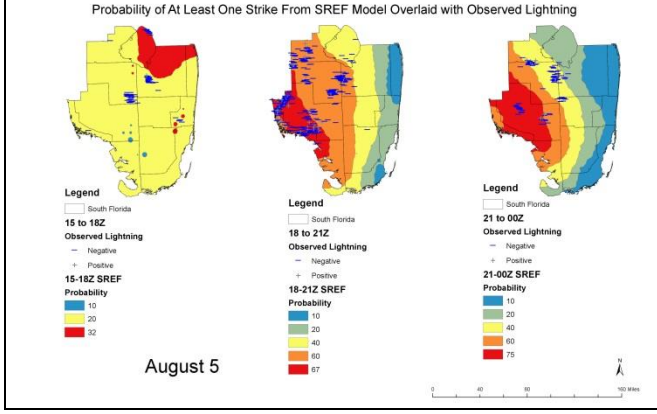
Probability of At Least One Strike From SREF Model Overlaid with Observed Lightning
Legend
South Florida
15 to 18Z
Observed Lightning
Negative
Positive
15-18Z SREF
Probability
10
20
32
Legend
South Florida
18 to 21Z
Observed Lightning
Negative
Positive
18-21Z SREF
Probability
10
20
40
60
67
Legend
South Florida
21 to 00Z
Observed Lightning
Negative
Positive
21-00Z SREF
Probability
10
20
40
60
75
August 5

h.

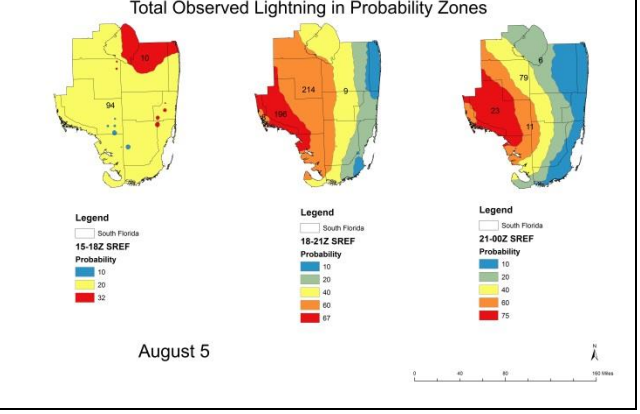
Total Observed Lightning in Probability Zones
10
94
214
9
196
6
79
23
11
Legend
South Florida
15-18Z SREF
Probability
10
20
32
Legend
South Florida
18-21Z SREF
Probability
10
20
40
60
67
Legend
South Florida
21-00Z SREF
Probability
10
20
40
60
75
August 5

i.

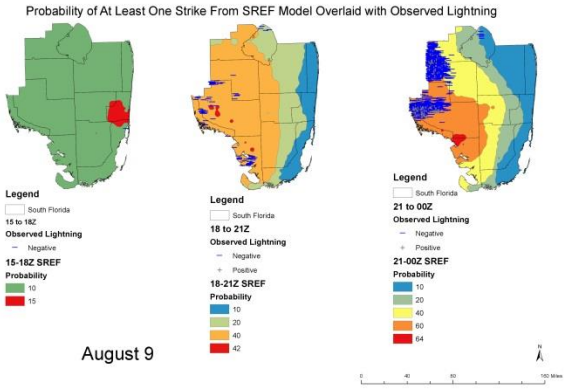
Probability of At Least One Strike From SREF Model Overlaid with Observed Lightning
Legend
South Florida
15 to 18Z
Observed Lightning
Negative
15-18Z SREF
Probability
10
15
Legend
South Florida
18 to 21Z
Observed Lightning
Negative
Positive
18-21Z SREF
Probability
10
20
40
42
Legend
South Florida
21 to 00Z
Observed Lightning
Negative
Positive
21-00Z SREF
Probability
10
20
40
60
64
August 9

j.

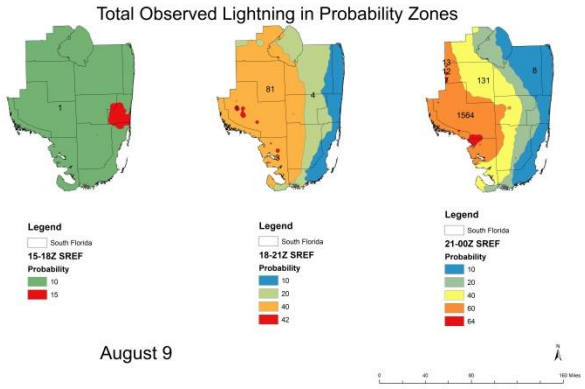
Total Observed Lightning in Probability Zones
1
Legend
South Florida
15-18Z SREF
Probability
10
15
81
4
Legend
South Florida
18-21Z SREF
Probability
10
20
40
42
131
8
1564
Legend
South Florida
21-00Z SREF
Probability
10
20
40
60
64
August 9

k.

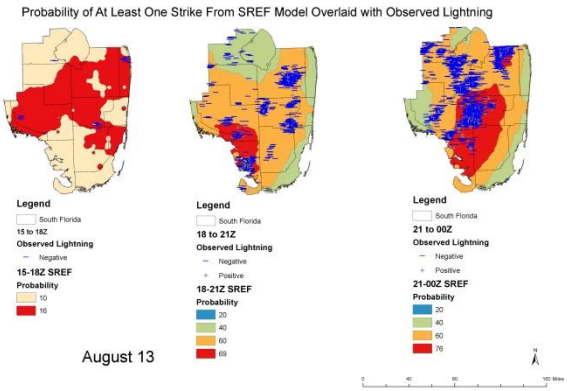
Probability of At Least One Strike From SREF Model Overlaid with Observed Lightning
Legend
South Florida
15 to 18Z
Observed Lightning
Negative
15-18Z SREF
Probability
10
16
Legend
South Florida
18 to 21Z
Observed Lightning
Negative
Positive
18-21Z SREF
Probability
20
40
60
69
Legend
South Florida
21 to 00Z
Observed Lightning
Negative
Positive
21-00Z SREF
Probability
20
40
60
76
August 13

l.

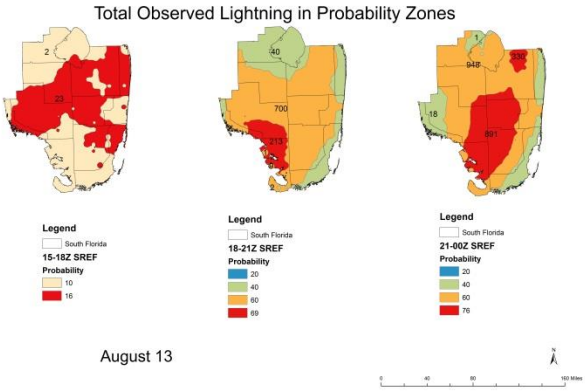
Total Observed Lightning in Probability Zones
2
23
Legend
South Florida
15-18Z SREF
Probability
10
16
40
700
213
Legend
South Florida
18-21Z SREF
Probability
20
40
60
89
1
330
948
18
881
Legend
South Florida
21-00Z SREF
Probability
20
40
60
76
August 13

m.

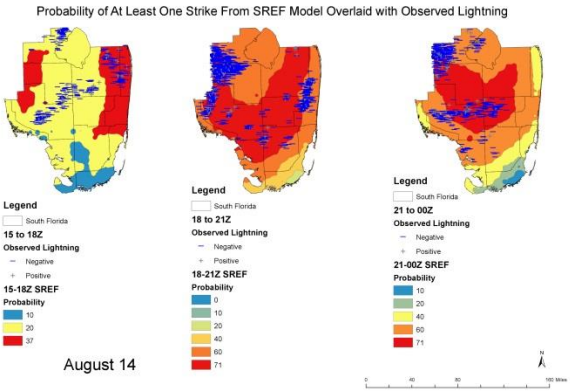
Probability of At Least One Strike From SREF Model Overlaid with Observed Lightning
Legend
South Florida
15 to 18Z
Observed Lightning
Negative
Positive
15-18Z SREF
Probability
10
20
37
Legend
South Florida
18 to 21Z
Observed Lightning
Negative
Positive
18-21Z SREF
Probability
0
10
20
40
60
71
Legend
South Florida
21 to 00Z
Observed Lightning
Negative
Positive
21-00Z SREF
Probability
10
20
40
60
71
August 14

n.

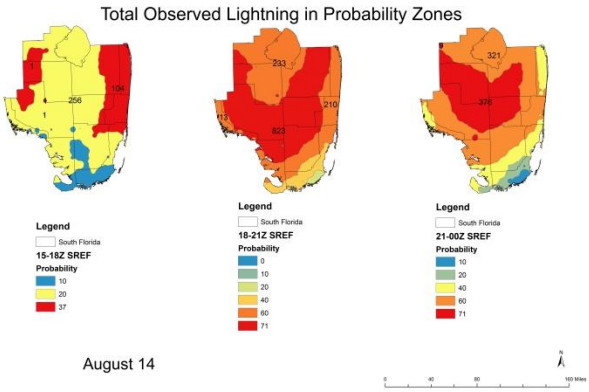
Total Observed Lightning in Probability Zones
1
256
19
1
Legend
South Florida
15-18Z SREF
Probability
10
20
37
233
13
823
210
Legend
South Florida
18-21Z SREF
Probability
0
10
20
40
60
71
321
376
Legend
South Florida
21-00Z SREF
Probability
10
20
40
60
71
August 14

o.

p.

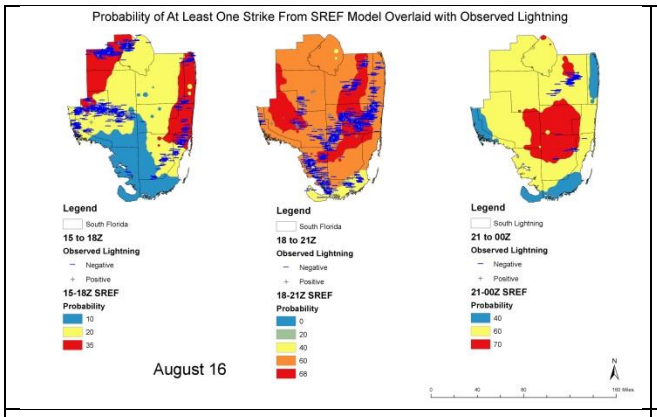
Probability of At Least One Strike From SREF Model Overlaid with Observed Lightning
Legend
South Florida
15 to 18Z
Observed Lightning
Negative
Positive
15-18Z SREF
Probability
10
20
35
Legend
South Florida
18 to 21Z
Observed Lightning
Negative
Positive
18-21Z SREF
Probability
0
20
40
60
68
Legend
South Lightning
21 to 00Z
Observed Lightning
Negative
Positive
21-00Z SREF
Probability
40
60
70
August 16

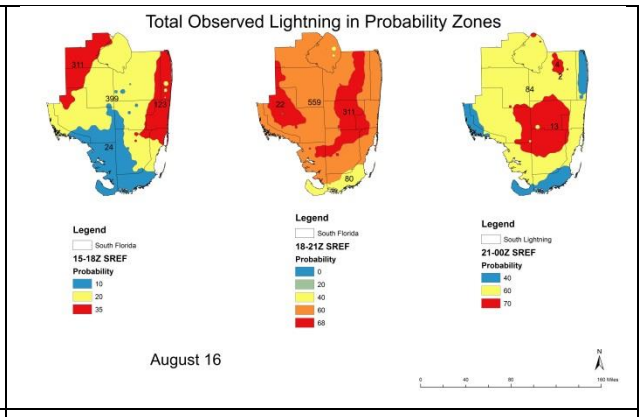
Total Observed Lightning in Probability Zones
311
399
127
24
32
559
911
60
84
2
13
Legend
South Florida
15-18Z SREF
Probability
10
20
35
Legend
South Florida
18-21Z SREF
Probability
0
20
40
60
68
Legend
South Lightning
21-00Z SREF
Probability
40
60
70
August 16

q.

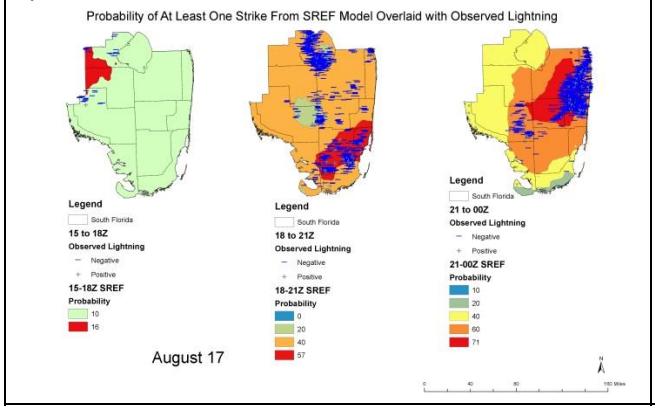
Probability of At Least One Strike From SREF Model Overlaid with Observed Lightning
Legend
South Florida
15 to 18Z
Observed Lightning
Negative
Positive
15-18Z SREF
Probability
10
16
Legend
South Florida
18 to 21Z
Observed Lightning
Negative
Positive
18-21Z SREF
Probability
0
20
40
57
Legend
South Florida
21 to 00Z
Observed Lightning
Negative
Positive
21-00Z SREF
Probability
10
20
40
60
71
August 17

r.

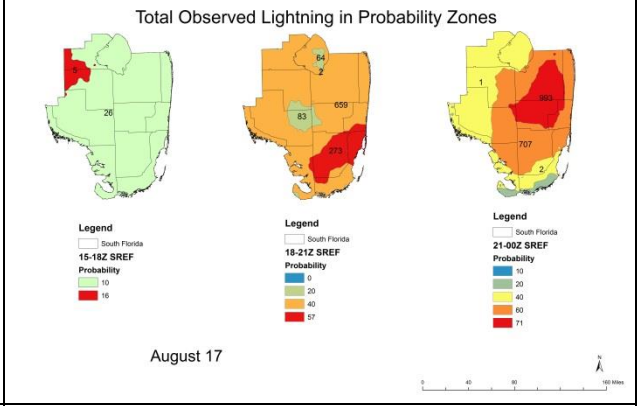
Total Observed Lightning in Probability Zones
26
64
2
659
83
273
1
983
707
2
Legend
South Florida
15-18Z SREF
Probability
10
16
Legend
South Florida
18-21Z SREF
Probability
0
20
40
57
Legend
South Florida
21-00Z SREF
Probability
10
20
40
60
71
August 17

s.

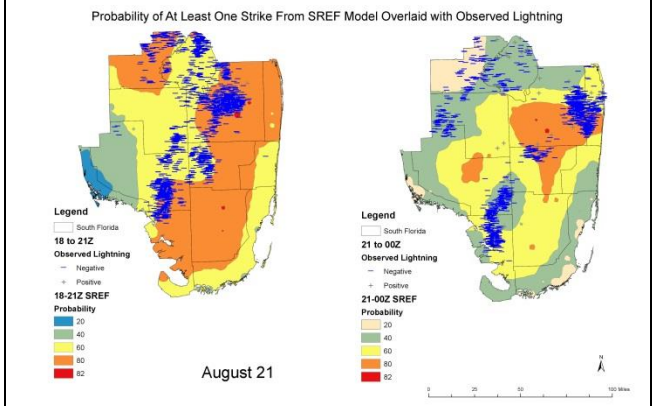
Probability of At Least One Strike From SREF Model Overlaid with Observed Lightning
Legend
South Florida
18 to 21Z
Observed Lightning
Negative
Positive
18-21Z SREF
Probability
20
40
60
80
82
Legend
South Florida
21 to 00Z
Observed Lightning
Negative
Positive
21-00Z SREF
Probability
20
40
60
80
82
August 21

t.

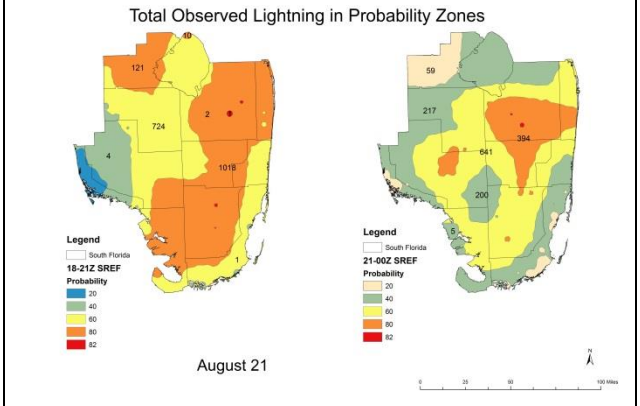
Total Observed Lightning in Probability Zones
121
724
4
2
1018
1
59
217
394
641
200
5
Legend
South Florida
18-21Z SREF
Probability
20
40
60
80
82
Legend
South Florida
21-00Z SREF
Probability
20
40
60
80
82
August 21

u.

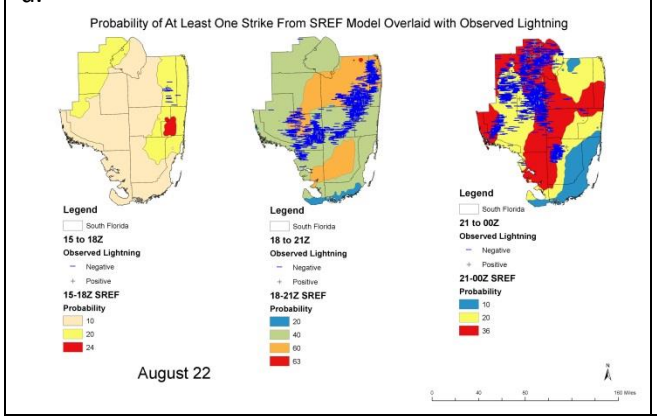
Probability of At Least One Strike From SREF Model Overlaid with Observed Lightning
Legend
South Florida
15 to 18Z
Observed Lightning
Negative
Positive
15-18Z SREF
Probability
10
20
24
Legend
South Florida
18 to 21Z
Observed Lightning
Negative
Positive
18-21Z SREF
Probability
20
40
60
63
Legend
South Florida
21 to 00Z
Observed Lightning
Negative
Positive
21-00Z SREF
Probability
10
20
36
August 22

v.

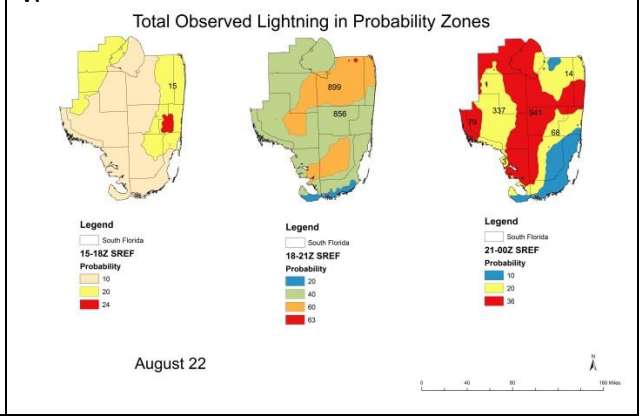
Total Observed Lightning in Probability Zones
15
899
856
14
1
337
941
68
Legend
South Florida
15-18Z SREF
Probability
10
20
24
Legend
South Florida
18-21Z SREF
Probability
20
40
60
63
Legend
South Florida
21-00Z SREF
Probability
10
20
36
August 22

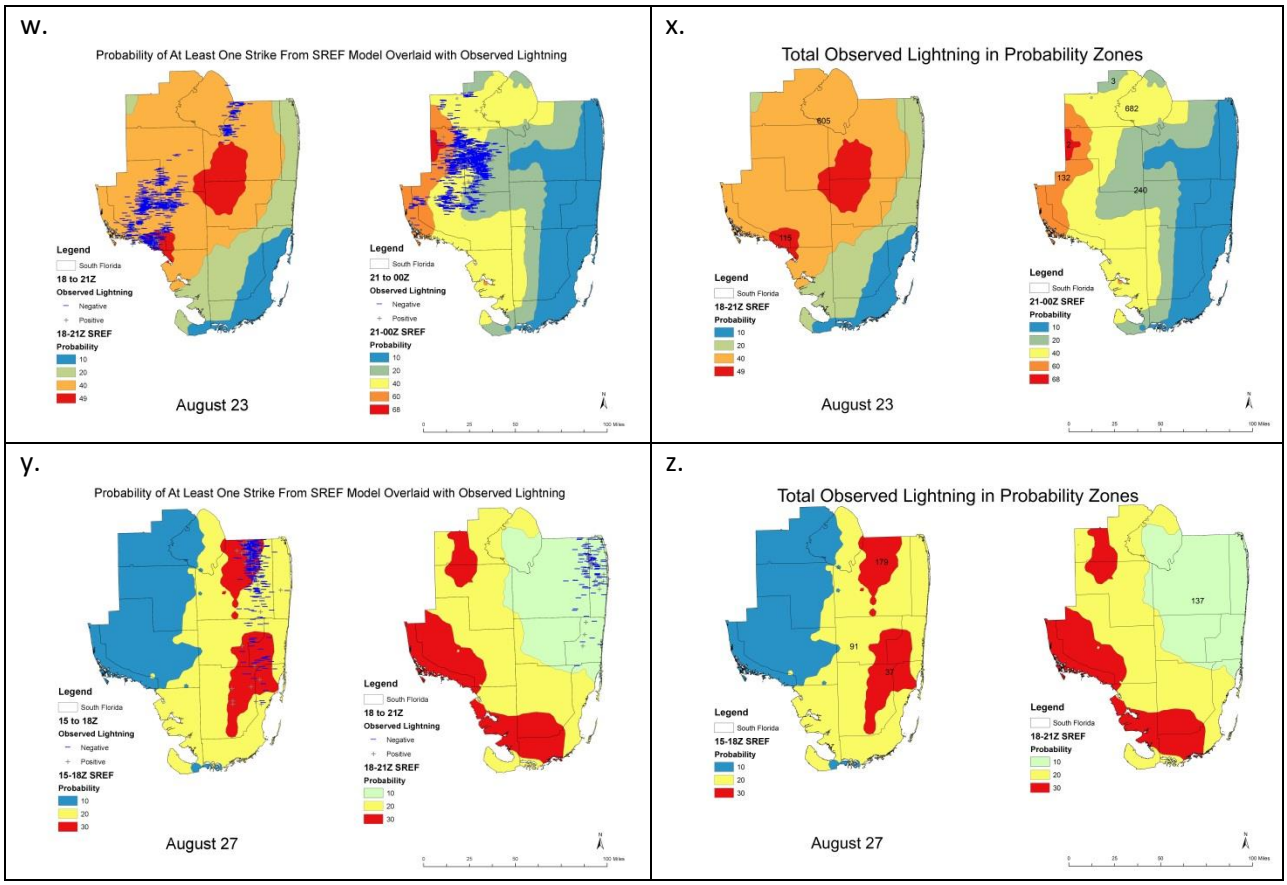

ArcGIS maps produced from analyzing the SREF model for active days in September depicting in a, c, e, g, i where the observed lightning occurred in respect to the model's predictions for each time period, 15Z, 18Z and 21Z and in b, d, f, h, j how many lightning strikes occurred in each probability range for each time period, 15Z, 18Z and 21Z. In figures a, c, e, g, i the observed lightning is represented by blue minus signs for negatively charged and gray positive signs for positively charged lightning and the probabilities are represented by colored polygons. In figures b, d, f, h, j the probabilities remain the same represented as colored polygons and the numbers represent the number of observed lightning strikes that occurred. Note that not all active days had lightning that occurred during all three time periods (15, 18 and 21Z). August 21, 23 and 27th did not have lightning activity during all three periods. August 21 and 23rd had activity only in the 18 and 21Z time periods, whereas August 27th had lightning during the 15 and 18Z time periods. From the second map, figures b, d, f, h, j, l, n, p, r, t, v, x, and z, the statistics were calculated to evaluate the accuracy of the SREF model.

Appendix D. September Lightning Maps

a.	b.

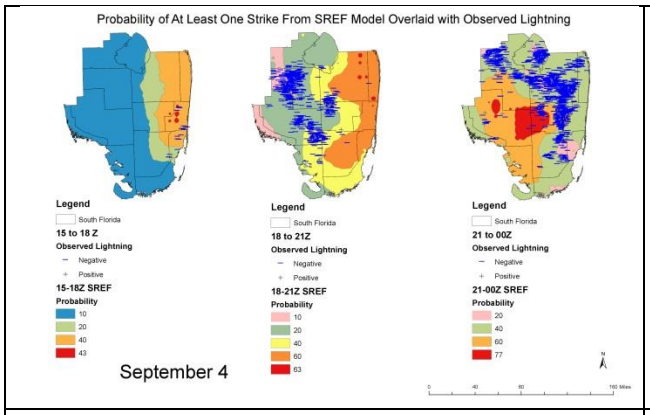
Probability of At Least One Strike From SREF Model Overlaid with Observed Lightning
Legend
South Florida
15 to 18 Z
Observed Lightning
Negative
Positive
15-18Z SREF
Probability
10
20
40
43
Legend
South Florida
18 to 21Z
Observed Lightning
Negative
Positive
18-21Z SREF
Probability
10
20
40
60
63
Legend
South Florida
21 to 00Z
Observed Lightning
Negative
Positive
21-00Z SREF
Probability
20
40
60
77
September 4

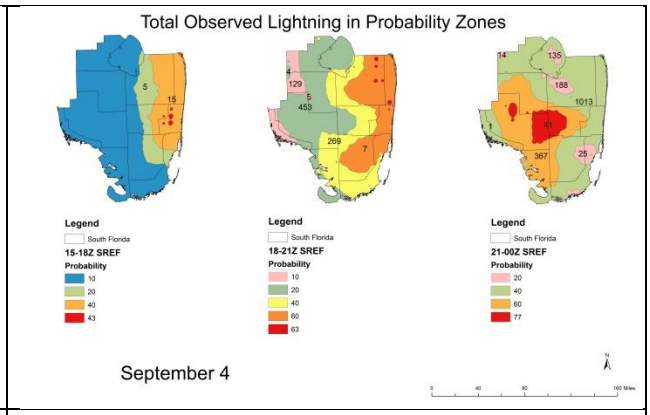
Total Observed Lightning in Probability Zones
5
15
Legend
South Florida
15-18Z SREF
Probability
10
20
40
43
4
129
5
453
269
7
Legend
South Florida
18-21Z SREF
Probability
10
20
40
60
63
14
135
188
1013
41
367
25
Legend
South Florida
21-00Z SREF
Probability
20
40
60
77
September 4

c.

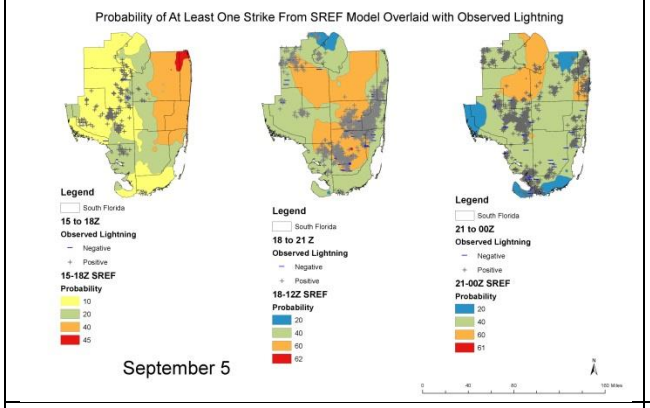
Probability of At Least One Strike From SREF Model Overlaid with Observed Lightning
Legend
South Florida
15 to 18Z
Observed Lightning
Negative
Positive
15-18Z SREF
Probability
10
20
40
45
Legend
South Florida
18 to 21 Z
Observed Lightning
Negative
Positive
18-12Z SREF
Probability
20
40
60
62
Legend
South Florida
21 to 00Z
Observed Lightning
Negative
Positive
21-00Z SREF
Probability
20
40
60
61
September 5

d.

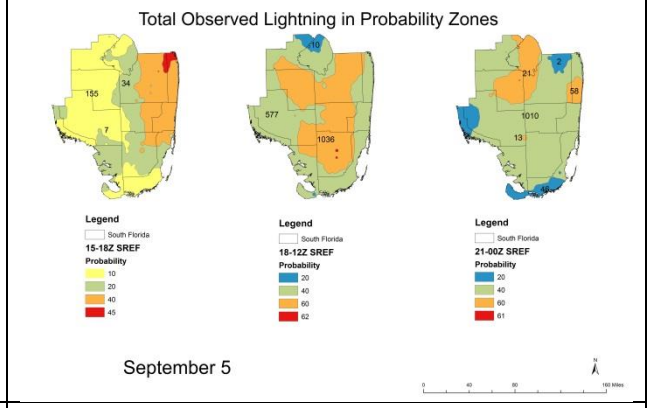
Total Observed Lightning in Probability Zones
155
34
7
Legend
South Florida
15-18Z SREF
Probability
10
20
40
45
577
10
1036
Legend
South Florida
18-12Z SREF
Probability
20
40
60
62
21
2
58
1010
13
Legend
South Florida
21-00Z SREF
Probability
20
40
60
61
September 5

e.

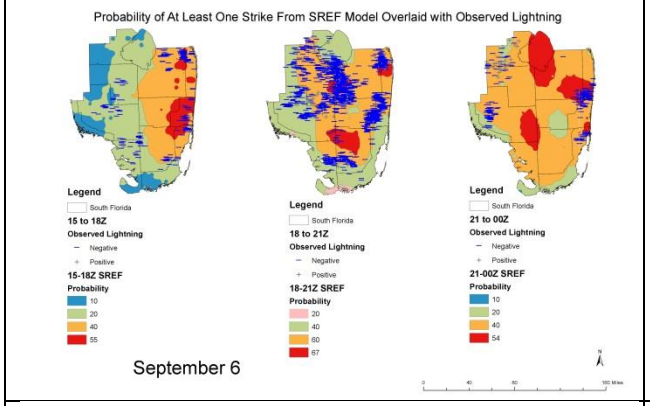
Probability of At Least One Strike From SREF Model Overlaid with Observed Lightning
Legend
South Florida
15 to 18Z
Observed Lightning
Negative
Positive
15-18Z SREF
Probability
10
20
40
55
Legend
South Florida
18 to 21Z
Observed Lightning
Negative
Positive
18-21Z SREF
Probability
20
40
60
67
Legend
South Florida
21 to 00Z
Observed Lightning
Negative
Positive
21-00Z SREF
Probability
10
20
40
54
September 6

f.

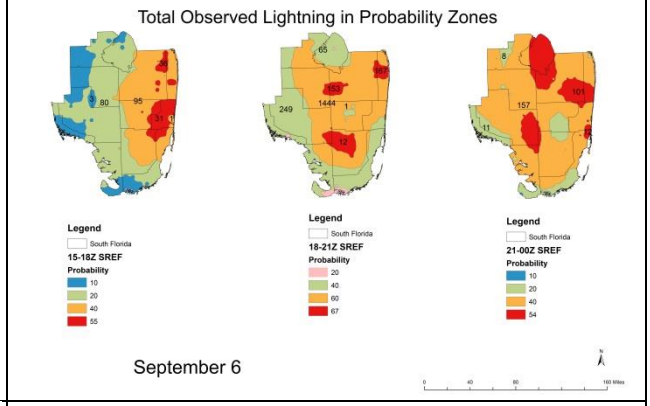
Total Observed Lightning in Probability Zones
80
95
Legend
South Florida
15-18Z SREF
Probability
10
20
40
55
65
249
1444
1
12
Legend
South Florida
18-21Z SREF
Probability
20
40
60
67
8
157
101
11
Legend
South Florida
21-00Z SREF
Probability
10
20
40
54
September 6

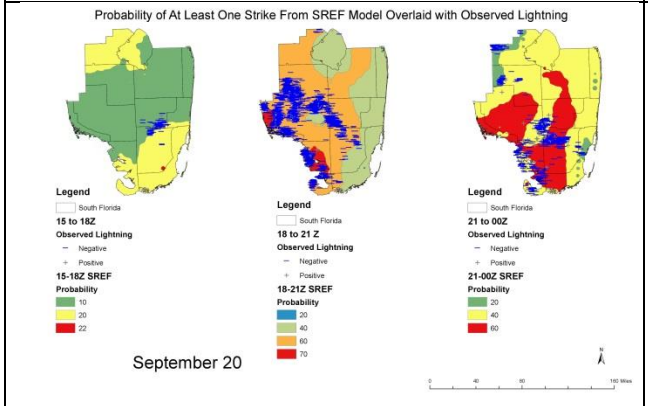
Probability of At Least One Strike From SREF Model Overlaid with Observed Lightning
Legend
South Florida
15 to 18Z
Observed Lightning
Negative
Positive
15-18Z SREF
Probability
10
20
22
Legend
South Florida
18 to 21 Z
Observed Lightning
Negative
Positive
18-21Z SREF
Probability
20
40
60
70
Legend
South Florida
21 to 00Z
Observed Lightning
Negative
Positive
21-00Z SREF
Probability
20
40
60
September 20

g.

h.

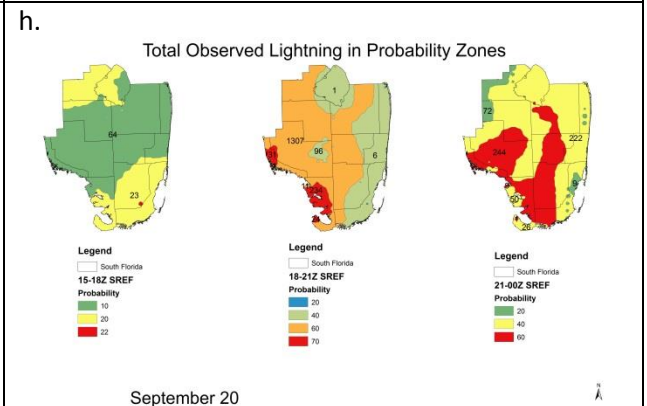
Total Observed Lightning in Probability Zones
64
23
Legend
South Florida
15-18Z SREF
Probability
10
20
22
1307
96
6
Legend
South Florida
18-21Z SREF
Probability
20
40
60
70
72
244
222
Legend
South Florida
21-00Z SREF
Probability
20
40
60
September 20

i. 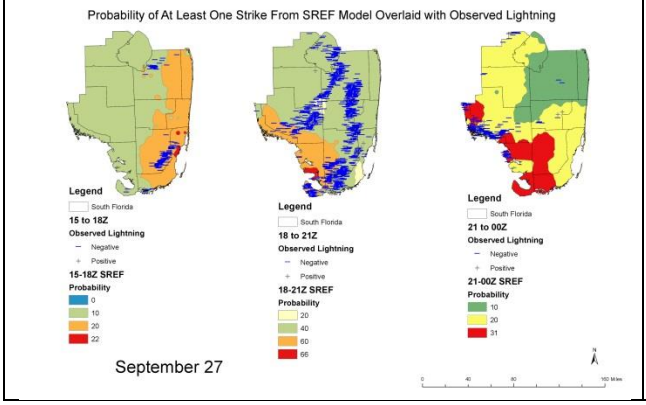	j. 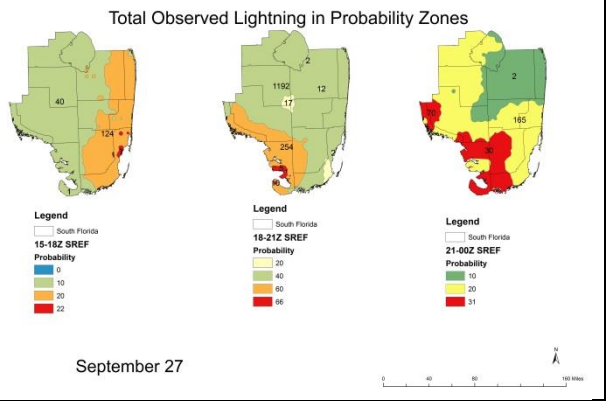

ArcGIS maps produced from analyzing the SREF model for active days in September depicting in a, c, e, g, i where the observed lightning occurred in respect to the model's predictions for each time period, 15Z, 18Z and 21Z and in b, d, f, h, j how many lightning strikes occurred in each probability range for each time period, 15Z, 18Z and 21Z. In figures a, c, e, g, i the observed lightning is represented by blue minus signs for negatively charged and gray positive signs for positively charged lightning and the probabilities are represented by colored polygons. In figures b, d, f, h, j the probabilities remain the same represented as colored polygons and the numbers represent the number of observed lightning strikes that occurred. From the second map, figures b, d, f, h, and j the statistics were calculated to evaluate the accuracy of the SREF model.

Appendix E. 500 mb Temperatures

a. 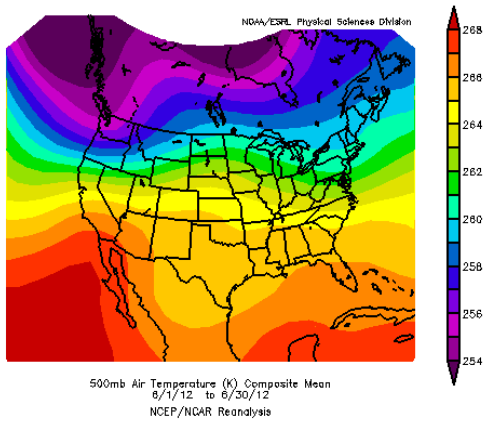	b. 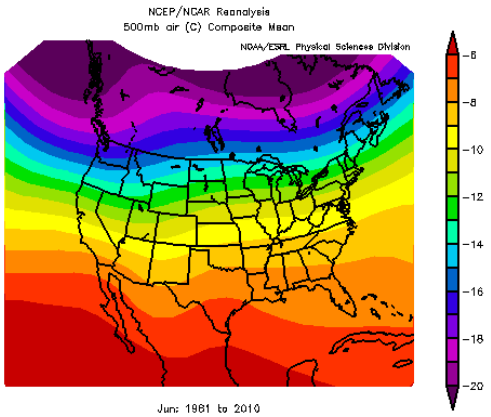
c.	d.

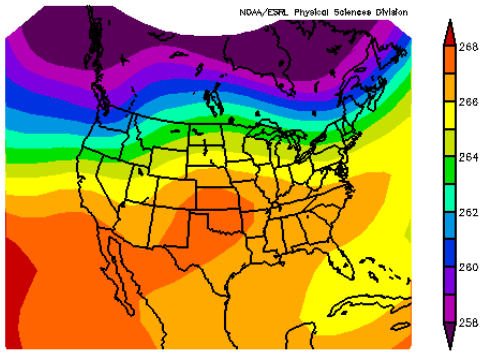

500mb Air Temperature (K) Composite Mean
7/1/12 to 7/31/12
NCEP/NCAR Reanalysis

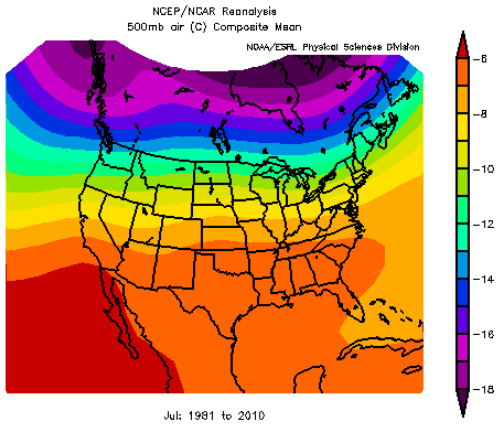

Jul: 1981 to 2010

e.

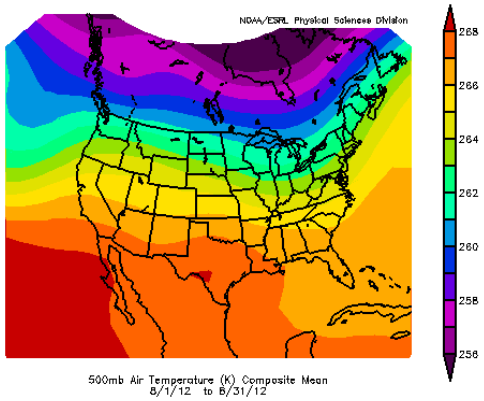

500mb Air Temperature (K) Composite Mean
8/1/12 to 8/31/12
NCEP/NCAR Reanalysis

f.

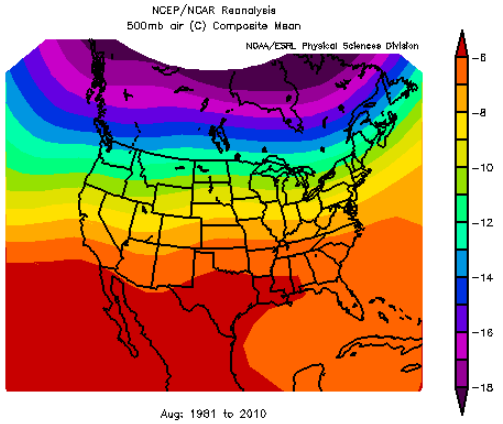

Aug: 1981 to 2010

g.

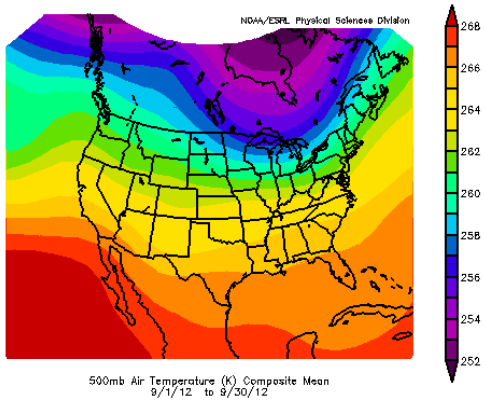

500mb Air Temperature (K) Composite Mean
9/1/12 to 9/30/12
NCEP/NCAR Reanalysis

h.

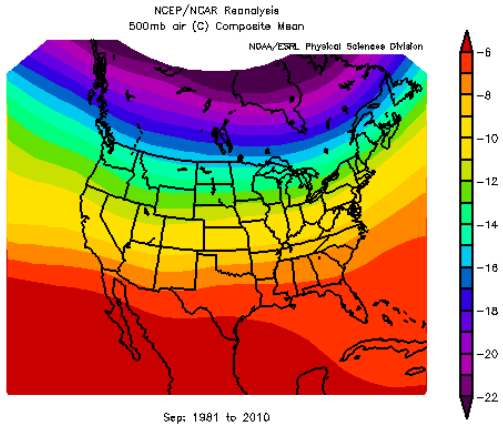

Sep: 1981 to 2010

Figures of each month in the convective season depicting in a, c, e, g the mean 500 mb temperatures for the month in 2012 and for figures b, d, f, h, a 29 year climatology from 1981 to 2010. Figures obtained from NOAA's Earth System Research Laboratory (ESRL) reanalysis. The June 500 mb temperature climatology indicates a 500 mb temperature of about -7 to -8 degrees C. The July 500 mb temperature climatology from the reanalysis shows a temperature of about -7 to -8 degrees C. The August 500 mb temperature climatology indicates a temperature of about -6 to -7 degrees C. The September 500 mb temperature climatology indicates a temperature of about -6 to -7 degrees C. Comparing these with the 2012 monthly averages for each month (figures a, c, e, g) June had a range of -6 to -7 coming in a degree warmer than the climatology, and the rest of the months, July, August and September had the same range as climatology for the 2012 average.

Appendix F. June Analysis

<table>
<tr>
<td> 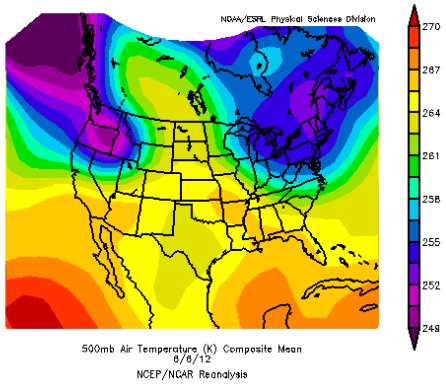

a.</td>
<td> 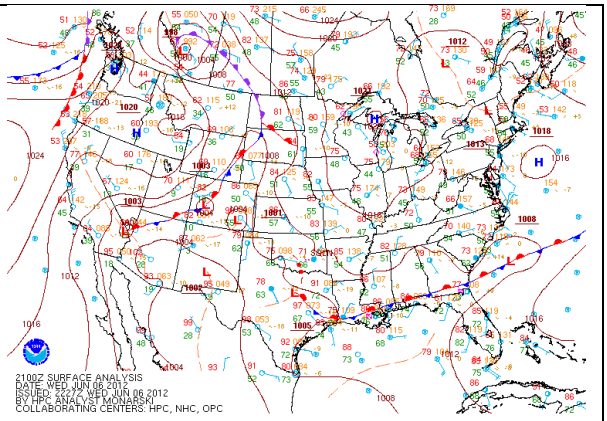

b.</td>
</tr>
<tr>
<td>c. 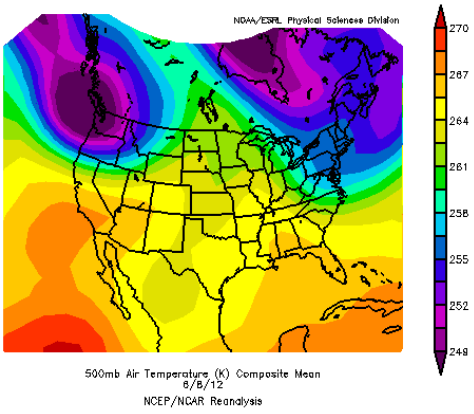
</td>
<td>d. 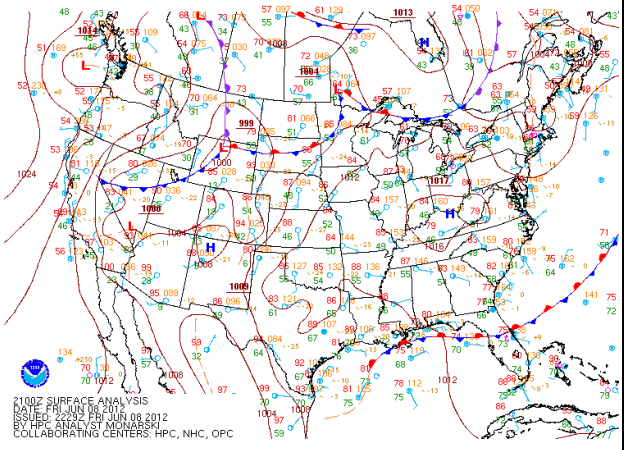
</td>
</tr>
<tr>
<td>e.</td>
<td>f.</td>
</tr>
</table>

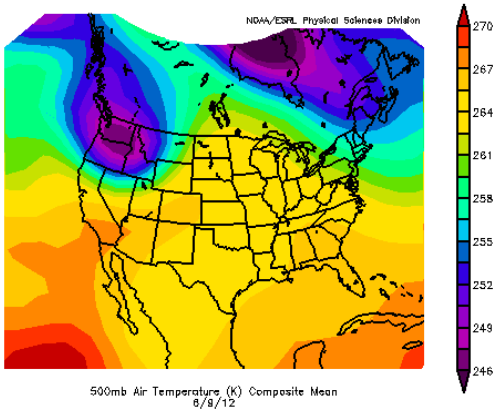

500mb Air Temperature (K) Composite Mean
6/9/12
NCEP/NCAR Reanalysis

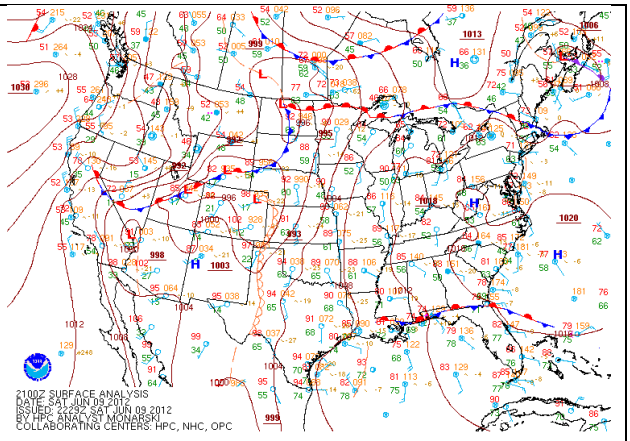

g.

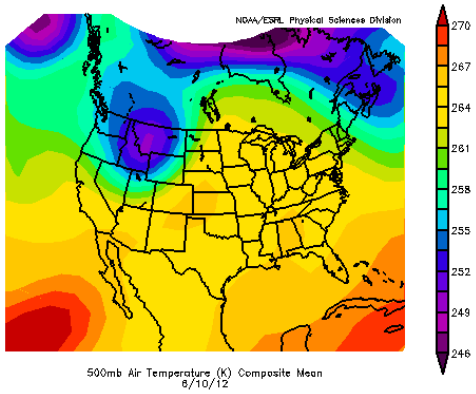

500mb Air Temperature (K) Composite Mean
6/10/12
NCEP/NCAR Reanalysis

h.

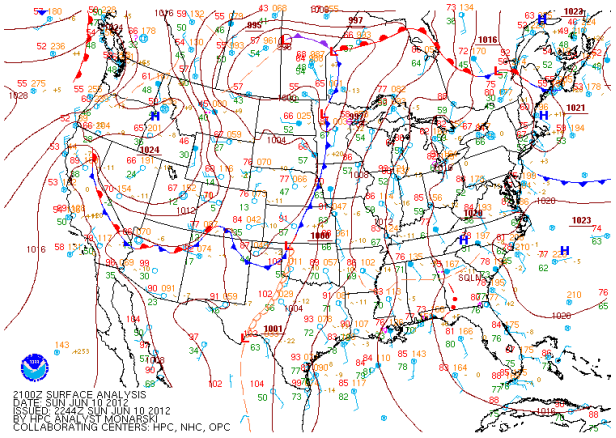

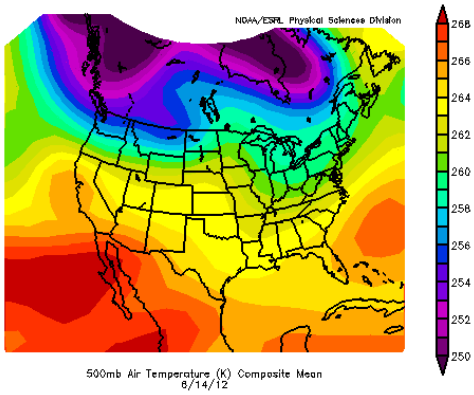

500mb Air Temperature (K) Composite Mean
6/14/12
NCEP/NCAR Reanalysis

i.

j.

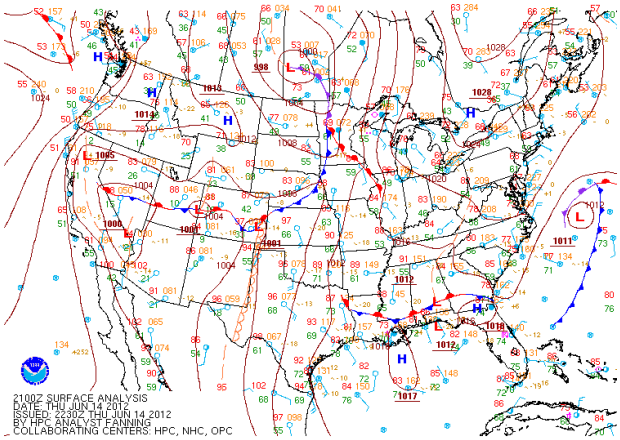

k.

l.

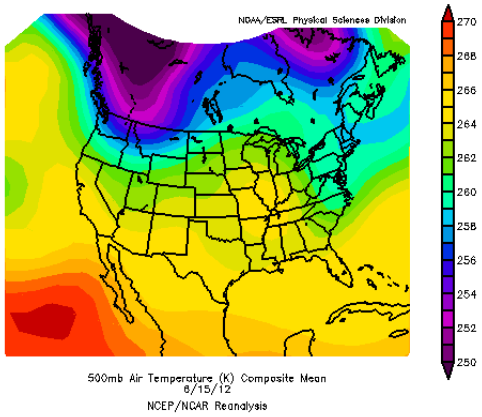

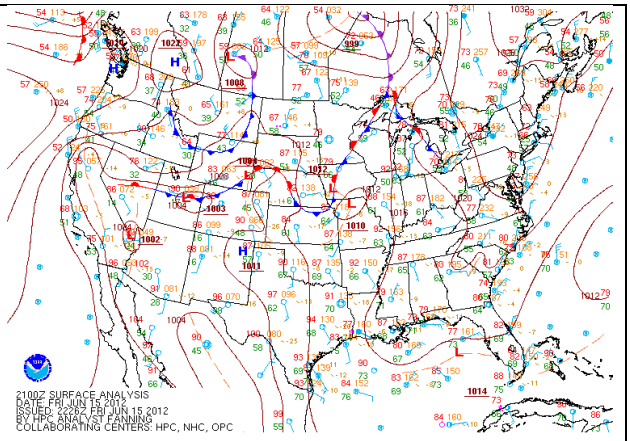

m.

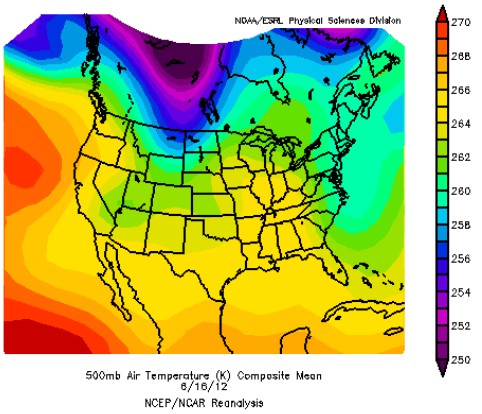

n.

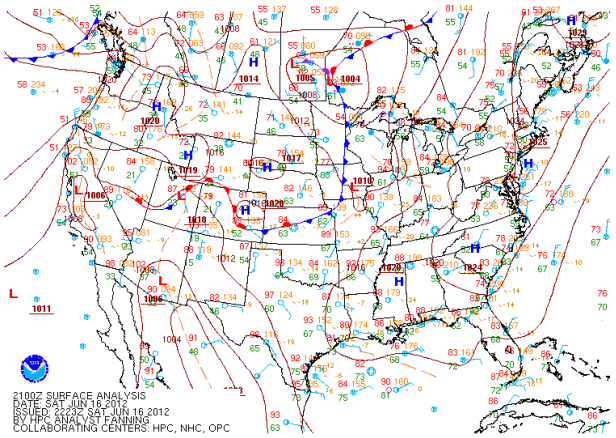

The two figures are of the synoptic set-up for the active days in June with a, c, e, g, i, k, m being a reanalysis map from NOAA's Earth System Research Laboratory (ESRL) daily mean composites of the 500 mb temperatures and b, d, f, h, j, l, n being a surface analysis map for 21Z from NOAA's Hydrometeorological Predication Center (HPC). Upon examination of all the mean 500 mb temperatures, the pattern seems to be the same for each day. There is an area of warmer temperatures located in the central United States with lower temperatures located along the Northeastern coast of the United States.

Appendix G. July Analysis

a.	b.

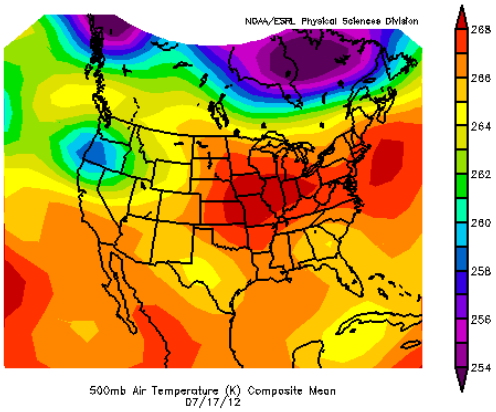
NOAA/ESRL Physical Sciences Division
268
266
264
262
260
258
256
254
500mb Air Temperature (K) Composite Mean
07/17/12
NCEP/NCAR Reanalysis

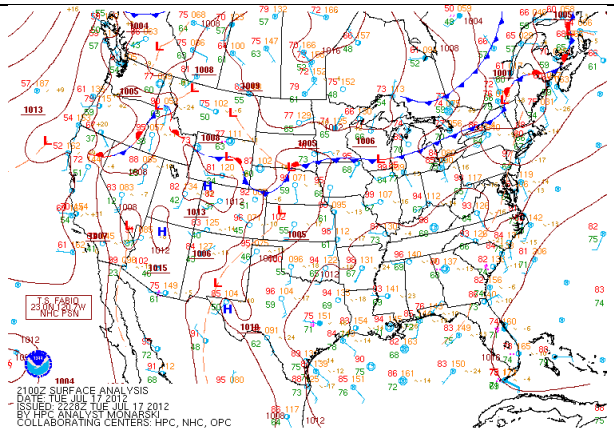
T.S. FABIO
23.0N 130.7W
NHC FSN
2100Z SURFACE ANALYSIS
DATE: TUE JUL 17 2012
ISSUED: 2228Z TUE JUL 17 2012
BY HPC ANALYST MONARSKI
COLLABORATING CENTERS: HPC, NHC, OPC

c.

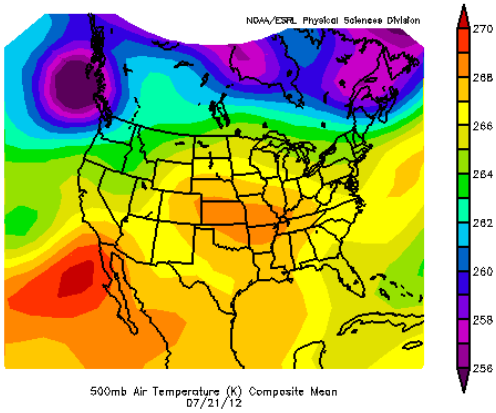
NOAA/ESRL Physical Sciences Division
270
268
266
264
262
260
258
256
500mb Air Temperature (K) Composite Mean
07/21/12
NCEP/NCAR Reanalysis

d.

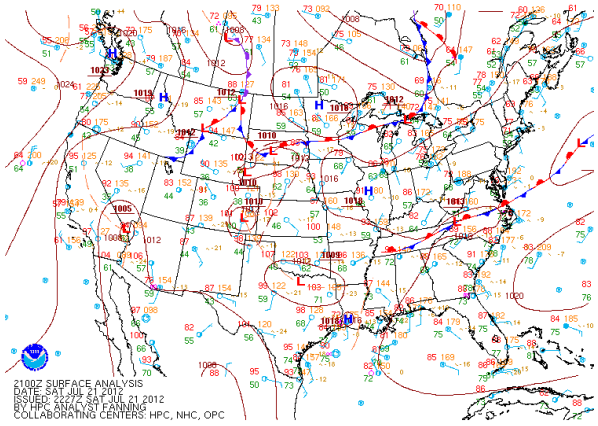
2100Z SURFACE ANALYSIS
DATE: SAT JUL 21 2012
ISSUED: 2227Z SAT JUL 21 2012
BY HPC ANALYST FANNING
COLLABORATING CENTERS: HPC, NHC, OPC

e.

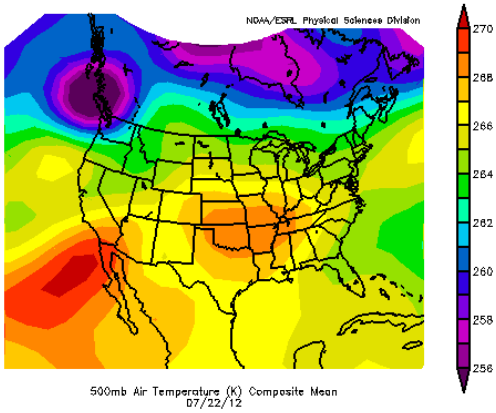
NOAA/ESRL Physical Sciences Division
270
268
266
264
262
260
258
256
500mb Air Temperature (K) Composite Mean
07/22/12
NCEP/NCAR Reanalysis

f.

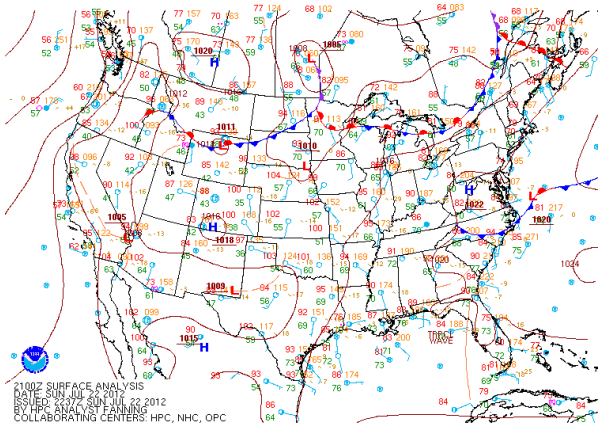
2100Z SURFACE ANALYSIS
DATE: SUN JUL 22 2012
ISSUED: 2227Z SUN JUL 22 2012
BY HPC ANALYST FANNING
COLLABORATING CENTERS: HPC, NHC, OPC

g.

h.

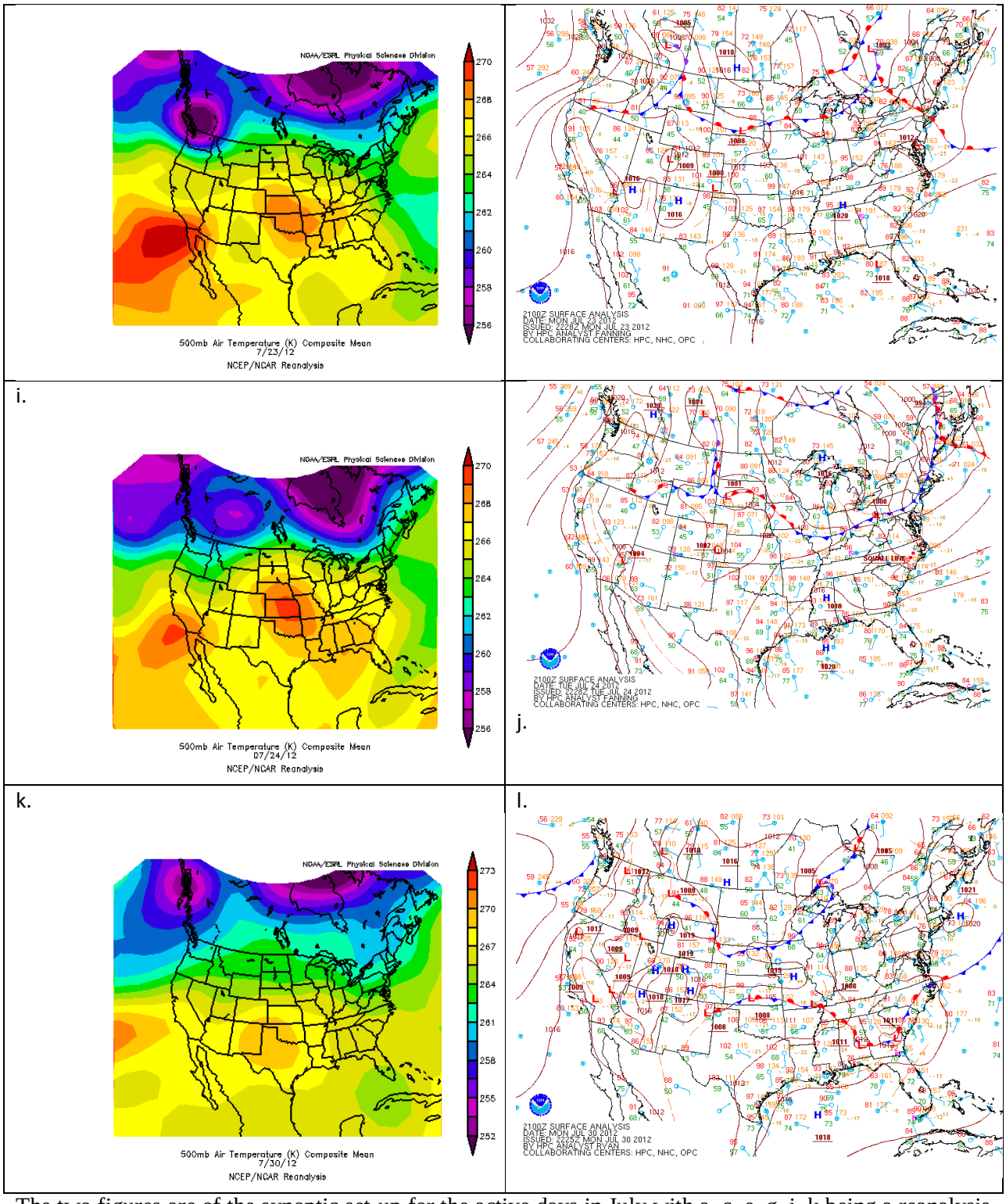

The two figures are of the synoptic set-up for the active days in July with a, c, e, g, i, k being a reanalysis map from NOAA's Earth System Research Laboratory (ESRL) daily mean composites of the 500 mb temperatures and b, d, f, h, j, l being a surface analysis map for 21Z from NOAA's Hydrometeorological Predication Center (HPC). Upon examination of all the mean 500 mb temperatures, the pattern seems to be the same for each day. There is an area of warmer temperatures located in the central United States

with lower temperatures located along the Northeastern coast of the United States. There is a slight difference to three of the days in July. For July 17th (figure a), July 21st (figure c) and July 30th (figure k) there is a cold pool located south of South Florida.

Appendix H. August Analysis

a.

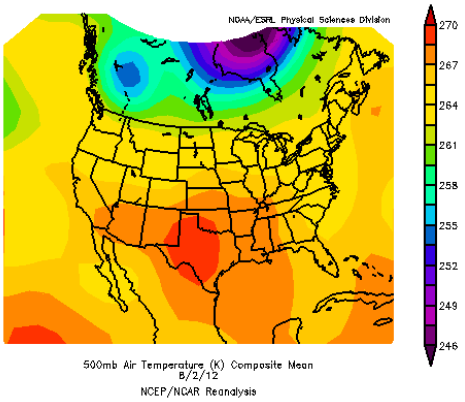

b.

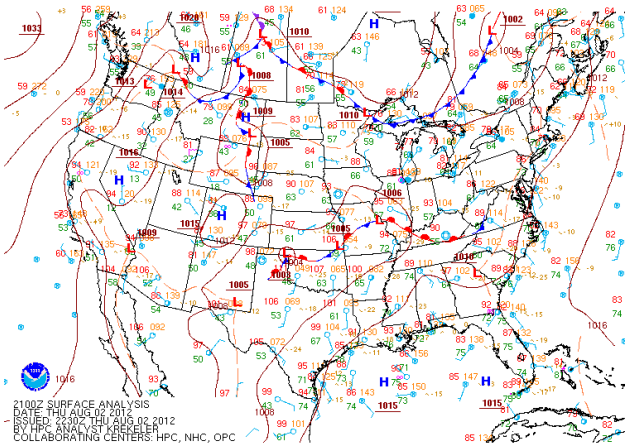

c.

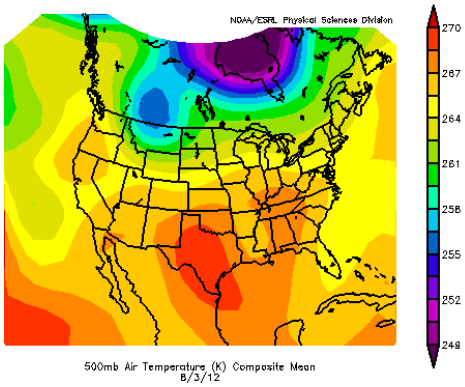

d.

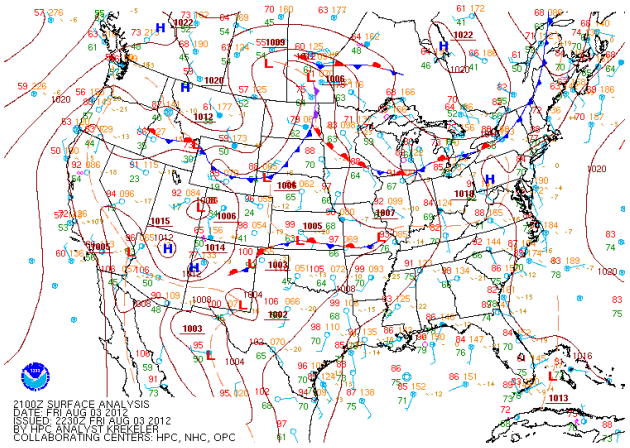

e.

f.

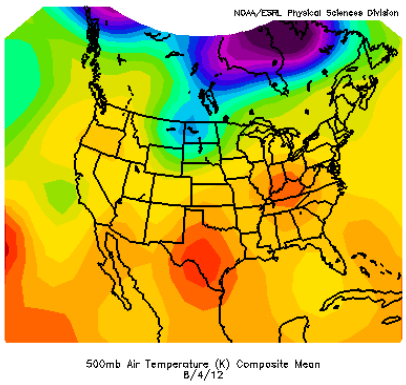

500mb Air Temperature (K) Composite Mean
8/4/12
NCEP/NCAR Reanalysis

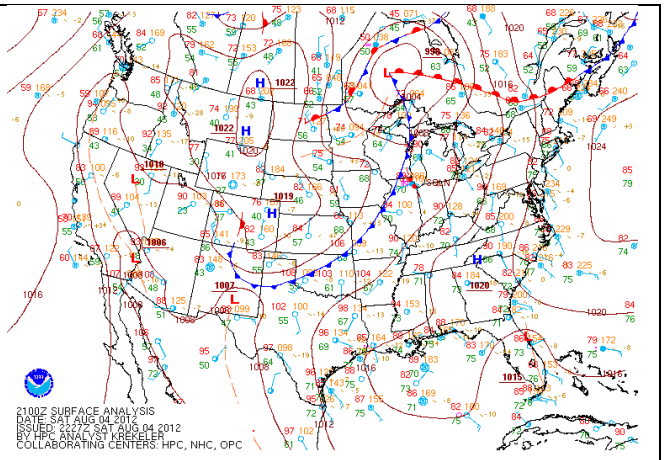

g.

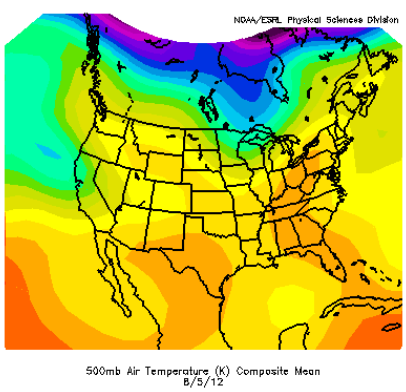

500mb Air Temperature (K) Composite Mean
8/5/12
NCEP/NCAR Reanalysis

h.

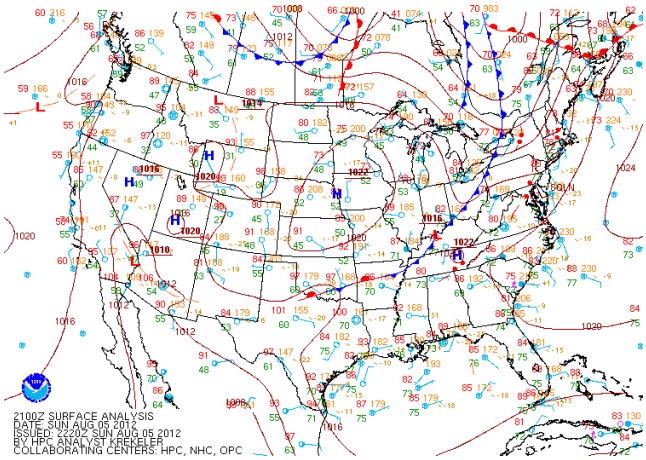

i.

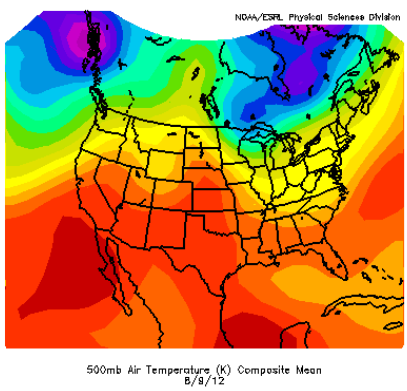

500mb Air Temperature (K) Composite Mean
8/9/12
NCEP/NCAR Reanalysis

j.

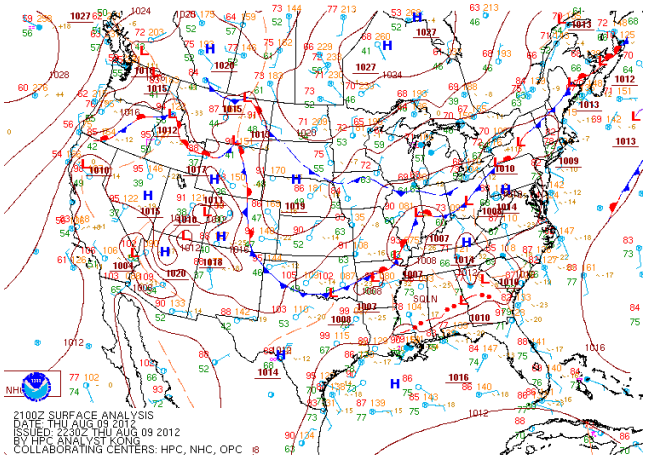

k.

l.

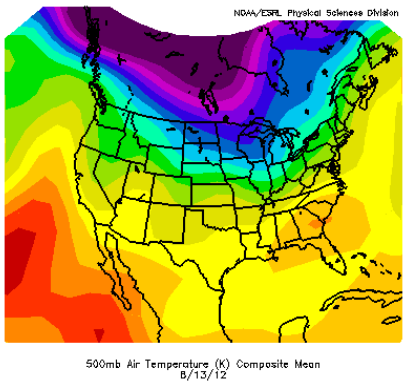

500mb Air Temperature (K) Composite Mean
8/13/12
NCEP/NCAR Reanalysis

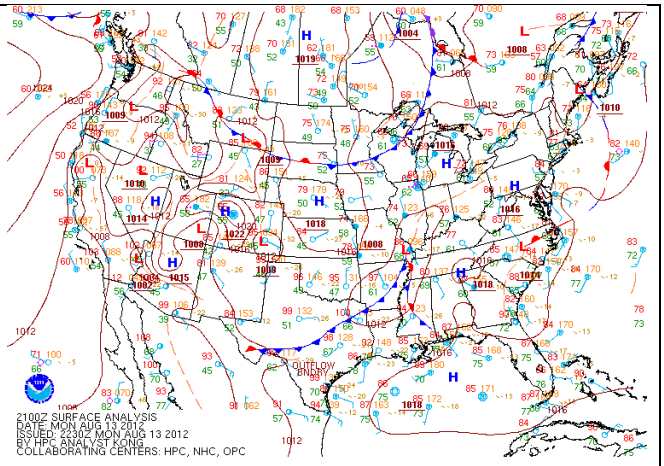

m.

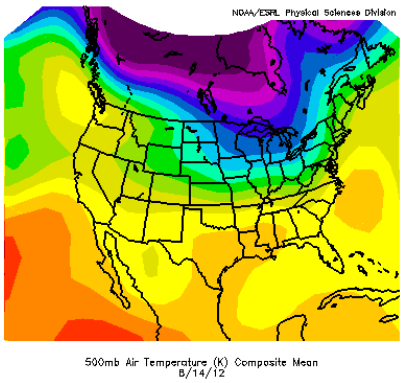

500mb Air Temperature (K) Composite Mean
8/14/12
NCEP/NCAR Reanalysis

n.

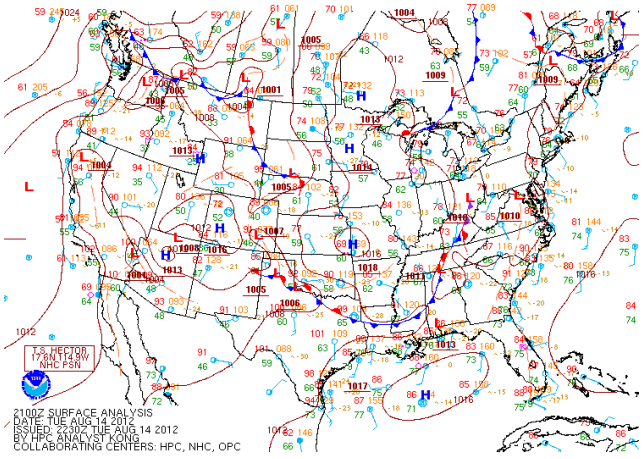

o.

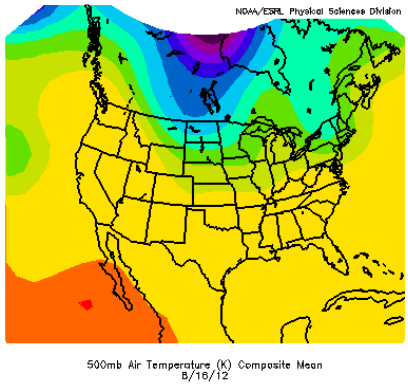

500mb Air Temperature (K) Composite Mean
8/16/12
NCEP/NCAR Reanalysis

p.

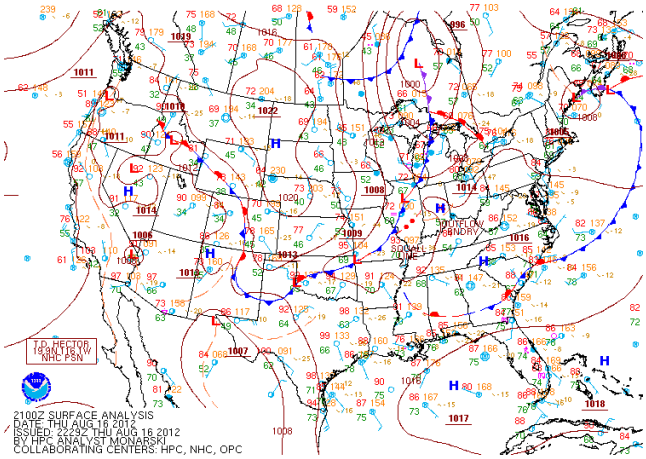

q.

r.

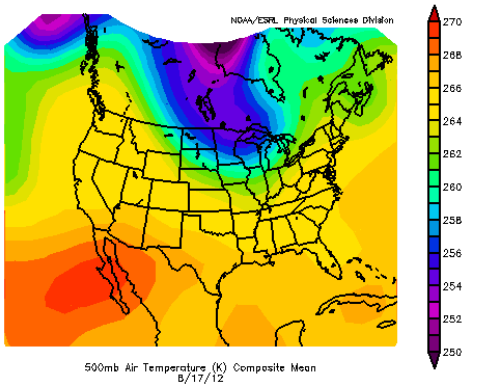

500mb Air Temperature (K) Composite Mean
8/17/12
NCEP/NCAR Reanalysis

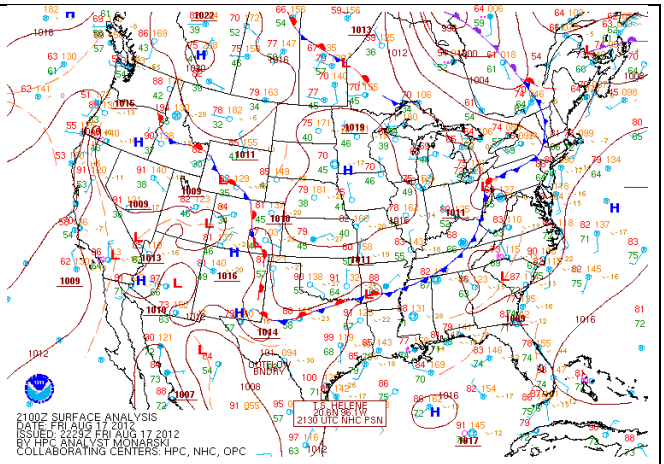

s.

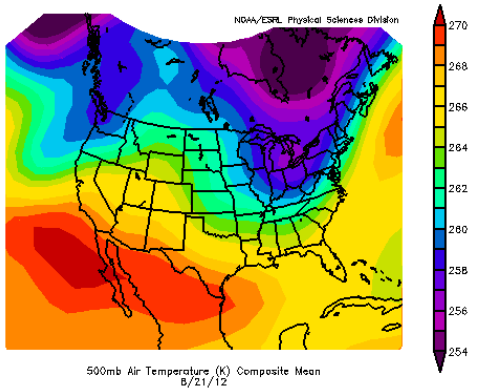

500mb Air Temperature (K) Composite Mean
8/21/12
NCEP/NCAR Reanalysis

t.

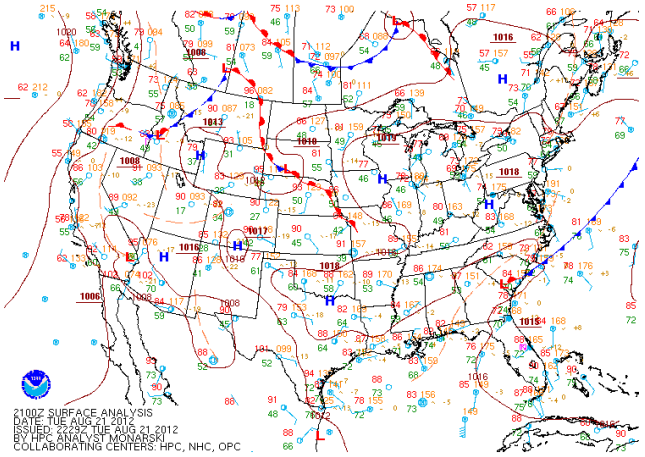

u.

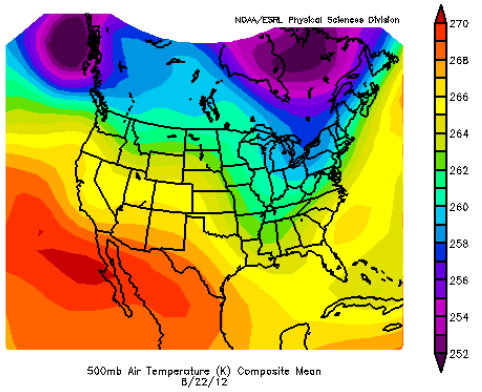

500mb Air Temperature (K) Composite Mean
8/22/12
NCEP/NCAR Reanalysis

v.

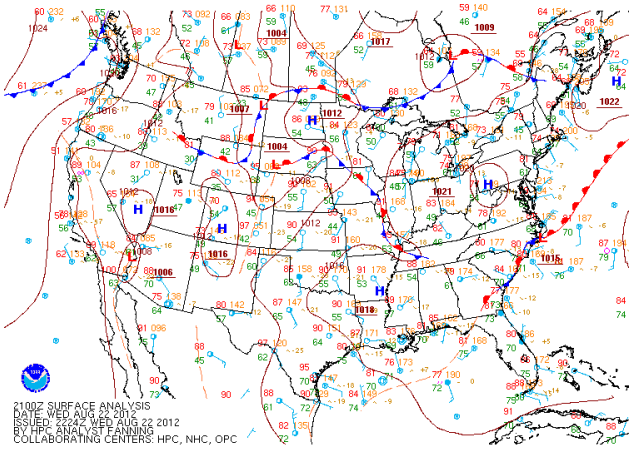

w.

x.

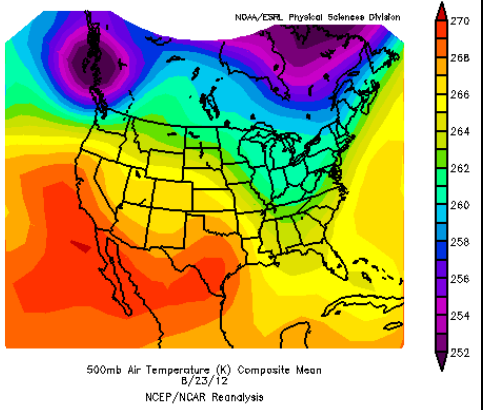

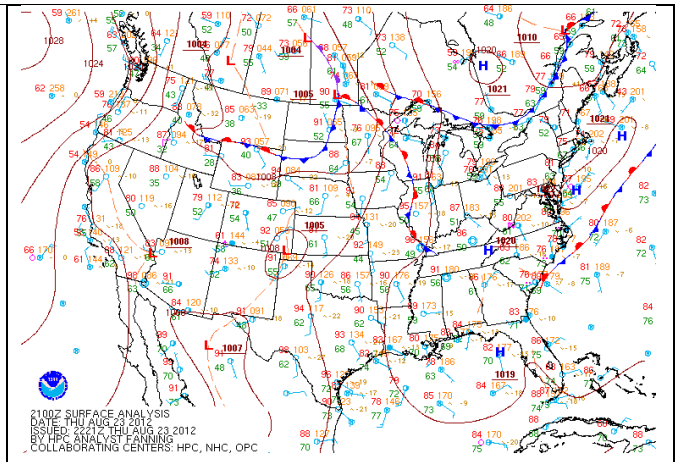

y.

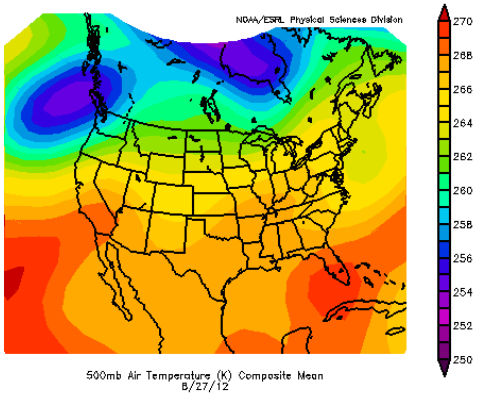

z.

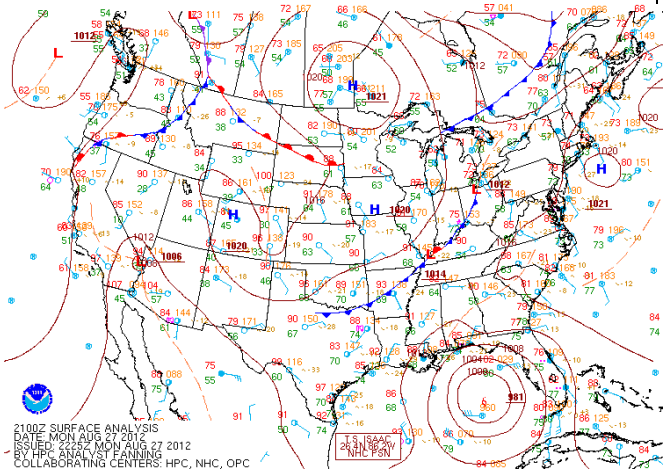

The two figures are of the synoptic set-up for the active days in August with a, c, e, g, i, k, m, o, q, s, u, w, y being a reanalysis map from NOAA's Earth System Research Laboratory (ESRL) daily mean composites of the 500 mb temperatures and b, d, f, h, j, l, n, p, r, t, v, x, z being a surface analysis map for 21Z from NOAA's Hydrometeorological Predication Center (HPC). Upon examination of all the mean 500 mb temperatures, the pattern seems to be the same for each day. There is an area of warmer temperatures located in the central United States with lower temperatures located along the Northeastern coast of the United States. Just like in July there are days that include a cold pool south of South Florida. For August there a lot more days that do so than in July. One day that was different was August 27th (figure y) that had a warm pool over and south of South Florida rather than a cold pool.

Appendix I. September Analysis

a.	b.

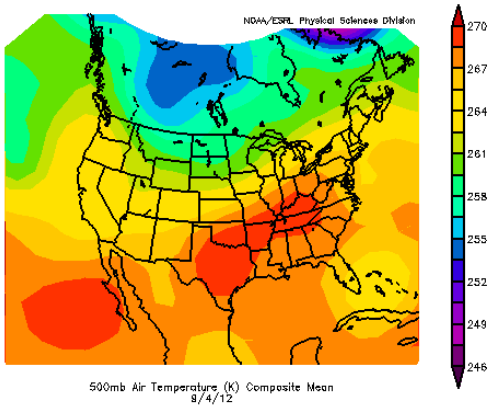

500mb Air Temperature (K) Composite Mean
9/4/12
NCEP/NCAR Reanalysis

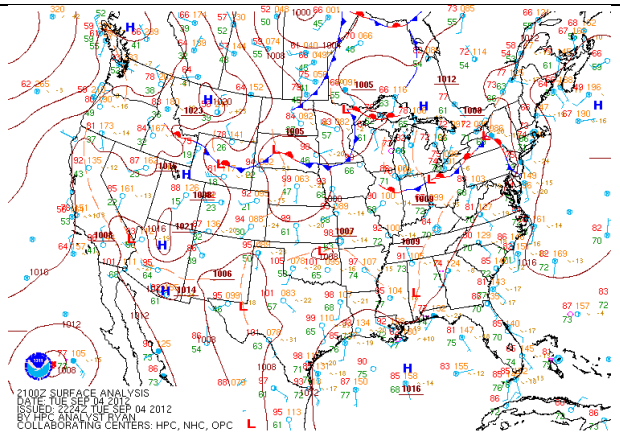

c.

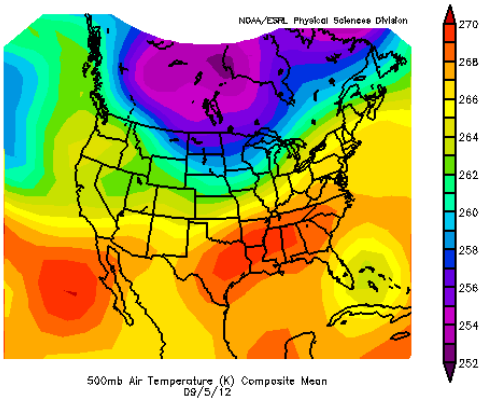

500mb Air Temperature (K) Composite Mean
09/5/12
NCEP/NCAR Reanalysis

d.

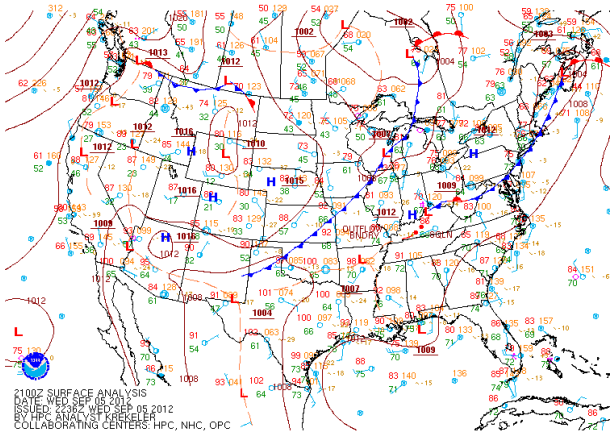

e.

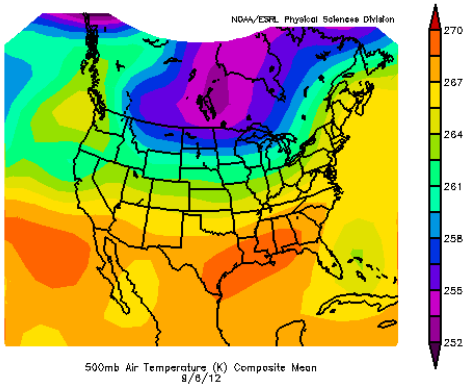

500mb Air Temperature (K) Composite Mean
9/6/12
NCEP/NCAR Reanalysis

f.

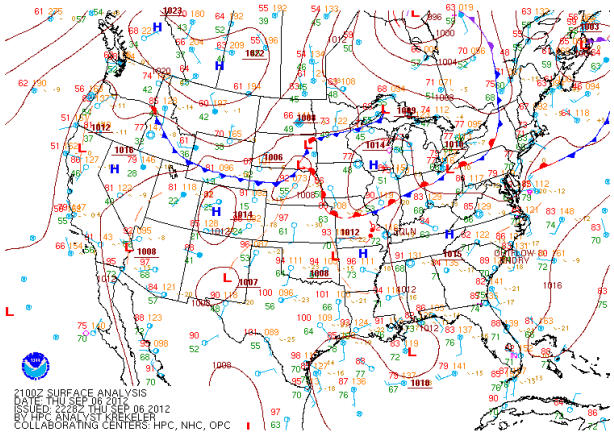

g.

h.

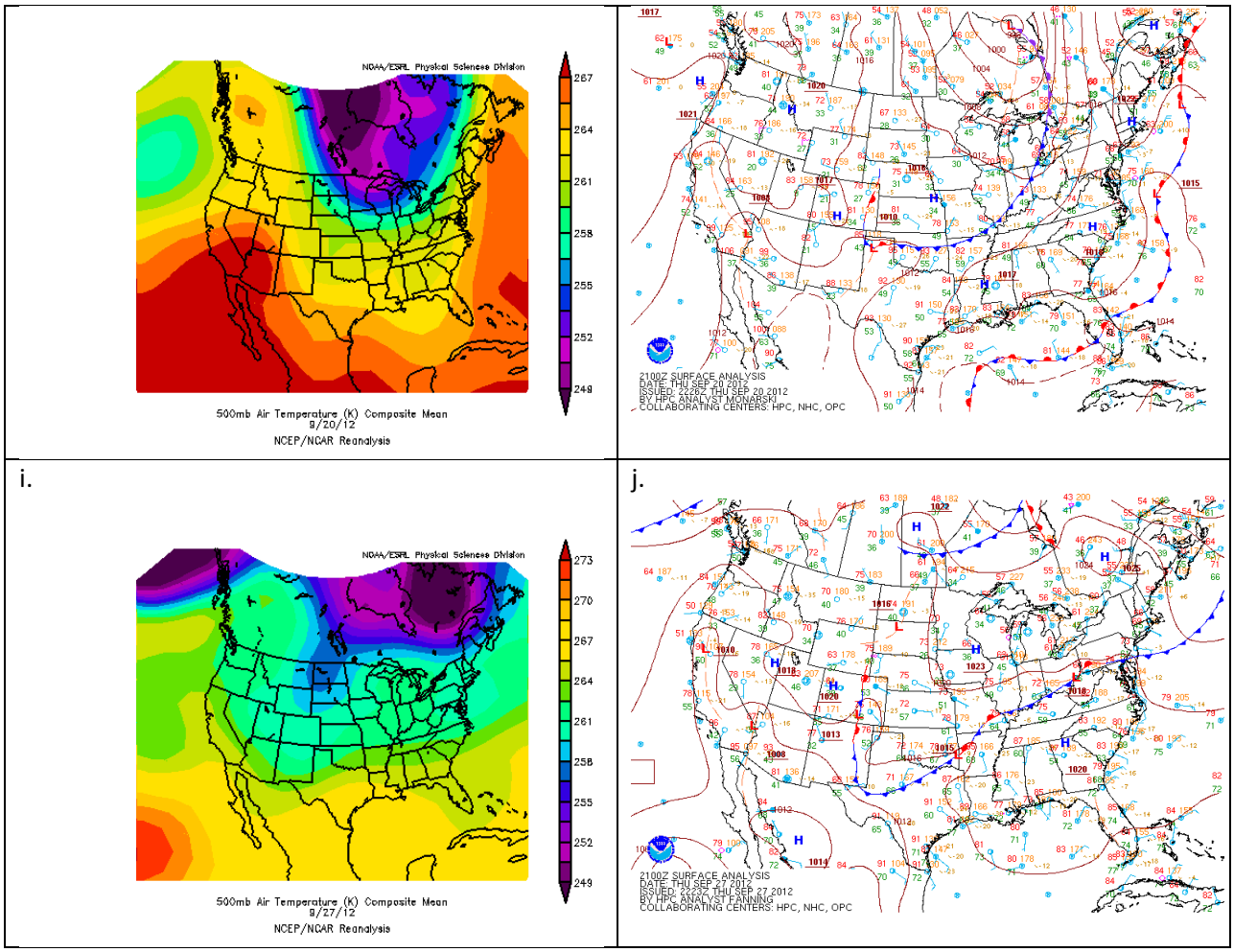

The two figures are of the synoptic set-up for the active days in September with a, c, e, g, i being a reanalysis map from NOAA's Earth System Research Laboratory (ESRL) daily mean composites of the 500 mb temperatures and b, d, f, h, j being a surface analysis map for 21Z from NOAA's Hydrometeorological Predication Center (HPC). Upon examination of all the mean 500 mb temperatures, the pattern seems to be the same for each day. There is an area of warmer temperatures located in the central United States with lower temperatures located along the Northeastern coast of the United States. For every active day in September, besides September 20th (figure g) and September 27th (figure i), there was a cold pool located around the South Florida area. The difference with the 20th and the 27th was that the cooler temperatures covered the entire United States.

Appendix J. Active Days 00Z Skew T Diagrams

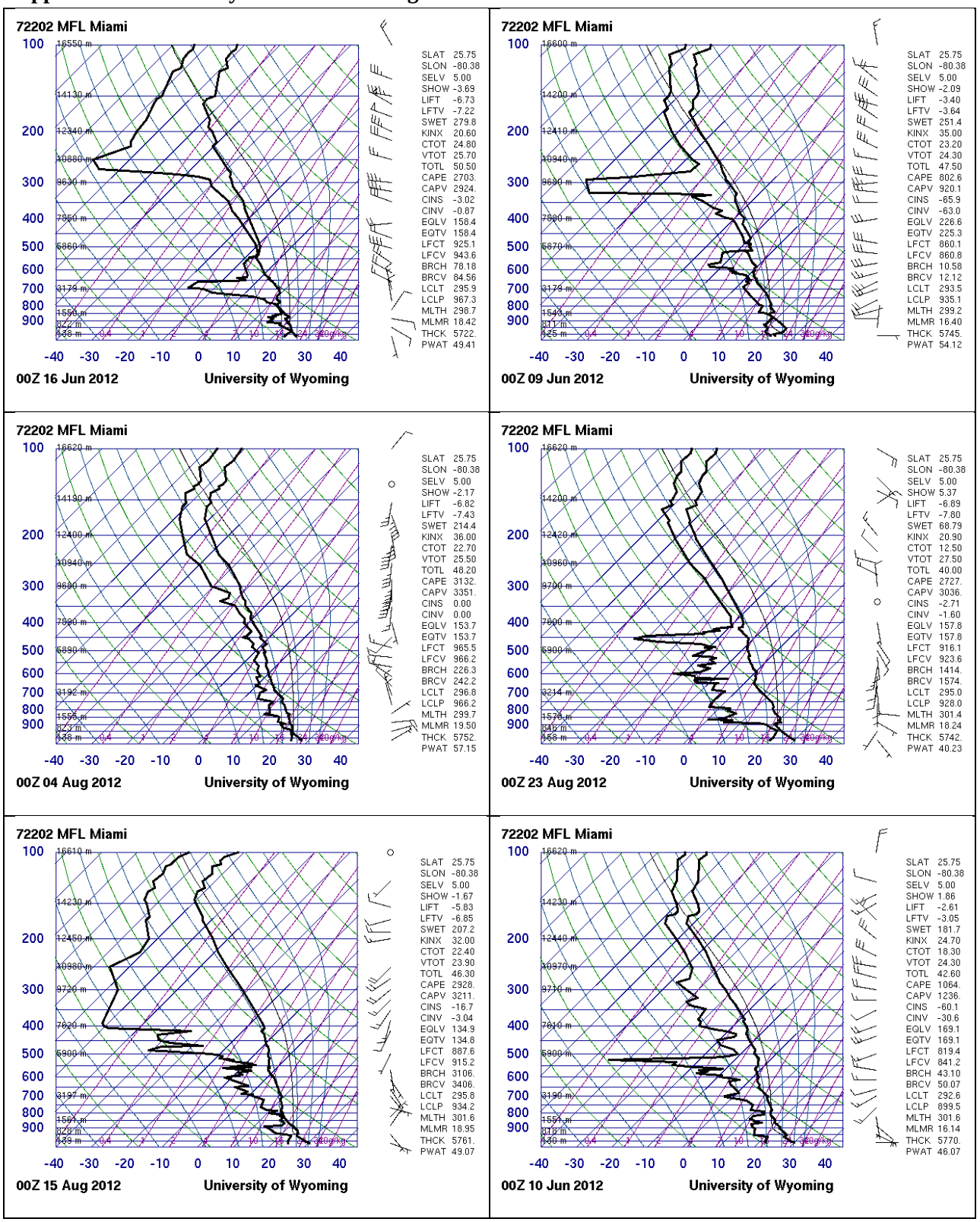

72202 MFL Miami

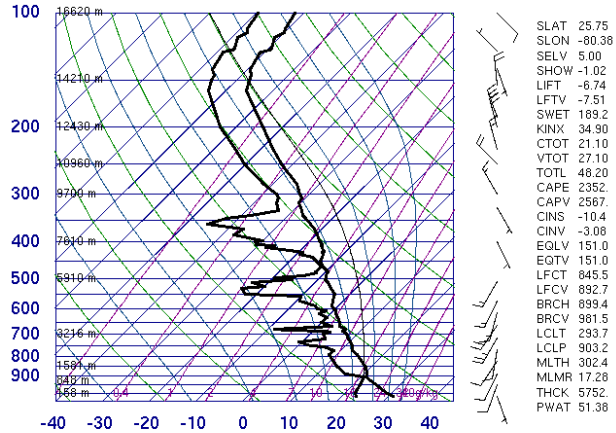

SLAT 25.75
SLON -80.38
SELV 5.00
SHOW -1.02
LIFT -6.74
LFTV -7.51
SWET 189.2
KINX 34.90
CTOT 21.10
VTOT 27.10
TOTL 48.20
CAPE 2352.
CAPV 2567.
CINS -10.4
CINV -3.08
EQLV 151.0
EQTV 151.0
LFCT 845.5
LFCV 892.7
BRCH 899.4
BRCV 981.5
LCLT 293.7
LCLP 903.2
MLTH 302.4
MLMR 17.28
THCK 5752.
PWAT 51.38

00Z 22 Aug 2012 University of Wyoming

72202 MFL Miami

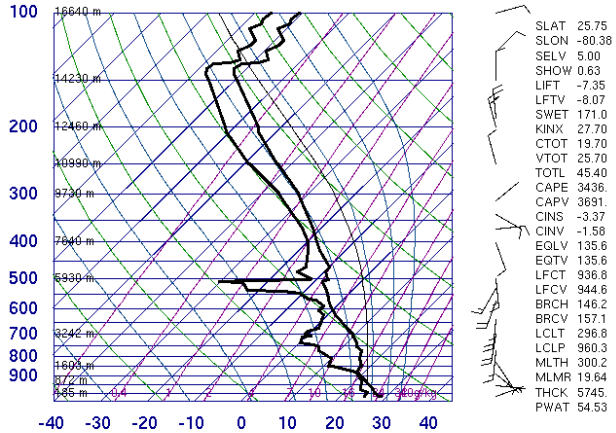

SLAT 25.75
SLON -80.38
SELV 5.00
SHOW 0.63
LIFT -7.35
LFTV -8.07
SWET 171.0
KINX 27.70
CTOT 19.70
VTOT 25.70
TOTL 45.40
CAPE 3436.
CAPV 3691.
CINS -3.37
CINV -1.58
EQLV 135.6
EQTV 135.6
LFCT 936.8
LFCV 944.6
BRCH 146.2
BRCV 157.1
LCLT 296.8
LCLP 960.3
MLTH 300.2
MLMR 19.64
THCK 5745.
PWAT 54.53

00Z 24 Jul 2012 University of Wyoming

72202 MFL Miami

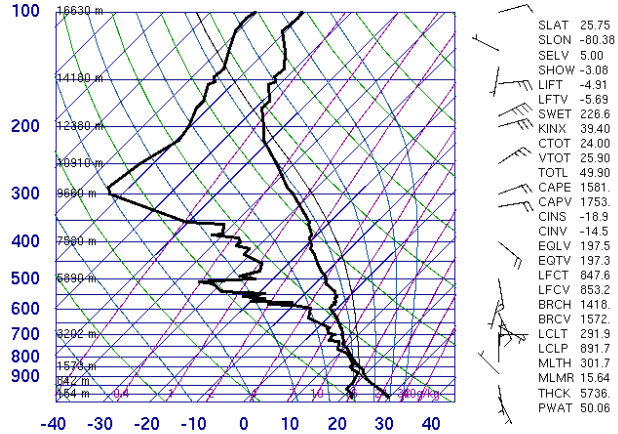

SLAT 25.75
SLON -80.38
SELV 5.00
SHOW -3.08
LIFT -4.91
LFTV -5.69
SWET 226.6
KINX 39.40
CTOT 24.00
VTOT 25.90
TOTL 49.90
CAPE 1581.
CAPV 1753.
CINS -18.9
CINV -14.5
EQLV 197.5
EQTV 197.3
LFCT 847.6
LFCV 853.2
BRCH 1418.
BRCV 1572.
LCLT 291.9
LCLP 891.7
MLTH 301.7
MLMR 15.64
THCK 5736.
PWAT 50.06

00Z 31 Jul 2012 University of Wyoming

72202 MFL Miami

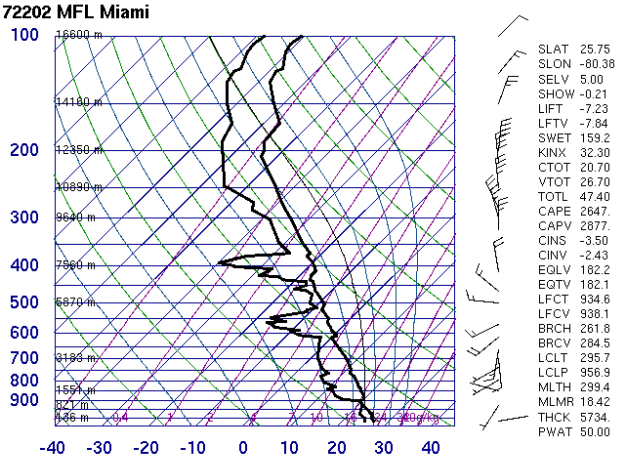

SLAT 25.75
SLON -80.38
SELV 5.00
SHOW -0.21
LIFT -7.23
LFTV -7.84
SWET 159.2
KINX 32.30
CTOT 20.70
VTOT 26.70
TOTL 47.40
CAPE 2647.
CAPV 2877.
CINS -3.50
CINV -2.43
EQLV 182.2
EQTV 182.1
LFCT 934.6
LFCV 938.1
BRCH 261.6
BRCV 284.5
LCLT 295.7
LCLP 956.9
MLTH 299.4
MLMR 18.42
THCK 5734.
PWAT 50.00

00Z 06 Sep 2012 University of Wyoming

72202 MFL Miami

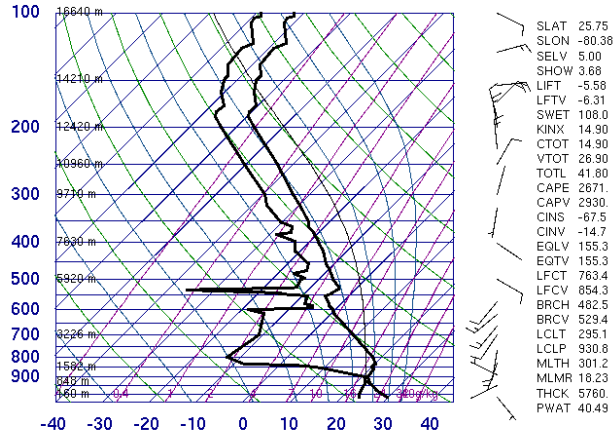

SLAT 25.75
SLON -80.38
SELV 5.00
SHOW 3.68
LIFT -5.58
LFTV -6.31
SWET 108.0
KINX 14.90
CTOT 14.90
VTOT 26.90
TOTL 41.80
CAPE 2671.
CAPV 2930.
CINS -67.5
CINV -14.7
EQLV 155.3
EQTV 155.3
LFCT 763.4
LFCV 854.3
BRCH 462.5
BRCV 529.4
LCLT 295.1
LCLP 930.8
MLTH 301.2
MLMR 18.23
THCK 5760.
PWAT 40.49

00Z 25 Jul 2012 University of Wyoming

72202 MFL Miami

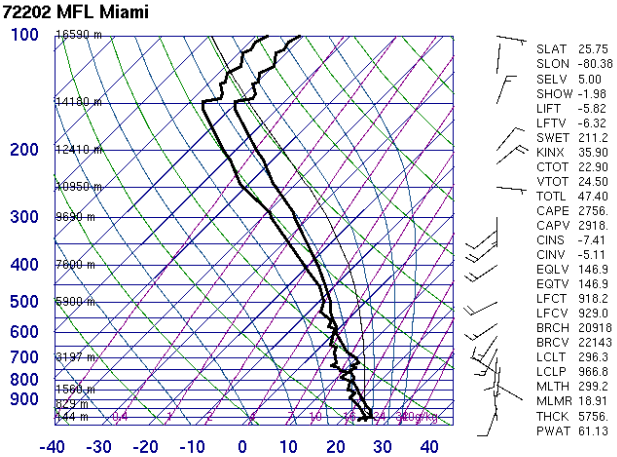

SLAT 25.75
SLON -80.38
SELV 5.00
SHOW -1.98
LIFT -5.82
LFTV -6.32
SWET 211.2
KINX 35.90
CTOT 22.90
VTOT 24.50
TOTL 47.40
CAPE 2756.
CAPV 2918.
CINS -7.41
CINV -5.11
EQLV 146.9
EQTV 146.9
LFCT 918.2
LFCV 929.0
BRCH 20916
BRCV 22143
LCLT 296.3
LCLP 966.8
MLTH 299.2
MLMR 18.91
THCK 5756.
PWAT 61.13

00Z 18 Aug 2012 University of Wyoming

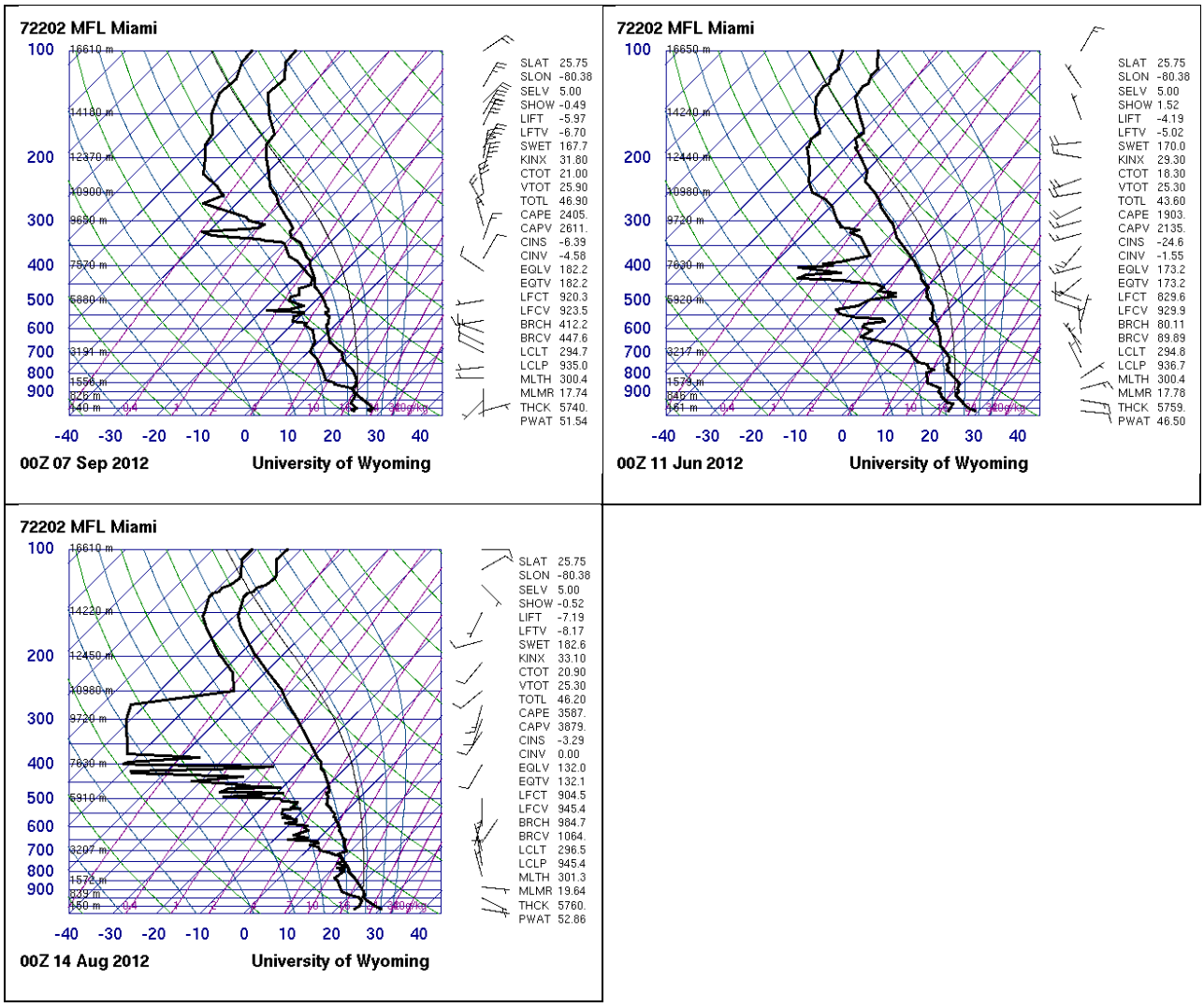

Skew-T diagrams at 00Z for 15 of the 31 active days obtained from Wyoming Weather Web. The order of the soundings is placed from left to right by greatest number of strikes. The order goes as follows: June 15, June 8, August 3, August 22, August 14, June 9, August 21, July 23, July 30, September 5, July 24, August 17, September 6, June 10, and August 13.

Appendix K. Non- Active Days 00Z Skew T Diagrams

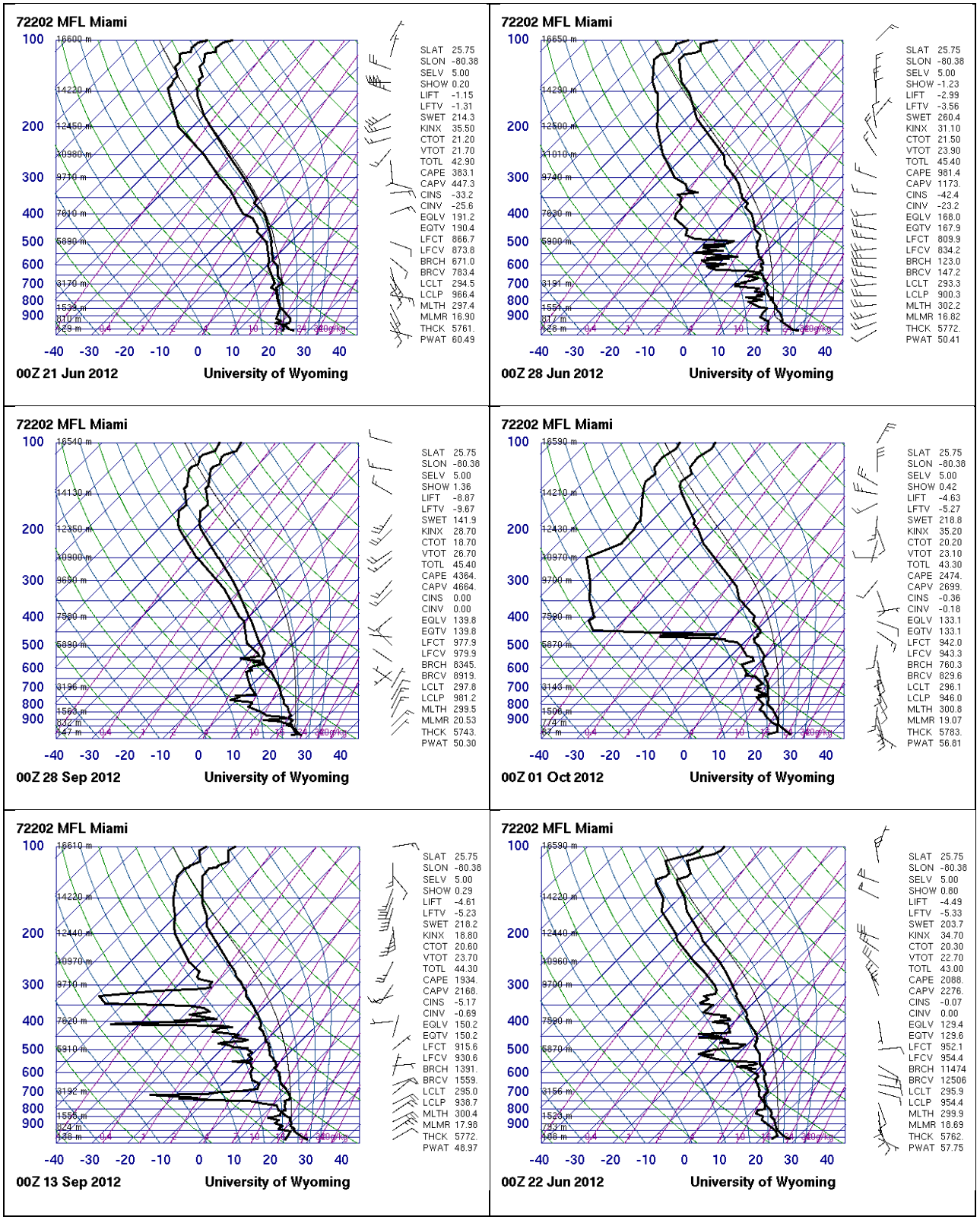

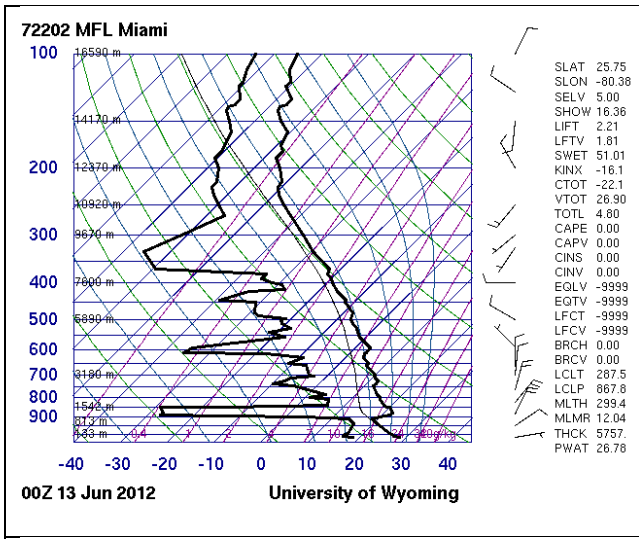
72202 MFL Miami
SLAT 25.75
SLON -80.38
SELV 5.00
SHOW 16.36
LIFT 2.21
LFTV 1.81
SWET 51.01
KINX -16.1
CTOT -22.1
VTOT 26.90
TOTL 4.80
CAPE 0.00
CAPV 0.00
CINS 0.00
CINV 0.00
EQLV -9999
EQTV -9999
LFCT -9999
LFCV -9999
BRCH 0.00
BRCV 0.00
LCLT 287.5
LCLP 867.6
MLTH 299.4
MLMR 12.04
THCK 5757.
PWAT 26.78
00Z 13 Jun 2012
University of Wyoming

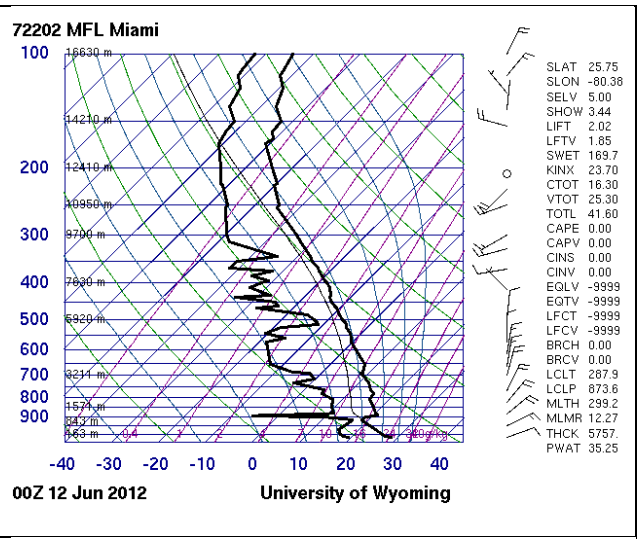
72202 MFL Miami
SLAT 25.75
SLON -80.38
SELV 5.00
SHOW 3.44
LIFT 2.02
LFTV 1.85
SWET 169.7
KINX 23.70
CTOT 16.30
VTOT 25.30
TOTL 41.60
CAPE 0.00
CAPV 0.00
CINS 0.00
CINV 0.00
EQLV -9999
EQTV -9999
LFCT -9999
LFCV -9999
BRCH 0.00
BRCV 0.00
LCLT 287.9
LCLP 873.6
MLTH 299.2
MLMR 12.27
THCK 5757.
PWAT 35.25
00Z 12 Jun 2012
University of Wyoming

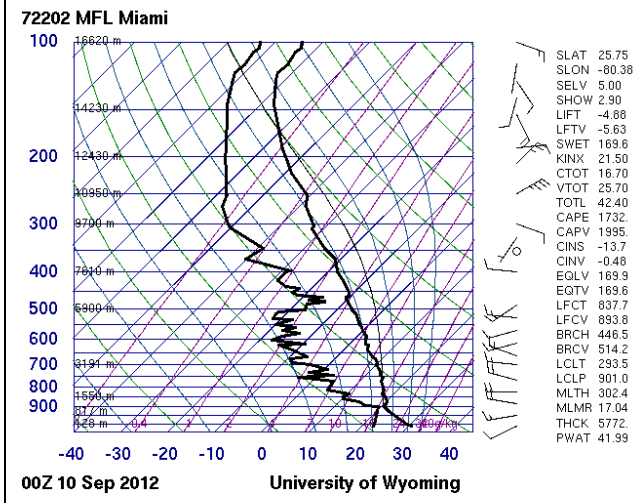
72202 MFL Miami
SLAT 25.75
SLON -80.38
SELV 5.00
SHOW 2.90
LIFT -4.88
LFTV -5.63
SWET 169.6
KINX 21.50
CTOT 16.70
VTOT 25.70
TOTL 42.40
CAPE 1732.
CAPV 1995.
CINS -13.7
CINV -0.48
EQLV 169.9
EQTV 169.6
LFCT 837.7
LFCV 893.8
BRCH 446.5
BRCV 514.2
LCLT 293.5
LCLP 901.0
MLTH 302.4
MLMR 17.04
THCK 5772.
PWAT 41.99
00Z 10 Sep 2012
University of Wyoming

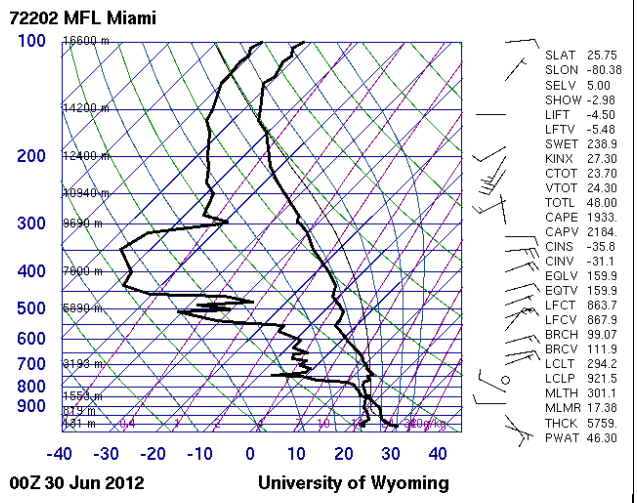
72202 MFL Miami
SLAT 25.75
SLON -80.38
SELV 5.00
SHOW -2.98
LIFT -4.50
LFTV -5.48
SWET 238.9
KINX 27.30
CTOT 23.70
VTOT 24.30
TOTL 48.00
CAPE 1933.
CAPV 2184.
CINS -35.8
CINV -31.1
EQLV 159.9
EQTV 159.9
LFCT 863.7
LFCV 867.9
BRCH 99.07
BRCV 111.9
LCLT 294.2
LCLP 921.5
MLTH 301.1
MLMR 17.38
THCK 5759.
PWAT 46.30
00Z 30 Jun 2012
University of Wyoming

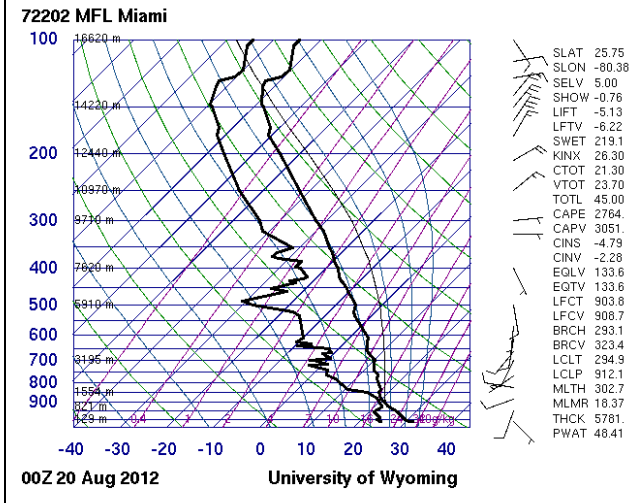
72202 MFL Miami
SLAT 25.75
SLON -80.38
SELV 5.00
SHOW -0.76
LIFT -5.13
LFTV -6.22
SWET 219.1
KINX 26.30
CTOT 21.30
VTOT 23.70
TOTL 45.00
CAPE 2764.
CAPV 3051.
CINS -4.79
CINV -2.28
EQLV 133.6
EQTV 133.6
LFCT 903.8
LFCV 908.7
BRCH 293.1
BRCV 323.4
LCLT 294.9
LCLP 912.1
MLTH 302.7
MLMR 18.37
THCK 5781.
PWAT 48.41
00Z 20 Aug 2012
University of Wyoming

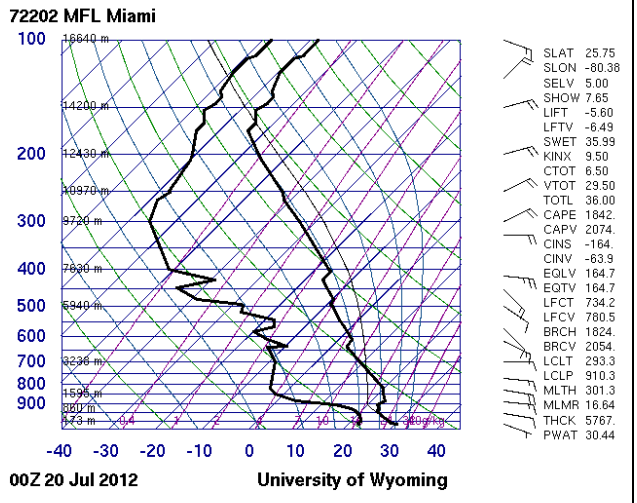
72202 MFL Miami
SLAT 25.75
SLON -80.38
SELV 5.00
SHOW 7.65
LIFT -5.60
LFTV -6.49
SWET 35.99
KINX 9.50
CTOT 6.50
VTOT 29.50
TOTL 36.00
CAPE 1642.
CAPV 2074.
CINS -164.
CINV -63.9
EQLV 164.7
EQTV 164.7
LFCT 734.2
LFCV 780.5
BRCH 1824.
BRCV 2054.
LCLT 293.3
LCLP 910.3
MLTH 301.3
MLMR 16.64
THCK 5767.
PWAT 30.44
00Z 20 Jul 2012
University of Wyoming

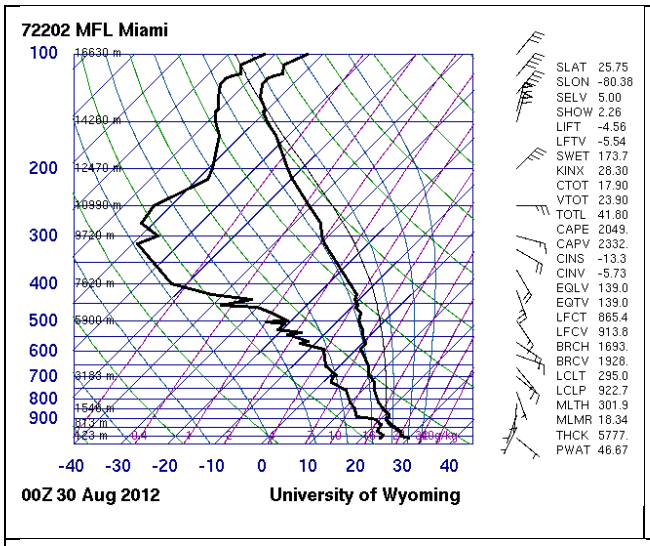
72202 MFL Miami
100
200
300
400
500
600
700
800
900
16630 m
14260 m
12470 m
10990 m
9720 m
7620 m
6900 m
3183 m
1546 m
813 m
423 m
-40 -30 -20 -10 0 10 20 30 40
00Z 30 Aug 2012
University of Wyoming
SLAT 25.75
SLON -80.38
SELV 5.00
SHOW 2.26
LIFT -4.56
LFTV -5.54
SWET 173.7
KINX 28.30
CTOT 17.90
VTOT 23.90
TOTL 41.80
CAPE 2049.
CAPV 2332.
CINS -13.3
CINV -5.73
EQLV 139.0
EQTV 139.0
LFCT 865.4
LFCV 913.8
BRCH 1693.
BRCV 1928.
LCLT 295.0
LCLP 922.7
MLTH 301.9
MLMR 18.34
THCK 5777.
PWAT 46.67

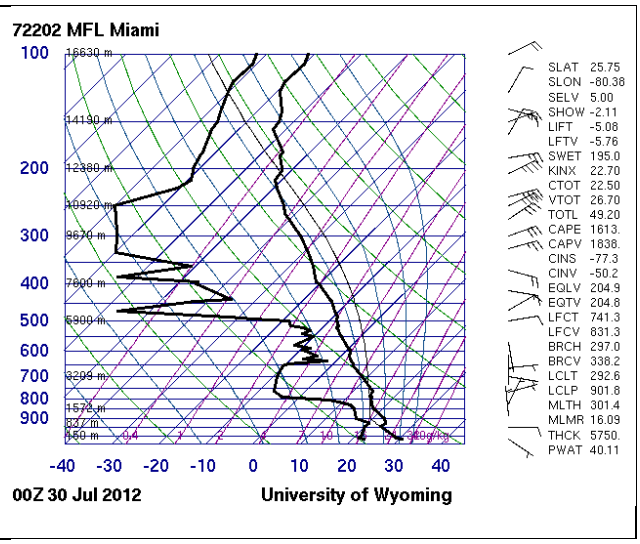
72202 MFL Miami
100
200
300
400
500
600
700
800
900
16630 m
14190 m
12380 m
10920 m
9670 m
7600 m
6900 m
3209 m
1574 m
837 m
450 m
-40 -30 -20 -10 0 10 20 30 40
00Z 30 Jul 2012
University of Wyoming
SLAT 25.75
SLON -80.38
SELV 5.00
SHOW -2.11
LIFT -5.08
LFTV -5.76
SWET 195.0
KINX 22.70
CTOT 22.50
VTOT 26.70
TOTL 49.20
CAPE 1613.
CAPV 1838.
CINS -77.3
CINV -50.2
EQLV 204.9
EQTV 204.8
LFCT 741.3
LFCV 831.3
BRCH 297.0
BRCV 338.2
LCLT 292.6
LCLP 901.8
MLTH 301.4
MLMR 16.09
THCK 5750.
PWAT 40.11

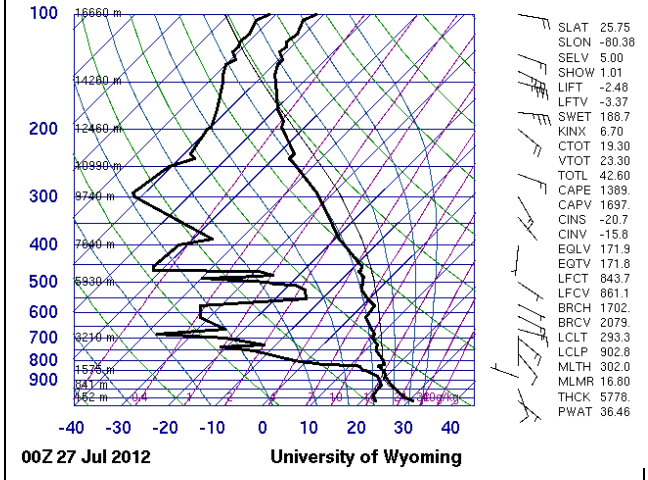
72202 MFL Miami
100
200
300
400
500
600
700
800
900
16660 m
14260 m
12460 m
10990 m
9740 m
7840 m
6930 m
3210 m
1575 m
841 m
452 m
-40 -30 -20 -10 0 10 20 30 40
00Z 27 Jul 2012
University of Wyoming
SLAT 25.75
SLON -80.38
SELV 5.00
SHOW 1.01
LIFT -2.48
LFTV -3.37
SWET 188.7
KINX 6.70
CTOT 19.30
VTOT 23.30
TOTL 42.60
CAPE 1389.
CAPV 1697.
CINS -20.7
CINV -15.8
EQLV 171.9
EQTV 171.8
LFCT 843.7
LFCV 861.1
BRCH 1702.
BRCV 2079.
LCLT 293.3
LCLP 902.8
MLTH 302.0
MLMR 16.80
THCK 5778.
PWAT 36.46

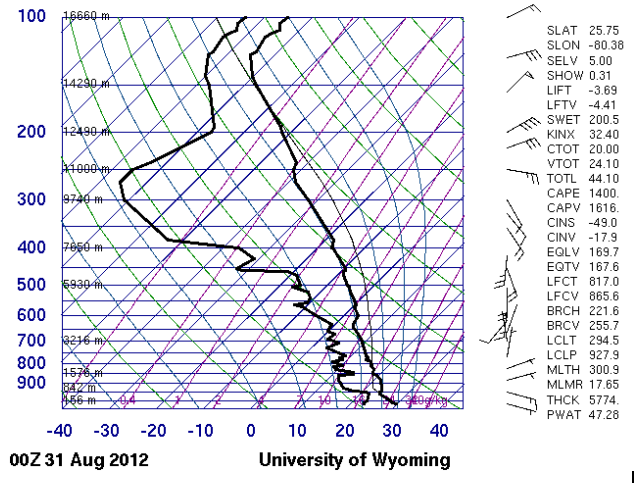
72202 MFL Miami
100
200
300
400
500
600
700
800
900
16660 m
14230 m
12490 m
11000 m
9740 m
7850 m
6930 m
3216 m
1576 m
842 m
456 m
-40 -30 -20 -10 0 10 20 30 40
00Z 31 Aug 2012
University of Wyoming
SLAT 25.75
SLON -80.38
SELV 5.00
SHOW 0.31
LIFT -3.69
LFTV -4.41
SWET 200.5
KINX 32.40
CTOT 20.00
VTOT 24.10
TOTL 44.10
CAPE 1400.
CAPV 1616.
CINS -49.0
CINV -17.9
EQLV 169.7
EQTV 167.6
LFCT 817.0
LFCV 865.6
BRCH 221.6
BRCV 255.7
LCLT 294.5
LCLP 927.9
MLTH 300.9
MLMR 17.65
THCK 5774.
PWAT 47.28

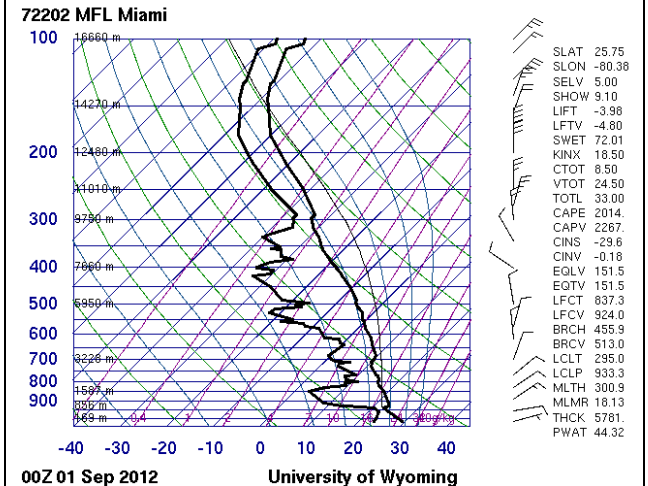
72202 MFL Miami
100
200
300
400
500
600
700
800
900
16660 m
14270 m
12480 m
11010 m
9790 m
7660 m
6950 m
3228 m
1585 m
859 m
469 m
-40 -30 -20 -10 0 10 20 30 40
00Z 01 Sep 2012
University of Wyoming
SLAT 25.75
SLON -80.38
SELV 5.00
SHOW 9.10
LIFT -3.98
LFTV -4.80
SWET 72.01
KINX 18.50
CTOT 8.50
VTOT 24.50
TOTL 33.00
CAPE 2014.
CAPV 2267.
CINS -29.6
CINV -0.18
EQLV 151.5
EQTV 151.5
LFCT 837.3
LFCV 924.0
BRCH 455.9
BRCV 513.0
LCLT 295.0
LCLP 933.3
MLTH 300.9
MLMR 18.13
THCK 5781.
PWAT 44.32

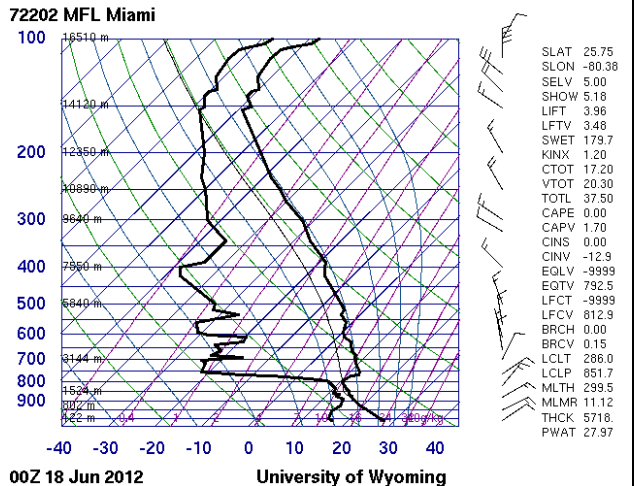
72202 MFL Miami
100
200
300
400
500
600
700
800
900
16510 m
14120 m
12350 m
10890 m
9640 m
7850 m
6840 m
3144 m
1524 m
802 m
422 m
-40 -30 -20 -10 0 10 20 30 40
00Z 18 Jun 2012
University of Wyoming
SLAT 25.75
SLON -80.38
SELV 5.00
SHOW 5.18
LIFT 3.96
LFTV 3.48
SWET 179.7
KINX 1.20
CTOT 17.20
VTOT 20.30
TOTL 37.50
CAPE 0.00
CAPV 1.70
CINS 0.00
CINV -12.9
EQLV -9999
EQTV 792.5
LFCT -9999
LFCV 812.9
BRCH 0.00
BRCV 0.15
LCLT 286.0
LCLP 851.7
MLTH 299.5
MLMR 11.12
THCK 5718.
PWAT 27.97

72202 MFL Miami

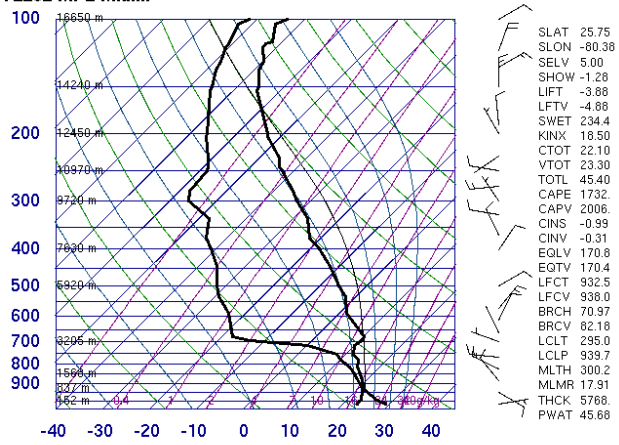

SLAT 25.75
SLON -80.38
SELV 5.00
SHOW -1.28
LIFT -3.88
LFTV -4.88
SWET 234.4
KINX 18.50
CTOT 22.10
VTOT 23.30
TOTL 45.40
CAPE 1732.
CAPV 2006.
CINS -0.99
CINV -0.31
EQLV 170.8
EQTV 170.4
LFCT 932.5
LFCV 938.0
BRCH 70.97
BRCV 82.16
LCLT 295.0
LCLP 939.7
MLTH 300.2
MLMR 17.91
THCK 5768.
PWAT 45.66

00Z 29 Jun 2012 University of Wyoming

72202 MFL Miami

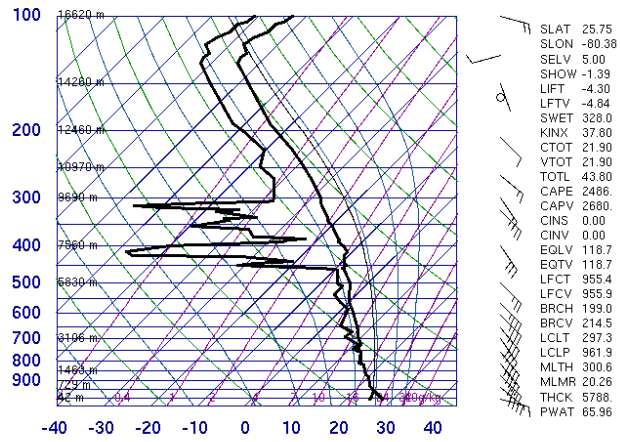

SLAT 25.75
SLON -80.38
SELV 5.00
SHOW -1.39
LIFT -4.30
LFTV -4.84
SWET 328.0
KINX 37.80
CTOT 21.90
VTOT 21.90
TOTL 43.80
CAPE 2486.
CAPV 2680.
CINS 0.00
CINV 0.00
EQLV 118.7
EQTV 118.7
LFCT 955.4
LFCV 955.9
BRCH 199.0
BRCV 214.5
LCLT 297.3
LCLP 961.9
MLTH 300.6
MLMR 20.26
THCK 5788.
PWAT 65.96

00Z 27 Aug 2012 University of Wyoming

72202 MFL Miami

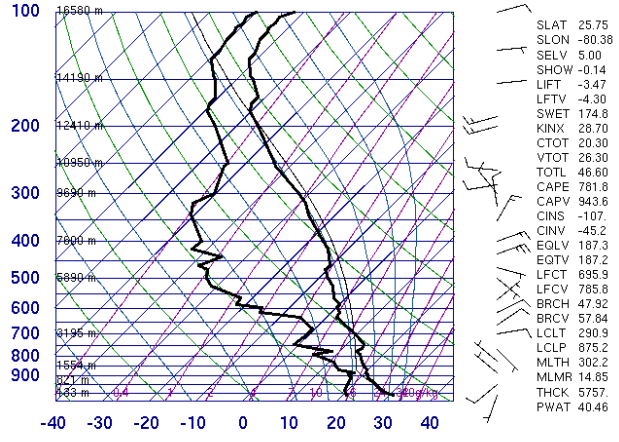

SLAT 25.75
SLON -80.38
SELV 5.00
SHOW -0.14
LIFT -3.47
LFTV -4.30
SWET 174.8
KINX 28.70
CTOT 20.30
VTOT 26.30
TOTL 46.60
CAPE 781.8
CAPV 943.6
CINS -107.
CINV -45.2
EQLV 187.3
EQTV 187.2
LFCT 695.9
LFCV 765.8
BRCH 47.92
BRCV 57.84
LCLT 290.9
LCLP 875.2
MLTH 302.2
MLMR 14.85
THCK 5757.
PWAT 40.46

00Z 01 Jul 2012 University of Wyoming

72202 MFL Miami

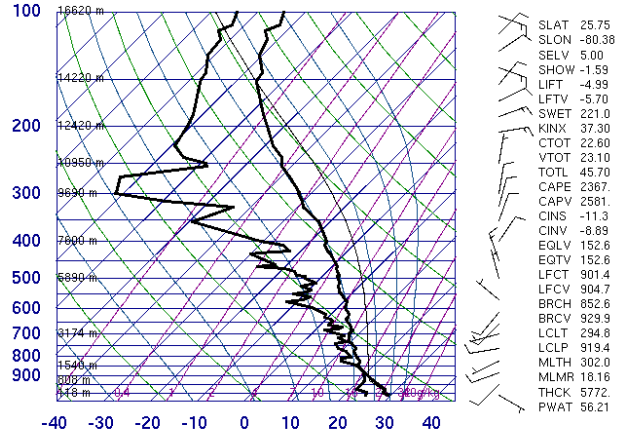

SLAT 25.75
SLON -80.38
SELV 5.00
SHOW -1.59
LIFT -4.99
LFTV -5.70
SWET 221.0
KINX 37.30
CTOT 22.60
VTOT 23.10
TOTL 45.70
CAPE 2367.
CAPV 2581.
CINS -11.3
CINV -8.89
EQLV 152.6
EQTV 152.6
LFCT 901.4
LFCV 904.7
BRCH 852.6
BRCV 929.9
LCLT 294.8
LCLP 919.4
MLTH 302.0
MLMR 18.16
THCK 5772.
PWAT 56.21

00Z 09 Sep 2012 University of Wyoming

72202 MFL Miami

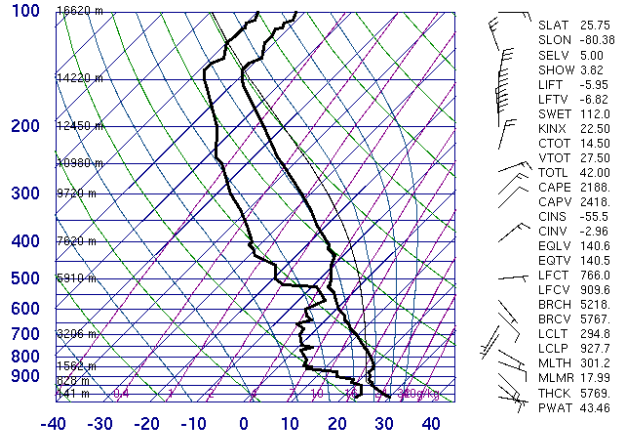

SLAT 25.75
SLON -80.38
SELV 5.00
SHOW 3.82
LIFT -5.95
LFTV -6.82
SWET 112.0
KINX 22.50
CTOT 14.50
VTOT 27.50
TOTL 42.00
CAPE 2188.
CAPV 2418.
CINS -55.5
CINV -2.96
EQLV 140.6
EQTV 140.5
LFCT 766.0
LFCV 909.6
BRCH 5218.
BRCV 5767.
LCLT 294.8
LCLP 927.7
MLTH 301.2
MLMR 17.99
THCK 5769.
PWAT 43.46

00Z 08 Aug 2012 University of Wyoming

72202 MFL Miami

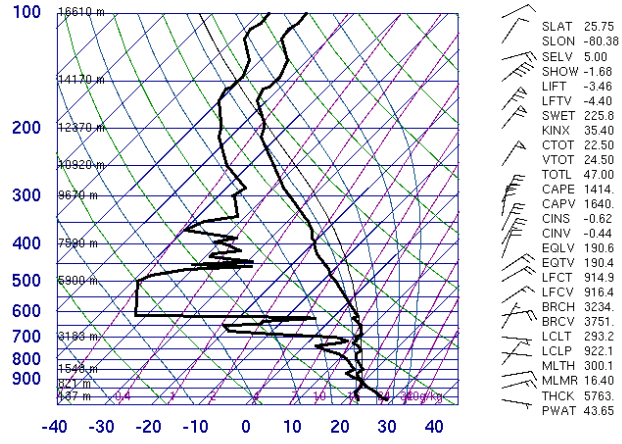

SLAT 25.75
SLON -80.38
SELV 5.00
SHOW -1.68
LIFT -3.46
LFTV -4.40
SWET 225.8
KINX 35.40
CTOT 22.50
VTOT 24.50
TOTL 47.00
CAPE 1414.
CAPV 1640.
CINS -0.62
CINV -0.44
EQLV 190.6
EQTV 190.4
LFCT 914.9
LFCV 916.4
BRCH 3234.
BRCV 3751.
LCLT 293.2
LCLP 922.1
MLTH 300.1
MLMR 16.40
THCK 5763.
PWAT 43.65

00Z 03 Sep 2012 University of Wyoming

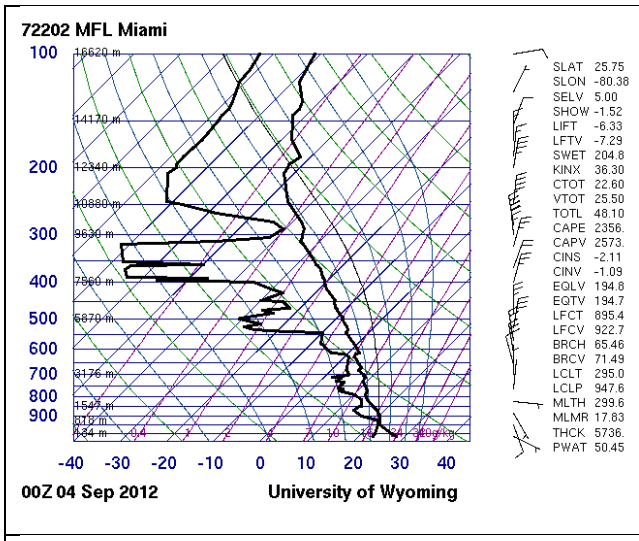
72202 MFL Miami
SLAT 25.75
SLON -80.38
SELV 5.00
SHOW -1.52
LIFT -6.33
LFTV -7.29
SWET 204.8
KINX 36.30
CTOT 22.60
VTOT 25.50
TOTL 48.10
CAPE 2356.
CAPV 2573.
CINS -2.11
CINV -1.09
EQLV 194.8
EQTV 194.7
LFCT 895.4
LFCV 922.7
BRCH 65.46
BRCV 71.49
LCLT 295.0
LCLP 947.6
MLTH 299.6
MLMR 17.83
THCK 5736.
PWAT 50.45
00Z 04 Sep 2012
University of Wyoming

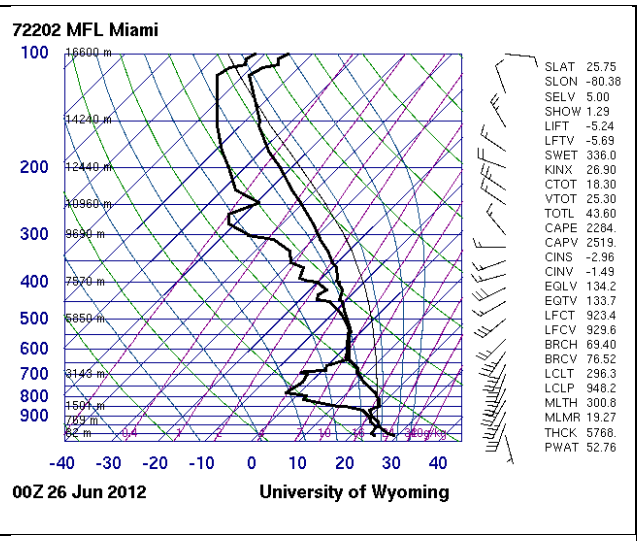
72202 MFL Miami
SLAT 25.75
SLON -80.38
SELV 5.00
SHOW 1.29
LIFT -5.24
LFTV -5.69
SWET 336.0
KINX 26.90
CTOT 18.30
VTOT 25.30
TOTL 43.60
CAPE 2284.
CAPV 2519.
CINS -2.96
CINV -1.49
EQLV 134.2
EQTV 133.7
LFCT 923.4
LFCV 929.6
BRCH 69.40
BRCV 76.52
LCLT 296.3
LCLP 948.2
MLTH 300.8
MLMR 19.27
THCK 5768.
PWAT 52.76
00Z 26 Jun 2012
University of Wyoming

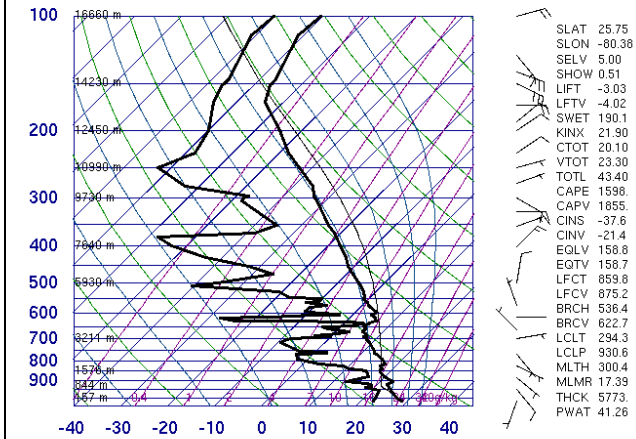
72202 MFL Miami
SLAT 25.75
SLON -80.38
SELV 5.00
SHOW 0.51
LIFT -3.03
LFTV -4.02
SWET 190.1
KINX 21.90
CTOT 20.10
VTOT 23.30
TOTL 43.40
CAPE 1598.
CAPV 1855.
CINS -37.6
CINV -21.4
EQLV 158.8
EQTV 158.7
LFCT 859.8
LFCV 875.2
BRCH 536.4
BRCV 622.7
LCLT 294.3
LCLP 930.6
MLTH 300.4
MLMR 17.39
THCK 5773.
PWAT 41.26
00Z 28 Jul 2012
University of Wyoming

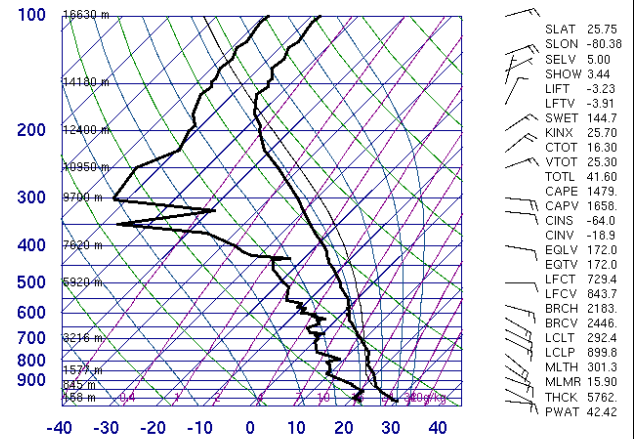
72202 MFL Miami
SLAT 25.75
SLON -80.38
SELV 5.00
SHOW 3.44
LIFT -3.23
LFTV -3.91
SWET 144.7
KINX 25.70
CTOT 16.30
VTOT 25.30
TOTL 41.60
CAPE 1479.
CAPV 1658.
CINS -64.0
CINV -18.9
EQLV 172.0
EQTV 172.0
LFCT 729.4
LFCV 843.7
BRCH 2183.
BRCV 2446.
LCLT 292.4
LCLP 899.8
MLTH 301.3
MLMR 15.90
THCK 5762.
PWAT 42.42
00Z 21 Jul 2012
University of Wyoming

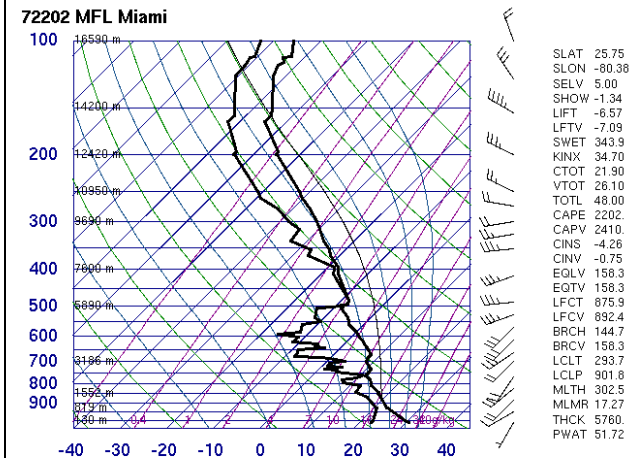
72202 MFL Miami
SLAT 25.75
SLON -80.38
SELV 5.00
SHOW -1.34
LIFT -6.57
LFTV -7.09
SWET 343.9
KINX 34.70
CTOT 21.90
VTOT 26.10
TOTL 48.00
CAPE 2202.
CAPV 2410.
CINS -4.26
CINV -0.75
EQLV 158.3
EQTV 158.3
LFCT 875.9
LFCV 892.4
BRCH 144.7
BRCV 158.3
LCLT 293.7
LCLP 901.8
MLTH 302.5
MLMR 17.27
THCK 5760.
PWAT 51.72
00Z 08 Jun 2012
University of Wyoming

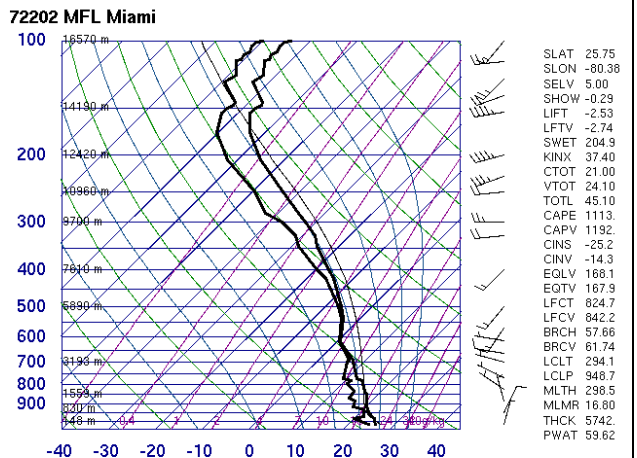
72202 MFL Miami
SLAT 25.75
SLON -80.38
SELV 5.00
SHOW -0.29
LIFT -2.53
LFTV -2.74
SWET 204.9
KINX 37.40
CTOT 21.00
VTOT 24.10
TOTL 45.10
CAPE 1113.
CAPV 1192.
CINS -25.2
CINV -14.3
EQLV 168.1
EQTV 167.9
LFCT 824.7
LFCV 842.2
BRCH 57.66
BRCV 61.74
LCLT 294.1
LCLP 948.7
MLTH 298.5
MLMR 16.80
THCK 5742.
PWAT 59.62
00Z 24 Sep 2012
University of Wyoming

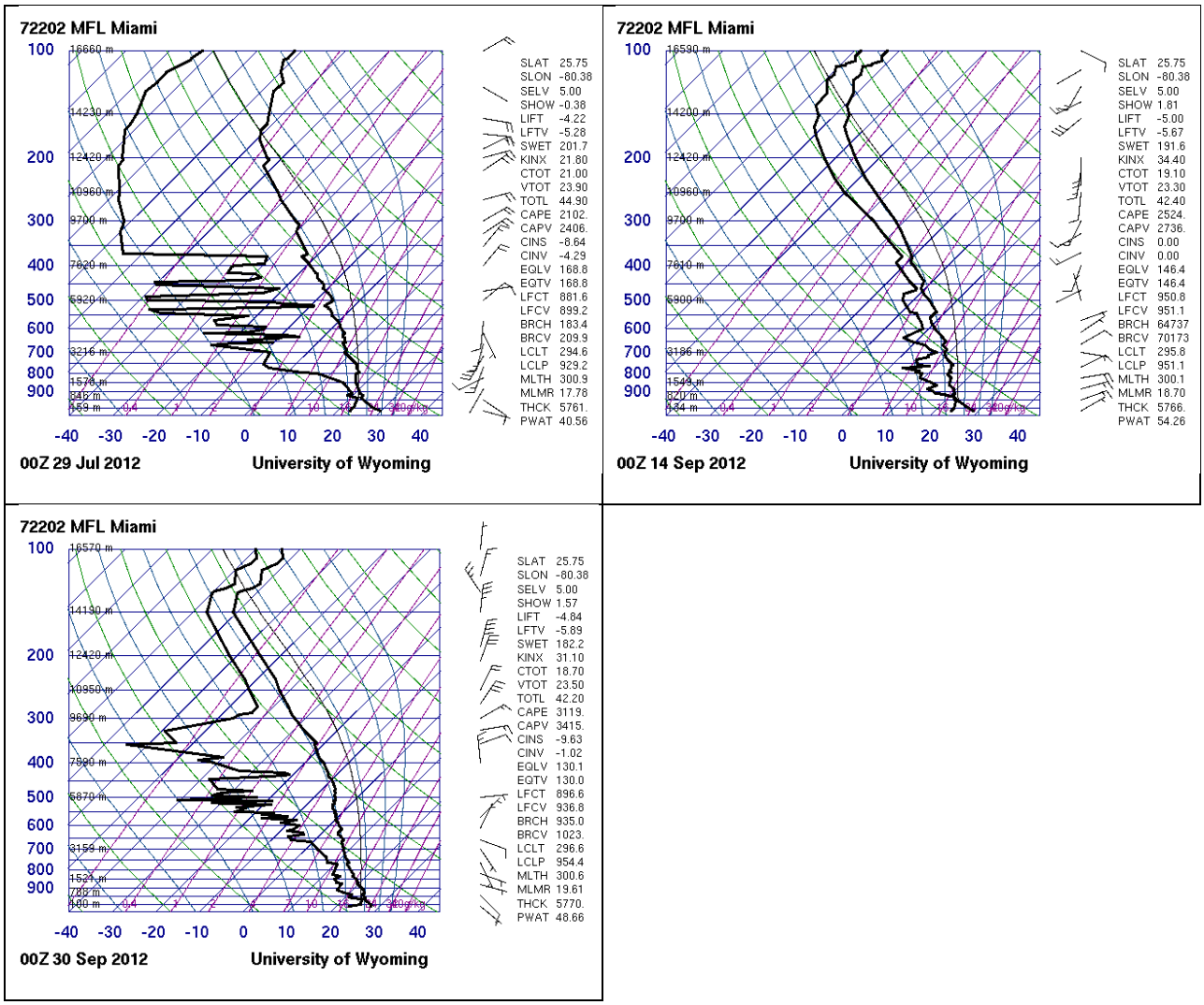

Skew T diagrams at 00Z for 33 of the 66 non-active days obtained from Wyoming Weather Web. The order of the soundings is placed from left to right by least number of strikes. The order goes as follows: June 20, June 27, September 27, September 30, September 12, June 21, June 12, June 11, September 9, June 29, August 19, July 29, July 26, August 30, August 31, June 17, June 28, August 26, June 30, September 8, August 7, September 2, September 3, June 25, July 27, July 20, June 7, September 23, July 28, September 13, and September 29.

Appendix L. Moisture Maps for Select Days

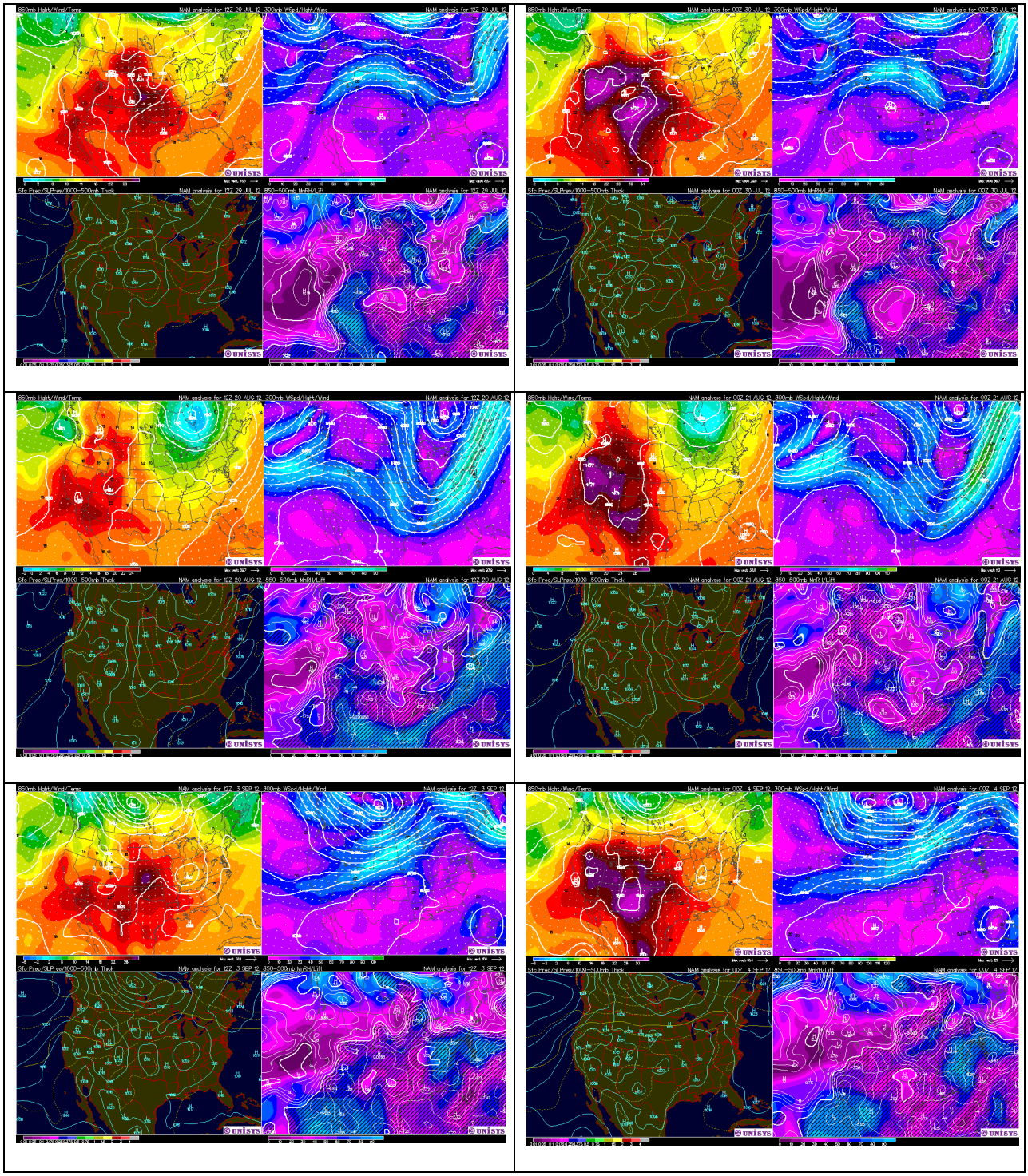

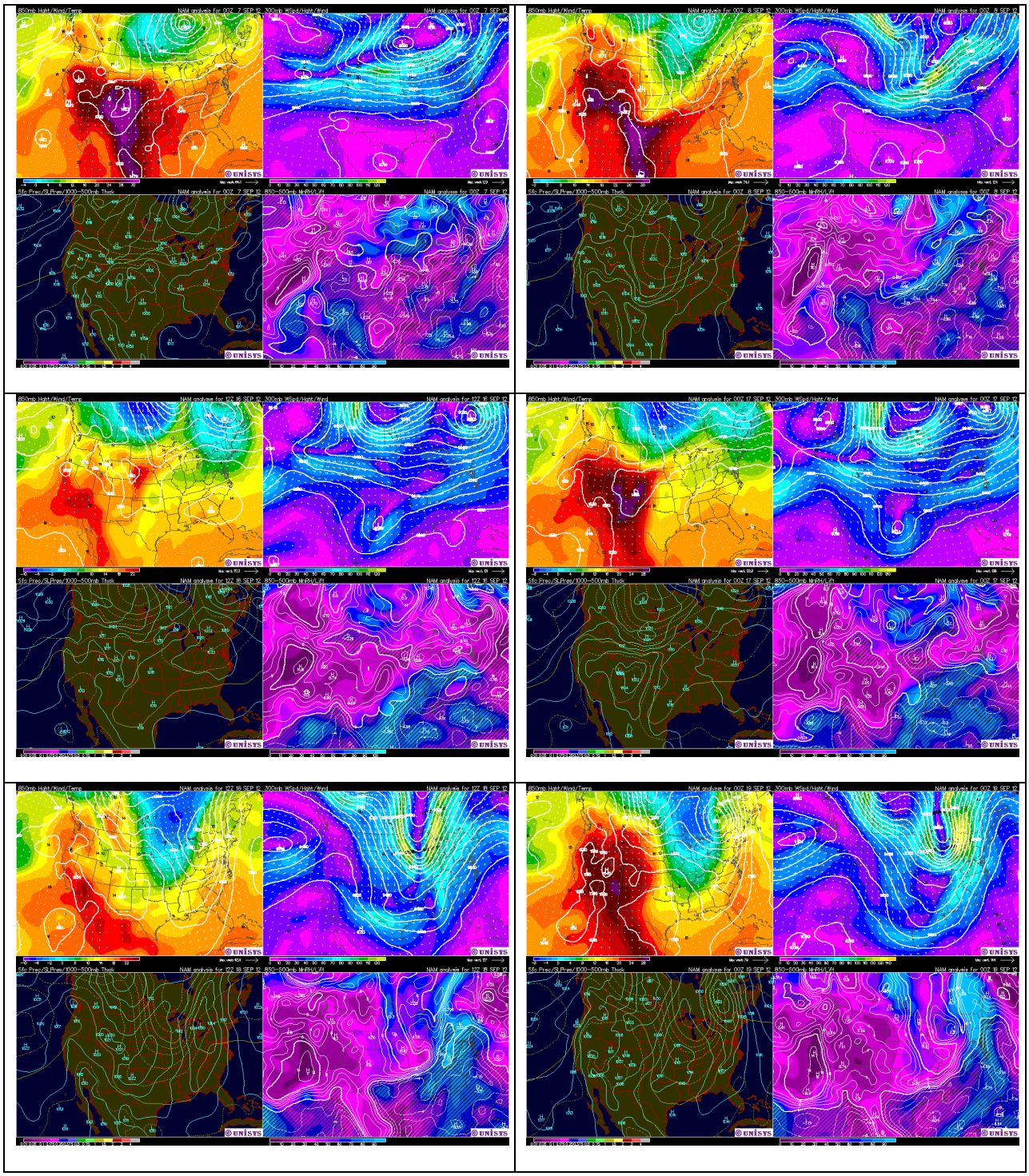
850mb Hght/Wind/Temp
300mb WSpd/Hght/Wind
Sfc Pres/SLPres/1000-500mb Thck
850-500mb MnRH/Hght
UNISYS

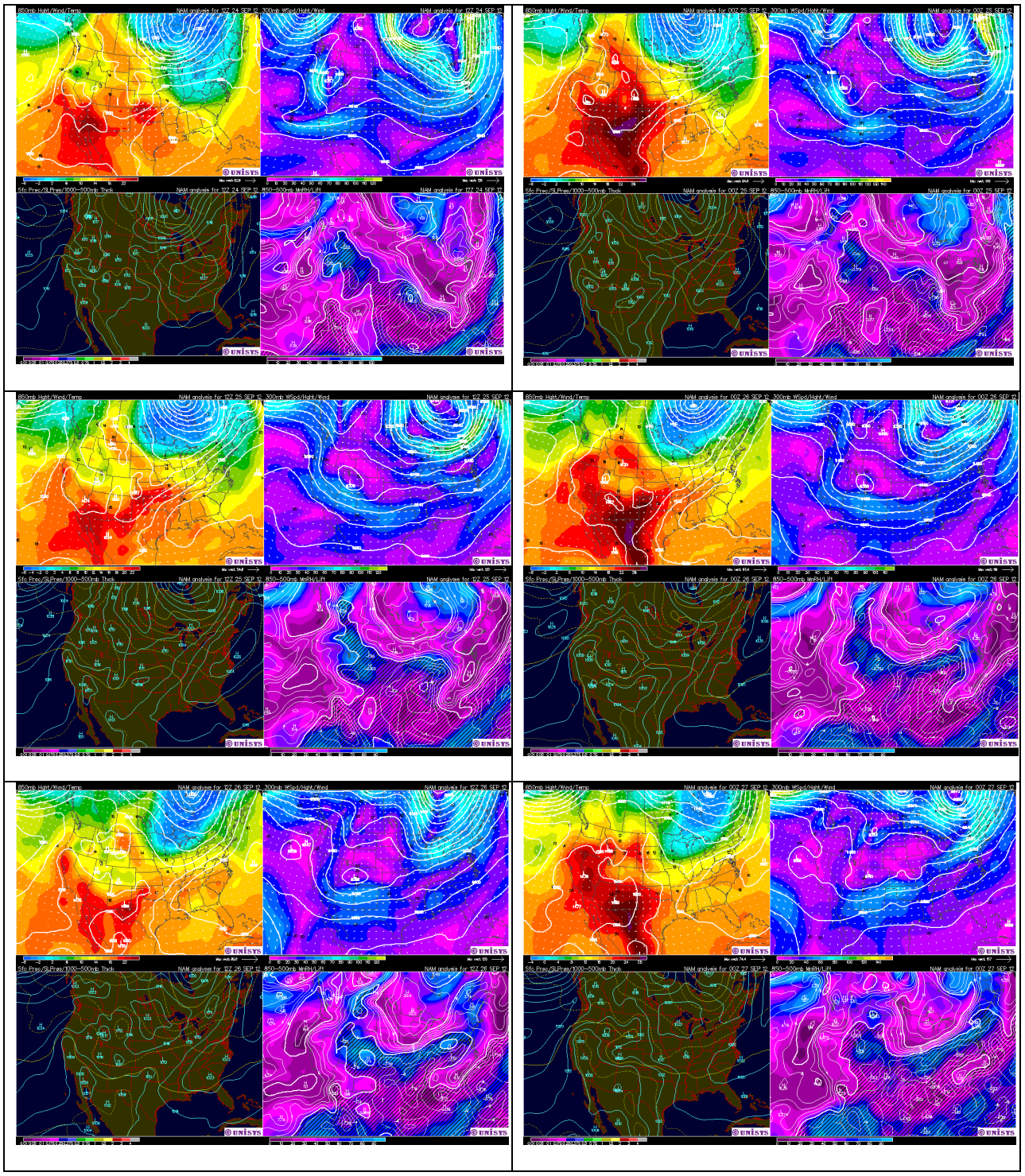
850mb Hght/Wind/Temp
NAM analysis for 127 24 SEP 12
300mb WSpd/Hght/Wind
NAM analysis for 127 24 SEP 12
Sfc Pres/SLPres/1000-500mb Thick
NAM analysis for 127 24 SEP 12
850-500mb MnRH/Lift
NAM analysis for 127 24 SEP 12
850mb Hght/Wind/Temp
NAM analysis for 007 25 SEP 12
300mb WSpd/Hght/Wind
NAM analysis for 007 25 SEP 12
Sfc Pres/SLPres/1000-500mb Thick
NAM analysis for 007 25 SEP 12
850-500mb MnRH/Lift
NAM analysis for 007 25 SEP 12
850mb Hght/Wind/Temp
NAM analysis for 127 25 SEP 12
300mb WSpd/Hght/Wind
NAM analysis for 127 25 SEP 12
Sfc Pres/SLPres/1000-500mb Thick
NAM analysis for 127 25 SEP 12
850-500mb MnRH/Lift
NAM analysis for 127 25 SEP 12
850mb Hght/Wind/Temp
NAM analysis for 007 26 SEP 12
300mb WSpd/Hght/Wind
NAM analysis for 007 26 SEP 12
Sfc Pres/SLPres/1000-500mb Thick
NAM analysis for 007 26 SEP 12
850-500mb MnRH/Lift
NAM analysis for 007 26 SEP 12
850mb Hght/Wind/Temp
NAM analysis for 127 26 SEP 12
300mb WSpd/Hght/Wind
NAM analysis for 127 26 SEP 12
Sfc Pres/SLPres/1000-500mb Thick
NAM analysis for 127 26 SEP 12
850-500mb MnRH/Lift
NAM analysis for 127 26 SEP 12
850mb Hght/Wind/Temp
NAM analysis for 007 27 SEP 12
300mb WSpd/Hght/Wind
NAM analysis for 007 27 SEP 12
Sfc Pres/SLPres/1000-500mb Thick
NAM analysis for 007 27 SEP 12
850-500mb MnRH/Lift
NAM analysis for 007 27 SEP 12

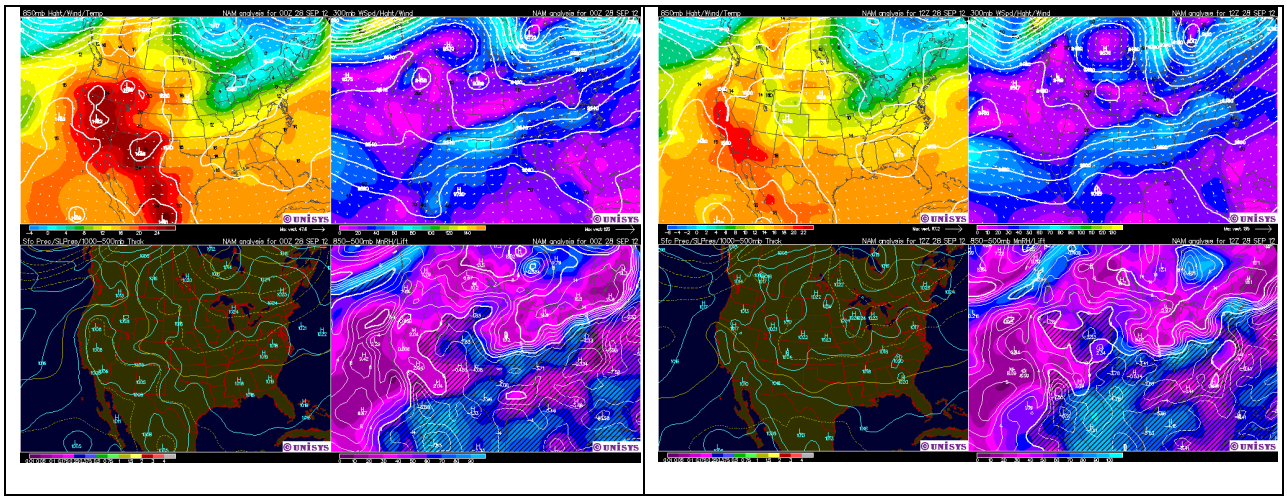

The maps are of the 850-500 mb relative humidity (RH) located in the bottom right corner and of 850 mb wind located in the top left corner for both 12 (left panels) and 00Z (right panels) for non-active days with cooler than average 500 mb temperatures. Maps obtained from the Unisys Weather archive of upper air charts.